Faculty of Science and Engineering
Department of Petroleum Engineering

Cuttings Transportation in Coiled Tubing Drilling for Mineral Exploration

Mohammadreza Kamyab

This thesis is presented for the Degree of
Doctor of Philosophy
of
Curtin University

June 2014

Declaration

To the best of my knowledge and belief this thesis contains no material previously published by any other person except where due acknowledgment has been made. This thesis contains no material which has been accepted for the award of any other degree or diploma in any university.

Name: Mohammadreza Kamyab
Signature: 
Date: 13 June 2014

Abstract

Due to fast growing in mineral consumption and quick reduction in surface ore bodies, exploration of the deep mineral resources seems crucial. To explore deeper hard rocks and determine the extent of the ore bodies, Deep Exploration Technologies Cooperative Research Centre (DET CRC) proposed the use of Coiled Tubing (CT) technology for mineral exploration drilling. The aim is to map the underground mineral resources which are deposited at large depths by drilling fast and at economic rate. To adapt the drilling technology from oil and gas industry into hard rock drilling application, investigations are needed.

The density and size of the cuttings in hard rock drilling varies in a broader range than oil and gas drilling where rocks are of softer nature. In addition, high rotational speed and low weight on bit is preferred in drilling hard rocks. This will need a high speed downhole motor associated with coiled tubing drilling in order to rotate the bit; this, in turn, means that the flow velocity and flow rate should be very high. Also, the size of the annulus space in the application of this study is narrow. This leads to the fact that the flow regime in the annulus space would be of turbulent nature. The study of cuttings transport in the small size annulus space with high fluid velocity at turbulent regime is the core part of this research study. This was done through both laboratory experiments using a flow loop and numerical modelling.

The experimental results indicated that fine particles generated with impregnated diamond bit will affect the rheological properties of the mud noticeably; this is not the case in oil and gas drilling where the cuttings are coarser. The results of flow loop experiments determined the minimum transportation velocity to effectively bring all the cuttings to the surface. Both vertical and directional boreholes were tested and the effect of cuttings size as well as mud properties was investigated. Testing cuttings from Brukunga mine site presented different results in terms of the effect of rheological properties of the drilling fluid and cuttings size on the minimum transportation velocity than those observed in the literature in oil and gas drilling.

Computational fluid dynamics numerical simulation was applied in this study to investigate the effect of different parameters in cuttings transportation. The simulation results were validated against the experimental results of the flow loop.

Various flow pattern profiles were simulated by changing different parameters and the results are presented.

Acknowledgements

I would like to appreciate the support of all those people who helped me during my PhD studies.

I express my special acknowledgment to my supervisor Prof Vamegh Rasouli for his continuous and timely support towards my project. I would like to express my gratitude to my associate supervisor Dr Swapan Mandal from Australian Mud Company for his technical support in particular with regards to the laboratory experiments component of my work.

The work has been supported by the Deep Exploration Technologies Cooperative Research Centre whose activities are funded by the Australian Government's Cooperative Research Centre Programme. This is DET CRC Document 2014/516.

I also would like to appreciate the support of my colleagues and friends at the Department of Petroleum Engineering in various occasions.

I owe a great debt to my parents, without their inspiration I was not able to bear the hardship of this journey.

Above all, I praise God who gave me the courage and strength to go through this phase of my life successfully.

To

those who fell down and got up again

Contents

List of Figures

List of Tables

Nomenclature

Latin letters

A	annulus area (m^2, in^2)
A_{bed}	area of the formed cuttings bed (m^2, in^2)
A_{ann}	cross sectional area of the annulus (m^2, in^2)
B_a	well geometry shear rate correction (-)
B_x	field viscometer shear rate correction (-)
C	constant (-)
C_c	volumetric cuttings concentration (v/v)
C_D	drag coefficient (-)
d	diameter, hydraulic diameter, average diameter of the particles (m, in)
d_1	$d_1 = 2R_1$ (m)
d_2	$d_2 = 2R_2$ (m)
d_{hyd}	hydraulic diameter (m, in)
D_ω	cross-diffusion term ($kg/\left(m^3 s^2\right)$)
e_{ss}	solid particles restitution coefficient (-)
f	Fanning friction factor (-)
f_{lam}	laminar regime friction factor (-)
$\vec{F}_{lift}$	lift force (N)
$\vec{F}_q$	external body force (N)
f_{trans}	transition regime friction factor (-)
f_{turb}	turbulent regime friction factor (-)
$\vec{F}_{vm}$	virtual mass force (N)
Fr	Froude number (-)
$g_{0,ss}$	radial distribution function (-)
G	Geometry factor (-)

G_k	production of turbulent kinetic energy (J/kg)
$\tilde{G}_k$	generation of k ($J/(m^3 s)$)
G_ω	generation of ω ($kg/(m^3 s^2)$)
h	annulus gap (m)
I	turbulent intensity (-)
K_{pq}	interphase momentum exchange coefficient ($kg \cdot m^{-3} \cdot s^{-1}$)
k	fluid consistency index ($Pa \cdot s^n$, $lb_f/(100\, ft^2)$), constants (-), turbulent kinetic energy (m^2/s^2)
k'	local power law flow consistency index ($Pa \cdot s^n$, $lb_f/(100\, ft^2)$)
k_{pq}	covariance of the velocities of the continuous phase q and the dispersed phase p (m^2/s^2)
k_q	turbulent kinetic energy for phase q (m^2/s^2)
l	turbulent length scale (m)
L	length (m, ft)
m	inverse of n (-)
M	number of secondary phases (-)
n	fluid behaviour index (-), number of phases (-)
n'	local power law fluid behaviour index (-)
N	number of solid phases (-)
p	static pressure (Pa)
q	given or actual flow rate (m^3/s), phase
q^*	estimated flow rate (m^3/s)
R_1	outer radius of inner pipe for annulus geometry; it is zero for pipe geometry (m)
R_2	inner radius of outer pipe for annulus geometry; inner radius of the pipe for pipe geometry (m)
Re	Reynolds number (-)
Re^*	estimated Reynolds number (-)
Re_c	critical Reynolds number (-)
R_t	transport ratio (-)

S_k	source term for turbulent kinetic energy ($J/\left(m^3 s\right)$)
S_ω	source term for specific dissipation rate ($kg/\left(m^3 s^2\right)$)
$\vec{\mathrm{u}}$	velocity (*m/s*)
$\vec{\mathrm{u}}_{dr}$	drift velocity (*m/s*)
$\vec{\mathrm{u}}_{pq}$	relative velocity (*m/s*)
u'	velocity fluctuation (*m/s*)
$u_{\text{Flow Direction}}$	velocity in the flow direction (*m/s*)
u_x	flow velocity in the *x* directions (*m/s*)
u_y	flow velocity in the *y* directions (*m/s*)
U	free stream velocity (*m/s*)
v	velocity (*m/s*, $ft/\min$)
v_a	annular fluid velocity (*m/s*, $ft/\min$)
v_s	cuttings slip velocity (*m/s*, $ft/\min$)
v_u	cuttings net upward velocity (*m/s*, $ft/\min$)
V	average velocity (m/s)
w	width of the slot (m)
y_i	measured values
$\hat{y}_i$	predicted values
$\bar{y}$	average value of the parameter
Y_k	turbulence dissipation of *k* ($J/\left(m^3 s\right)$)
Y_ω	turbulence dissipation of ω caused ($kg/\left(m^3 s^2\right)$)

Greek letters

α	hole inclination (*rad*), flow conduit constant (-), volume fraction (-)
α_s	total volume fraction of the solid phase (-)
$\alpha_{s,\max}$	packing limit (-)
γ	shear rate (s^{-1})
γ_{Nw}	Newtonian shear rate at the wall (s^{-1})
Γ_k	effective diffusivity of *k* ($kg/\left(ms\right)$)

Γ_ω	effective diffusivity of ω ($kg/(ms)$)
Δ	pressure loss per unit length (Pa/m)
ΔP	pressure loss (*Pa*, *psi*)
ε	rate of dissipation (m^2/s^3)
θ	granular temperature (*J*), hole inclination (*degree*)
λ_s	granular bulk viscosity ($Pa \cdot s$)
μ	viscosity ($Pa \cdot s$, *cP*)
μ_B	plastic viscosity in Bingham Plastic model ($Pa \cdot s$, *cP*)
μ_s	granular shear viscosity ($Pa \cdot s$)
$\mu_{s,col}$	collisional component of granular shear viscosity ($Pa \cdot s$)
$\mu_{s,f}$	frictional component of granular shear viscosity ($Pa \cdot s$)
$\mu_{s,kin}$	kinetic component of granular shear viscosity ($Pa \cdot s$)
μ_t	turbulent viscosity ($Pa \cdot s$)
ξ	$= \tau_y / \tau_w$ (-)
π	dimensionless parameter (-)
Π	influence of the dispersed phase on the continuous phase ($J \cdot m^3/kg^2$)
ρ	density (kg/m^3 , lb_m/gal)
σ_k	turbulent Prandtl numbers for *k* (-)
σ_ε	turbulent Prandtl numbers for ε (-)
τ	shear stress (Pa , $lb_f/(100\,ft^2)$)
$\overline{\overline{\tau_q}}$	q^{th} phase stress-strain tensor (Pa)
τ_w	wall shear stress (Pa)
τ_y	yield shear stress (Pa)
τ_{y1} , τ_{y2}	middle values of yield stress to determine the best value (Pa)
$\tau_{y\min}$, $\tau_{y\max}$	minimum and maximum values of the yield stress boundary (Pa)
ω	specific dissipation rate (s^{-1})

Abbreviations

AMC	Australian Mud Company

API	American Petroleum Institute
APL	annular pressure loss
BIV	best index value
CFD	computational fluid dynamics
CT	coiled tubing
CTD	coiled tubing drilling
CTU	coiled tubing unit
ECD	equivalent circulating density
EG	Eulerian Granular
FV	funnel viscosity
HB	Herschel-Bulkley
ID	inside diameter
minex	mineral exploration
MTV	minimum transportation velocity
O&G	oil and gas
OD	outside diameter
PDC	polycrystalline diamond compact bit
PHPA	partially hydrolysed polyacrylamide
PL	Power Law
RAB	rotary air-blast
RC	reverse circulation
ROP	rate of penetration
MBH	micro–borehole
MBHCTD	MBH CTD
SG	specific gravity
WOB	weight on bit

1 Introduction

This Chapter summarises the objectives, framework, methodologies and significance of the research work in this study. An overview of material presented in subsequent Chapters is also given.

1.1 Cuttings transportation

Due to the imminent shortage of easily accessible minerals at the surface and shallow subsurface depths there is a future necessity to drill and extract more deeply buried resources. Accordingly, a new project was initiated by the Deep Exploration Technologies Cooperative Research Centre (DET CRC) in Australia. The project aims at more economic, faster and deeper operation in mineral exploration (minex) using coiled tubing drilling (CTD) for hard rock (Hillis, 2012).

CT has been used largely in the oil and gas (O&G) industry applications in the past mainly in workover operations and to a little extend for drilling compared to the conventional drilling operation (Spears, 2003). However, due to the differences between its application in O&G and minex drilling there are aspects of CT technology which need to be modified specifically for hard rock drilling.

In O&G wells, the space between the drill string and bore-hole wall, known as the annulus, is larger than that in minex wells drilled with micro-borehole (MBH) CT. Hence, one of the challenges in such technology transfer, is cuttings transportation; particularly in the small annuli of MBH under very high flow rates. Consequently, cuttings transportation is the research topic here that has been studied through both laboratory experimental work and numerical simulations.

Ideally for CTD to replace diamond coring in minex, the cuttings recovered at the surface by CTD need to accurately represent the depth of their origin. This can be achieved only if the cuttings are not mixed together whilst they are transported up the annulus of a wellbore. Also unmixed clean cuttings are essential to allow their online analysis for potential mineral content.

Typically the density of cuttings from sediments drilled in O&G wells ranges between 2.2-2.7SG (18.36-22.53ppg) whereas in mineral drilling cuttings may have densities as high as that of gold; notably 19.3SG (161ppg). In addition to size, shape and density of the cuttings, many drilling parameters also affect annular cuttings transportation.

Percussive hammer bits and impregnated diamond bits are two types of drill bits used in MBHCTD. As CT does not rotate therefore the rotation of the bit is provided with a downhole turbine or motor. To activate the hammer bit, in addition to the downhole motor, a hammer is required. Moreover, CT cannot transmit a heavy weight or force to the bit without buckling and for rotary drilling the downhole turbine/motor and hammer require high flow rates to generate faster bit rotation and acceptable rates of penetration (ROP). In turn, increased annular velocities especially in MBHs cause turbulent flow, which in turn, result in higher annular pressure losses (APLs). Coupled with the drilling fluid flow through the entire length of CT, the higher pressure losses mean that the overall pump pressures are higher in minex CTD operations when compared to conventional O&G drilling.

Percussive hammer drilling has a higher ROP and generates broader range of particle sizes compared to the impregnated diamond bit. In fact the cuttings produced with an impregnated diamond bit are micron size powders.

The major differences between fluid flow and cuttings transport in drilling O&G and minex are listed in Table 1.1.

Table 1.1 Difference between fluid flow and cuttings transport in conventional O&G and MBHCTD wells

Parameter	Conventional oil and gas	Microborehole CT Drilling
Annular volume	Larger	Smaller
Velocity	Slower	Faster
Flow regime	Laminar	Laminar to Turbulent
Annular pressure loss	Lower	Higher
Cuttings size	Coarse	Mainly fine
Cuttings density (g/cc)	2.2-2.9	2.7-19.3

The effect of cuttings on the rheological properties of the slurry mixture is not considered to be important in O&G drilling. This is the result of a combination of mainly coarse cuttings and slower annular velocities. However, fine cuttings (rock flour) generated by an impregnated diamond bit will affect the rheological properties of the drilling fluid (mud) and this aspect is discussed in details in Chapter 3.

A minimum transportation velocity (MTV) to effectively transport and avoid intermixing of the cuttings in an annulus can be determined. MTV has been used under different nomenclature to quantify the cuttings transportation capacity in O&G wells. Ideally the annular flow rate has to be just above the MTV to put any stationary cuttings in motion.

From the above brief discussion, it appears that there are many different parameters affecting the efficiency of cuttings transport in the annulus. While many researches have been undertaken to study this in O&G applications, their effect in the applications related to this study is not yet investigated.

In O&G drilling there are recommendations for the minimum flow rate required for effective hole cleaning as a function of hole size and hole angle (Amoco, 1996). However in this study the objective is to investigate the minimum flow rate or velocity corresponding to MBH size environment with applications in minex drilling.

In order to be able to study the effect of various parameters on cuttings transportation, laboratory experiments are invaluable particularly because they allow sensitivity analyses of the effect of each parameter while other parameters in the system are kept constant.

For the purpose of this study a flow loop was designed and built to simulate cuttings transport behaviour in small size annuli. Real cuttings were tested using the flow loop and the results are presented in this thesis.

The use of numerical simulations would help to do the sensitivity analysis over a wide range of parameters. This is only valid if the model has been calibrated against some real or laboratory experimental data. In Chapter 5 the computational fluid dynamics (CFD) simulations with ANSYS Fluent 14.0 software to model cuttings transportation are reported.

1.2 Research objectives and methodology

Based on the discussion above, the main objectives of this study include:

- To investigate the effect of the fine cuttings (rock flour) on the rheological properties of the drilling fluids used in minex wells and an estimation of the resultant APL in MBHs;

- To carry out experimental laboratory tests using a flow loop to determine the effect of controlling parameters such as hole inclination, cuttings size and mud rheology on cuttings transportation;
- To perform numerical simulations of annular cuttings transportation with Eulerian Granular (EG) approach where the findings are verified by laboratory experiments; and to use of the EG model to determine the effect of other parameters such as cuttings density and concentration on cuttings transportation.

In order to achieve the above mentioned objectives the following methods were utilized:

- Real impregnated diamond bit cuttings were used to determine the effect of fine cuttings on the rheological properties of the drilling fluids. For this purpose different cuttings concentration and mud types were used to show the significance of this effect. The APL for each case was measured and the difference with the original mud (without cuttings) was found.
- An experimental flow loop setup was built to model the efficiency of cuttings transportation in MBHCTD minex wells from variations in hole inclination, cuttings size, and mud rheology.
- A numerical simulation model, performed in ANSYS Fluent 14.0 software, was developed to model cuttings transportation with EG approach and it was validated against the experimental results.

1.3 Research significance

The originality and significance of this research are as follows:

- This research is the adaptation of the CTD into minex and this study focuses on the cuttings transportation aspect in the small annular space of MBHCTD. This study has not been performed in the past with this specific focus.
- As mentioned in the previous section, in the O&G drilling the effect of particles on the rheological properties of the drilling fluid is not considered significant and this is due to the fact that the particles are bigger and the annular velocity is lower in comparison with MBHCTD that is discussed in this study. However, in minex when the impregnated diamond bit is used the cuttings are fine powders and the annular flow velocity is higher. Due to these

reasons, in this study experiments were performed which demonstrated that the effect of the particles on the rheological properties of the mud cannot be neglected.

- For initial investigation a mini flow loop was designed at a smaller scale to simulate the cuttings transportation in narrow annulus of CT drilling where the results were used to calibrate the corresponding numerical simulations.
- A fluid flow loop is specifically built for the applications of MBHCTD.
- The use of actual cuttings retrieved from percussive hammer drilling from Brukunga mine site in Adelaide added a significant value in terms of obtaining results which represent real drilling operation. The results can be compared with real drilling activities in the mine site and make some conclusions.
- The effect of different parameters in the flow loop such as hole inclination, mud rheological properties and cuttings size on cuttings transportation performance were investigated which showed different results to the literature corresponding to the O&G applications. This is an important finding from this work.
- EG model has not commonly been used for cuttings transportation studies in O&G applications, however, its use in applications of this study appear to be promising. This finding can be used for further studies in this topic.

1.4 Thesis structure

Figure 1.1 shows a summary of the thesis structure. In this Chapter an overview of the project topic, the objectives and methodologies used and the significance of this work were discussed.

In Chapter 2 a literature review of previous cuttings transportation studies in O&G application is presented. The requirements for transfer of CT technology from O&G into mining drilling are explained in detail and the associated challenges related to the cuttings transport are reviewed. The patterns of cuttings transportation in deviated holes are illustrated. Furthermore, the controlling parameters in cuttings movement are elucidated. In this Chapter also the need for further studies in the form of both laboratory work and numerical simulations is discussed.

The effect of fine powder inert cuttings on the rheological properties of the drilling fluid is covered in Chapter 3. Three mud samples were tested to display the

significance of change in the rheological properties of the drilling fluids due to addition of fine powders in terms of the total pressure losses that they introduce to the drilling system.

Chapter 4 presents the experimental set up and tests of the cuttings transportation carried out as part of this work. Detail of a mini flow loop that was designed for preliminary study is presented. The specifications of the full scale flow loop are illustrated and the capabilities of the system are explained with the controlling parameters that can be changed. Details of the mud and cuttings properties will be given and the MTV results at different hole inclinations are presented to show the effect of mud rheology and cuttings sizes on cuttings transport capacity.

In Chapter 5 the details of CFD model developed to simulate cuttings transportation for the purpose of this study in presented. The equations and models used to incorporate different parameters are given. The results of calibrating the models against laboratory experimental data are explained.

Chapter 6 presents the concluding remarks of this study and provides recommendations for future studies.

The procedure of preparing diamond coring cuttings powders for rheological tests and collecting real samples at the rig site for the flow loop tests are presented in Appendix A.

1.5 Summary

In this Chapter an overview of the research topic to emphasise the importance and necessity of understanding cuttings transport studies in minex is given. The differences of this study opposite to the applications in O&G industry were explained. Then the objectives, methodologies and significance of this research work were detailed. In the next Chapter a background for CTD is outlined and a review of the literature for annular cuttings transportation is offered.

Chapter 1 Introduction

- A brief discussion about the challenges of cuttings transportation in minex drilling
- Presenting the objective, methodology and significance of this study
- The layout and structure of the thesis

Chapter 2 Cuttings transportation in hard rock drilling

- Review of previous investigation of cuttings transportation in oil industry
- Presenting the effect of different parameters on cuttings carrying capacity
- Expressing the need for further experimental and numerical investigation to adapt cuttings transportation for hard rock drilling with coiled tubing

Chapter 3 Rheological properties and slurry behaviour in hard rock drilling

- Experimental investigation of the effect of fine powders on the rheological properties of the drilling mud
- Calculating the pressure losses corresponding to the rheology changes

Chapter 4 Experimental simulations of cuttings transport

- Mini and full scale flow loop specifications
- Presenting the experimental results and expressing the effect of hole inclination, cuttings size and mud rheology on MTV
- Expressing the difference in findings with cuttings transport investigation in O&G industry

Chapter 5 Numerical simulation

- Explaining the Eulerian Granular CFD model developed to simulate cuttings transportation in minex
- Validation of the model with experimental results
- Performing extra simulation to find the effect of other parameters

Chapter 6 Conclusions and recommendations

References

Appendix A Cuttings collection, preparation and analyses

Figure 1.1 Thesis structure

2 Cuttings transportation in hard rock drilling

2.1 Introduction

In this chapter the idea of coiled tubing drilling (CTD) for mineral exploration (minex) is presented and the justifications for selecting this technology to reach deep underground mineral ore bodies are discussed. The challenges in cuttings transportation in narrow annulus space with reference to the applications discussed in this study, i.e. drilling for minex, will be reviewed. The concept of minimum transportation velocity (MTV) will be introduced as a benchmark to study the carrying capacity of the drilling fluid in use. Some of the major literature arising from slurry transportation studies that used laboratory experiments and/or numerical simulation analyses will also be presented. As they are mainly concerned with drilling for oil and gas (O&G), the differences with cuttings transportation in minex drilling will be discussed.

2.2 Mineral exploration drilling

Mapping of underground ore bodies is a multi-fold task, one of which is the drilling operation. Increasing the drilling speed while quality geological data is collected at a minimum cost during minex is one ultimate goal of drilling operation in mining industry.

Various types of mineral drilling and coring methods are currently used, notably (Marjoribanks, 1997; DMP, 2013; Misiano, 2010):

- **Auger drilling**: in this method of drilling helical screw rods are used to drill shallow depth unconsolidated rocks fast and cheap. The cut rocks are brought to the surface by the screws' blades. Water is used to hydrate dry formations to

achieve quicker drilling. This method can be used for target depths of around 20m.

- **Percussion rotary air-blast (RAB) drilling**: In this method hallow rods are used and compressed air is injected into the rods and after energizing the hammer it passes through the bit and goes into the annulus space between the outer side of the rod and the wellbore wall. Then air carries the cuttings to the surface. Generated cuttings range from rock flour to 3mm chips and this method of drilling can target depths of more than 50m. This method is not effective when water table is reached. To avoid this situation stabilisers are attached to the drill string to ream and isolate the water bearing formations. Small drilling rigs with compressors that can provide around 600cfm at 250psi are used. If multiple compressors are utilized, the operation can reach up to about 1250m.
- **Rotary reverse dual tube drilling**: Dual tubes have inner tubes inside of the drill rods. The air (or water) is injected through the annulus space between the inner tubes and drill rods and after passing through the bit nozzles it goes to the surface throughout the inner tubes. Because the cuttings are transferred inside of the pipe without any contact with the formation, they are less contaminated and are more representative. These types of rods are used in the following drilling methods:
  - **Air core drilling**: In this method a small rig is used and the compressor can provide 600cfm at 250psi.
  - **Reverse circulation (RC) drilling**: The rig in this method is bigger than the air core drilling rig and can be used for deeper targets up to 500m. The compressor can provide up to 1000cfm at 500psi.
- **Diamond coring**: In this method cylindrical solid rocks are recovered instead of cuttings samples. Therefore this method is the slowest among all above methods; however, the samples are more representative. A hallow impregnated diamond bit is used to cut the rock and guide the core into a core barrel positioned inside of the drilling rods. After the core reaches a certain length a wireline system retrieves the core to the surface with a special tool called overshot. The drilling fluid usually used in this operation is water to lubricate and cool the bit. The fluid then goes to the surface throughout the annulus

space between the drilling rods and borehole wall. The drilling depths can reach up to 2500m.

- **Sonic drilling**: In this method high frequency, resonate energy is generated by an oscillator assembly at the rig and it is sent to the bit through the rods in order to increase the ROP. In addition, the friction between the rods and wellbore wall is reduced due to the resonation of the drill strings.

In the more commonly used methods drilling rods or drill pipes are used to make up the drill string. Male (pin) and female (box) joints are made up or broken out to, respectively, run the drill string in and out of the hole. “Tripping pipe” in stands, that are either double or triple drilling rods or drill pipes in length, carries a safety risk. It is also time consuming and costly. For O&G well drilling an approximate trip time estimation is one hour per 1000ft (305m). The use of CT therefore readily seen to reduce both the safety risk and time associated with pulling or running a drill bit (Misiano, 2010; Safaee Ardekani & Shadizadeh, 2013).

2.3 Coiled tubing drilling

Coiled tubing (CT) is a continuous length of tube often that is spooled or coiled around a reel. The tubing generally has an outside diameter (OD) of 19-114.3mm (0.75-4.5in) but can sometimes attain a 168mm (6.625in) OD for offshore flow line applications. The first development of spool-able steel tubulars is often attributed to the early 1940’s World War II, Project 99 - Pipeline under the Ocean (PLUTO) for oil transportation of allied armies (PLUTO, 2014). However the use of a continuous length of tubing in O&G wellbore services is first documented in a US Patent #1965563 entitled "Well Boring Machine" that was awarded on 1934 (Bannister, 1934). Since then the use of the CT system has rapidly grown and nowadays it serves as one of the tools for drilling in O&G industries.

A CT unit (CTU) consists of the following major components:

1. Reel: for storage of the CT string;
2. Guide arch and injector head: to straighten, run and retrieve the CT string;
3. Control cabin: to monitor and control different operations and house the crew;
4. Power pack: for the provision of hydraulic and pneumatic power;
5. Mud tank(s), solid control equipment and mud pump(s): for the provision, storage and treatment (maintenance) of the drilling fluid;

6. Blow-out preventer (BOP): the equipment dedicated to control the well in case of a kick (ICoTA, 2005).

Figure 2.1 displays the major constituents of the CTU.

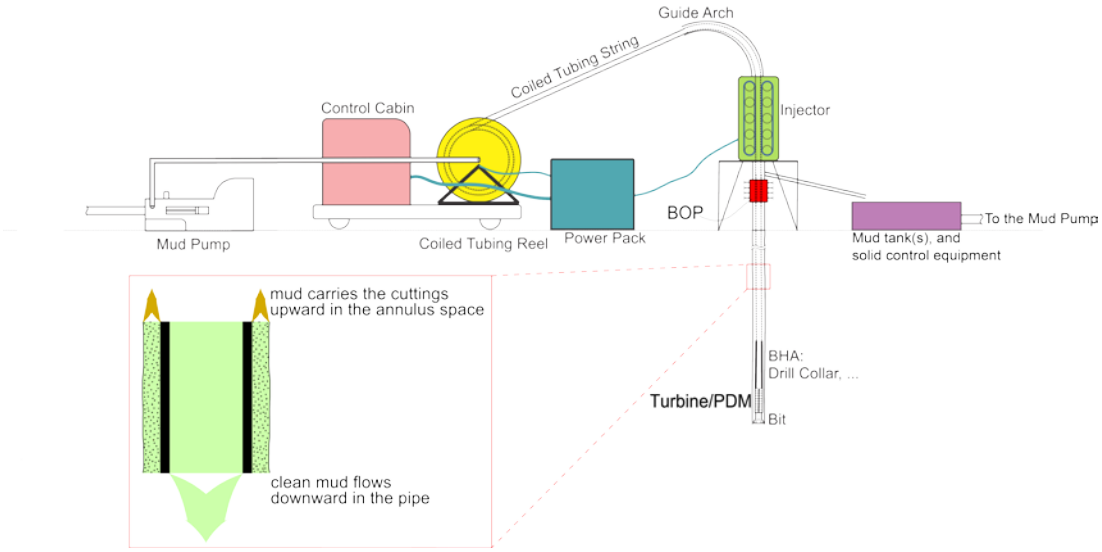

Figure 2.1 The main components of a CTU

A CTU and/or CTD have the following applications and capabilities (Byrom, 1999; Hyun et al., 2000; Kelessidis & Bandelis, 2004; Leising & Rike, 1994; Leising & Walton, 2002b; Perry, 2009) that are applicable to either or both O&G and minex drilling operations; all of which can lead to significant cost savings:

- Rapid mobilisation/demobilisation and rig up/down times
- Elimination of connection time
- Faster tripping in and out of the hole
- Faster drilling
- Small hole size capability
- Continuous circulation of the drilling fluid whilst tripping
- Smaller environmental footprint
- Reduction in the volumes of drilling fluids and cuttings
- Less operation time
- Underbalanced and managed pressure drilling operation
- Improved downhole to surface telemetry
- Ease of portability
- Reduced numbers of personnel
- Safer working environment
- Availability of thru-tubing re-entry for safe and efficient live well operations.

However CT and CTD have some limitations which may include:

- Short CT working life and ultimately higher string cost
- Inability to rotate which exacerbates good hole cleaning from cuttings transport difficulties especially in directional and horizontal wells
- CT strings cannot sustain tension
- Limited fishing operations
- Higher pressure losses in the coiled section specially at top hole
- Weight transfer problem to the bit
- Mud motor/turbine failures.

Consequently, there are still some obstacles to overcome before CTD is more widely adopted. For instance, it was expected to drill 18000-20000 wells to 5000ft in the US, however only 25 was selected to be drilled by CTD (Spears, 2003). Some investigators have a pessimistic perspective to CTD like Byrom (1999), however, of the upside for CTD applications is demonstrated, for example, by:

- Leising and Rike (1994) reported on the CTD jobs worldwide between 1991 and 1993. One job that they specifically mentioned was a re-entry into a conventionally drilled well. The production rate was increased by a factor of 3.5 times and at only one-fourth of the cost had a work-over rig been used.
- The Gas Technology Institute (GTI) with support of DOE/NETL drilled 220 wells in the Niobrara unconventional gas play of Kansas and Colorado. The trailer mounted CTU could drill a 3000ft well in one day and gave an overall project cost saving of about 30% relative to that achievable from a conventional drilling operation (Perry, 2009).
- Conoco Phillips performed a CTD project in the Chittim Ranch, Maverick county, West Texas between 2006 and 2009 where the objective was to drill infill wells with a rate of one well per day. The results were reductions in the drilling time and project costs by 60% and 14% respectively when compared to conventional rotary drilling operations (Littleton et al., 2010).

From this perspective, coiled tubing drilling (CTD) appears to be a better alternative as drilling progresses continuously with no interruption using this technique. This is in particular important when fast drilling is desired.

2.4 Coiled tubing drilling for mineral exploration

Surface minerals production has reached a level that demands more underground ore exploration. In addition to this, more deep mineral resources encourage deeper exploration drilling. For instance, in Australia, only 20% of the minerals are at the surface and the rest are deeply buried. Such deep mineral resources require deeper economic exploration drilling before higher rates of extraction can be achieved (McFadden, 2012). To help to achieve this goal, CTD technology was adapted for the exploration of deep mineral resources (Hillis, 2012).

While CT technology has advanced in O&G drilling, its application in minex has not been widely reported. However, it appears that CTD is a potentially suitable drilling and sampling technique; in particular for deep mining projects. For such minex purposes, CTD is an appropriate technique to drill micro-boreholes (MBH), with diameters less than 3in (76mm), where a significant reduction in the cost of the drilling operation is achievable. From a parallel effort the US Department of Energy (US DOE) developed a CTD technology for shallow O&G wells with depths less than 5000ft (1524m) with improved reservoir imaging ability and reduced environmental footprint (Lang, 2006).

Without compromising sample quality faster and potentially less expensive operations are the main drivers for using micro-borehole CTD (MBHCTD) instead of the existing methods for minex drilling (Hillis, 2012).

Small size boreholes can also be called slim-hole or MBH; and their sizes vary depending on required applications. Example of MBH diameters that have been reported in the past are 4.5in (114mm) (Lang, 2006), 4.75in (121mm) (Perry, 2009), 5.75in (146mm) (Albright et al., 2005) and 6in (152mm) (Enilari et al., 2006). Albright et al. (2005) suggested that holes with internal diameter of 2-3/8in (60mm) should be considered as MBHs. In this study MBHs are defined as those wells with internal sizes less than 3in (76mm).

For the transfer of CTD technology the differences in the requirements between the O&G and the mineral industries are summarised in Table 2.1.

Table 2.1 Major upstream differences between drilling in O&G and mining industries

	O&G drilling	Minex wells
Purpose of drilling	drill undamaged reservoir	mineral sampling and quantification
Final goal	O&G production	ore bodies extraction
Rock types to be drilled	soft to medium sedimentary	hard igneous, metamorphic and sedimentary
Exploration techniques before drilling	seismic surveys	magnetic, electric, electro-magnetic, induced polarization, gravimetric, and seismic surveys
Drilling method	rotary drilling	diamond coring, RC, and RAB
Samples type and size	cuttings, core and DST fluids	cores and cuttings
Target depth	underground reservoir	surface strip, pit and underground mines
Drilling bit types	tri-cone and PDC	impregnated diamond core bit, tri-cone, and hammer bits
Drilling problems	kick, lost circulation, wellbore instability, stuck pipe, hole cleaning, formation damage, and health, safety and environment	air compression safety, water tables, unconsolidated formations, gas kicks, slow ROP, stuck pipe, directional control, and health, safety and environment
Drilling fluid	water base and oil base muds, air, foam, and water	air, foam, water, and water base muds

Referring to Table 2.1, it can be seen that minex CTD needs to allow accurate quantitative sampling techniques. Therefore CTD must ideally transport cuttings effectively from a specific depth to the surface without any mixing with cuttings from other depths.

When combining CTD with percussive hammer drilling or impregnated diamond bit a downhole motor is required to rotate the bit because the CT string cannot be rotated. The size of the cuttings generated by the hammer drilling bit mainly vary in a wide range from 1 micron to 5mm in diameter compared to much finer cuttings and rock powder (flour) generated with diamond bits. In this study cuttings of the larger particle range were used for the simulation purposes.

When drilling with CT, clean mud travels through the coiled tubing (in a downward direction) and after passing through the bit's nozzles it travels through the annular space (in an upward direction) to the surface. Drilling fluid (mud) plays a multi-functional role in the drilling process: amongst its many functions a drilling fluid transfers hydraulic power into mechanical power through the downhole motor which rotates the bit. Mud also cools the bit and carries the cuttings in the annulus section to the surface. A clean hole is necessary as the CT (like a drill string in conventional drilling) can get stuck if the cuttings accumulate and pack-off.

Zhou and Shah (2004) carried out an extensive literature review on experimental and theoretical investigations for Newtonian and non-Newtonian fluid flow in the

CT. Studies of fluid flow inside the CT string for both of the coiled and straight sections of the tubing have been performed by many researchers. Several correlations have been developed and experimental procedures proposed to determine the friction factor along the spooled section (Zhou & Shah, 2006). As a result a secondary fluid flow inside the curve (coiled) section exists due to centrifugal forces that increase the pressure loss along this section. Accordingly, the use of some additives has been proposed to reduce the friction factor by 65% (Shah et al., 2006).

The objective of this research is to model the fluid flow and cuttings transport in the annular section of MBHCTD wells for applications in minex as discussed in detail in the following sections.

2.5 Annular cuttings transport

Slurry transport is the transportation of solid particles in a liquid medium. In this mode of transportation the liquid phase is the continuous phase that carries the solid particles within a confined space such a pipe or in the annulus between a drill string/CT and a borehole wall.

Slurry transportation has been the subject of study in the food, pharmaceuticals, chemical, construction, power generation and O&G industries (Doron et al., 1987; Eesa & Barigou, 2009; Kelessidis et al., 2007). From a drilling engineering perspective slurry transport is known as cuttings transport where the drilling mud (liquid phase) carries the cuttings (solid phase) along an annulus space in a well in an overall upward direction.

Many investigations have been performed to study slurry annular cuttings transportation. Such studies are based on field or laboratory test data, numerical simulations or other methods. Although field testing is the most valuable method to study cuttings transportation, it is both costly and time consuming and therefore field tests have often been restricted to a small number of studies. For example, Matousek (1996) performed tests with a 10km long pipeline.

A flow loop simulation is an alternative experimental laboratory method but its results need to be scaled up to the applicable field size. For instance, Doron et al. (1987) performed an experimental study of slurry transport in a horizontal pipe and used laboratory test results to calibrate the computer simulated models.

In numerical simulation, the domain of interest is divided into smaller portions or grids and the equations are solved for each grid. Two main governing continuity and momentum equations are combined with the constitutive equations. Based on the assumptions all equations are solved together to find the results.

In layer modelling the transporting conduit is divided into two or three sections, depending on type of the model, to simulate the occurrence of different layers. Initially, a two-layer model was introduced by Doron et al. (1987) which was later extended to a three-layer modelling (Doron & Barnea, 1993) where a bottom stationary bed layer, a middle moving bed layer and a top suspended layer were defined. Computational fluid dynamics (CFD) is a computer-aided technique which is widely used for simulation purposes. The numerical simulation in this study focuses on CFD simulations of cuttings transport in minex drilling.

In addition to field and experimental tests and numerical simulations, several correlations have been proposed by researchers in which the parameters governing the process of cuttings transportation are grouped together (Sorgun, 2010). Dimensional analysis is used to check the validity of an equation in terms of the units based on the Buckingham-π Theorem (Buckingham, 1914). Artificial neural network is another technique in which the input data is connected to the output data through functions and weights. The objective of this method is to find these weights and functions in a way that yields the output results as close as possible to the actual results. Ozbayoglu et al. (2002) used least square regression and neural network method to determine the cuttings bed thickness in horizontal and deviated wells. They encapsulated the parameters into dimensionless groups. The following dimensionless parameters had been defined:

$$\pi_1 = C_c,\ \pi_2 = \alpha,\ \pi_3 = \frac{A_{bed}}{A_{ann}},\ \pi_4 = \frac{\rho v d}{\mu} = \mathrm{Re},\ \text{and}\ \pi_5 = \frac{gd}{v^2} = \frac{1}{\mathrm{Fr}}$$

where,

C_c = volumetric cuttings concentration,

α = hole inclination,

A_{bed} = area of the formed cuttings bed,

A_{ann} = cross sectional area of the annulus,

ρ = density of the drilling fluid,

v = drilling fluid velocity,

d = hydraulic diameter,

μ = drilling fluid viscosity,

Re = Reynolds Number, and

Fr = Froude Number.

Then, the following equation has been defined based on the above parameters:

$$\frac{A_{bed}}{A_{ann}} = k_1 (C_c)^{k_2} (\mathrm{Re})^{k_3} (\mathrm{Fr})^{k_4} .$$

Ozbayoglu et al. (2002) used the least square fitting method to fit an equation over the experimental data and determine the *k* values (constants). In addition they developed a neural network fitting while the inputs are those parameters in the parentheses and the output is the dimensionless value of A_{bed}/A_{ann}.

In this study, a flow loop is designed and built to simulate transportation of cuttings inside the annular volume between an inner tube (CT) and outer tube (borehole wall). The process was simulated numerically to calibrate the model and then it was used to perform several sensitivity analyses to investigate the effect of various parameters influencing cuttings transport.

Before studying the aspects of annular cuttings transportation, it is important to understand the basics of fluid flow of a single liquid phase in the annulus space. This is briefly explained in the subsequent section.

2.5.1 Annular fluid flow

In this section the important models proposed for fluid flow simulations, in particular APL estimation are discussed. These include analytical models, numerical simulations and experimental studies.

In order to determine the pressure loss, fluid rheology needs to be identified first. This is then followed by determining whether the flow regime is laminar, transitional or turbulent. Using proposed friction factors it is possible to estimate the pressure loss inside the annulus. Detailed procedure for pressure drop calculations can be found in Zamora et al. (2005) which is similar to the API RP 13D standard for hydraulics in the oil industry. A brief review of this is given below.

Fluid rheological models

To determine the fluid flow characteristics, one of the major elements is the rheological properties of the drilling fluid. Many 2, 3, 4 and 5 parameter

mathematical models have been proposed to fit the experimental shear rate (γ) - shear stress (τ) relationship. Amongst these models, Bingham Plastic model (Bingham, 1922):

$$\tau = \tau_y + \mu_B \gamma ,$$

and Power Law (PL) model (Ostwald, 1929):

$$\tau = k\gamma^n ,$$

are the mostly used models. In Bingham model τ_y and μ are known as yield stress and plastic viscosity and are derived from measurements using a viscometer. k is the flow consistency and n is the flow behaviour index.

The standard American Petroleum Institute (API) methods for drilling fluid rheology and hydraulics often assume either a Power Law or a Bingham Plastic model but the Power Law model underestimates frictional pressure drops while the Bingham Plastic model overestimates. In reality, most drilling muds correspond much more closely to the Herschel-Bulkley (HB) (1926) rheological model which is a general form of Bingham and Power Law model as:

$$\tau = \tau_y + k\gamma^n .$$

Figure 2.2 shows the schematic illustration of the three models mentioned above.

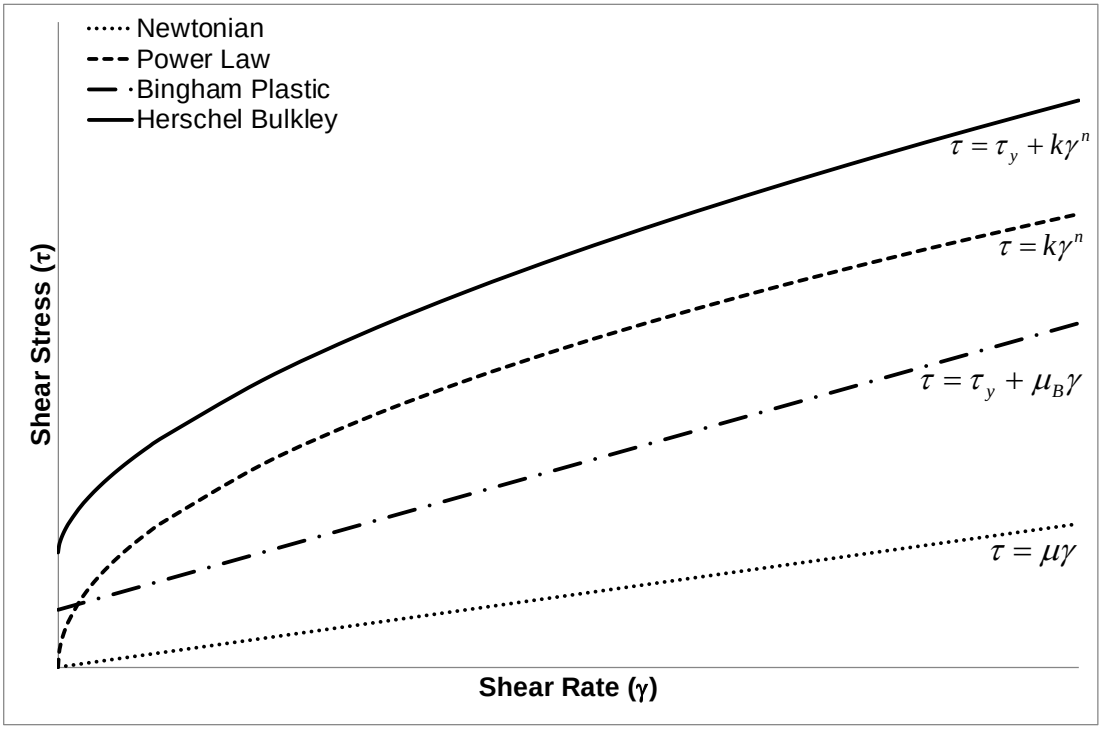

Figure 2.2 Illustration of mostly used rheological models for drilling fluids

Robertson-Stiff (1976) presented a three parameter model as:

$$\tau = C_1\left(C_2 + \gamma\right)^{C_3}.$$

This model is similar to the Power Law model but presents a yield strength value similar to the HB model. This model is not as popular as the other three models. It is to be noted that four and five parameters models are also available but their applications are limited in O&G industry.

Most of the drilling fluids used in drilling O&G wells show yield stress in their rheology, hence the Power Law model cannot be a good representative for very low shear rates. With a similar reason and that the HB is a general form of the power low model it can be said that theses rheological models may not fit well to the experimental data at low shear rate values.

In some instances it appears that defining the three parameters of HB's model results in a negative yield stress value; as for example the results of numerical analysis proposed by Hemphill et al. (1993). Kelessidis et al. (2006) performed an extensive literature review and offered an iterative method using the Fibonacci golden section method to determine a valid yield stress value.

Notably, when a rheological model changes to incorporate more parameters it becomes more computationally expensive but a better fit over the experimental data is obtained. In this research the HB model to determine fluid rheology is applied.

Frictional pressure loss

Several equations have been developed to determine the annular frictional pressure loss. Due to the complexity to develop pressure drop formulae for annulus geometry by solving rheological and equilibrium equations simultaneously, it is a common approach to simulate the geometry with a slot, using two parallel planes. This generates a simpler model that offers reasonably accurate results; especially when the annulus diameters ratio (outer diameter of the inner pipe divided by the hole diameter) is greater than 0.3 (Bourgoyne et al., 1986; Fordham et al., 1991; Founargiotakis et al., 2008).

The models developed for pressure drop estimation consider different flow regimes, fluid rheology model, pipe eccentricity and pipe rotation. For example, for HB fluids under a laminar flow regime Fordham et al. (1991) developed a semi analytical equation and Kelessidis et al. (2006) developed an analytical solution; which was extended by Founargiotakis et al. (2008) to allow the additional consideration of transitional and turbulent fluid flow regimes.

In API recommended practice (RP) 13D, the HB model was chosen as the main rheology model but due to the complexity of the equations the PL model was used for pressure loss calculations. To avoid confusion between HB and PL model parameters, PL parameters are shown with "p" subscripts (n_p, k_p). The following pressure loss equation is suggested by the API to be used for either a pipe or an annular section:

$$\Delta P = 1.076 \times 10^{-5} \frac{\rho v^2 f L}{d_{hyd}} \tag{2.1}$$

where,

ΔP = frictional pressure loss in a section in *psi*,

ρ = density of the flowing media in lb_m / gal,

v = mean velocity in $ft/\min$,

f = Fanning friction factor and to avoid confusion it is worth mentioning that Fanning friction factor is one-fourth of Darcy-Weisbach friction factor,

L = length of the section in *ft*, and

d_{hyd} = hydraulic diameter of the flowing conduit.

In Equation (2.1) four out of five of the parameters in the right hand side are easy to determine but the value of friction factor first requires the flow regime to be determined.

The flow regime is identified using the Reynolds number (Re): if this value is less than a certain threshold the flow is laminar otherwise it is turbulent. In laminar flow the fluid particles are moving in streamlines (parallel layers) without disturbance. The following equation is used to determine the transition point between the laminar and turbulent regime:

$$\mathrm{Re}_c = 3470 - 1370n, \tag{2.2}$$

where Re_c is the critical Reynolds number. Equation (2.2) shows that the transition boundary is only a single point. However, Equations (3.7) and (3.8) in Chapter 3 demonstrate that the conversion from laminar to turbulent flow does not occur sharply and a transition zone arises in between.

The following equation is the generalized Reynolds number that can be used for both pipe and annuli:

$$\mathrm{Re} = \frac{\rho v^2}{19.36\tau_w}. \tag{2.3}$$

In this equation τ_w is the wall shear stress in $lb_f/\left(100\,ft^2\right)$ and it is calculated using the following equation; that is again applicable to both pipe and annulus:

$$\tau_w = 1.066\left(\left(\frac{4-\alpha}{3-\alpha}\right)^n \tau_y + k\cdot {\gamma_w}^n\right). \tag{2.4}$$

However the value of α for pipe and annulus is 0 and 1, respectively. The only unknown in this equation is the wall shear rate, γ_w, that can be calculated using the following equation:

$$\gamma_w = \frac{1.6Gv}{d_{hyd}}. \tag{2.5}$$

The rheological properties of the drilling mud are measured with an oil field viscometer. Therefore to equate the measured results to the wall shear rate, a geometry factor *G* is applied. It is defined as the ratio of the well geometry shear rate correction, B_a, to the field viscometer shear rate correction, B_x:

$$\begin{aligned} G &= \frac{B_a}{B_x} \\ B_a &= \left[\frac{(3-\alpha)n+1}{(4-\alpha)n}\right]\left[1+\frac{\alpha}{2}\right] \\ B_x &= \left[\frac{x^{2/n_p}}{n_p x^2}\right]\left[\frac{x^2-1}{x^{2/n_p}-1}\right] \approx 1 \end{aligned} \tag{2.6}$$

The value of *x* depends on the viscometer, e.g. for a standard bob/sleeve combination R1B1, $x = 1.0678$. Starting from Equation (2.6) and then (2.5) and (2.4) the Reynolds number is finally calculated with Equation (2.3). Then Equation (2.7) can be used to determine the friction factor for the particular flow.

$$f = \left({f_{lam}}^{12} + \left({f_{trans}}^{-8} + {f_{turb}}^{-8} \right)^{-12/8} \right)^{1/12} \tag{2.7}$$

where,

$$\begin{aligned} f_{lam} &= \frac{16}{\mathrm{Re}}, \\ f_{trans} &= \frac{16\,\mathrm{Re}}{{\mathrm{Re}_c}^2}, \end{aligned} \tag{2.8}$$

$$f_{turb} = \frac{0.02\log_{10}(n_p) + 0.0786}{\mathrm{Re}^{(0.25-0.143\log_{10}(n_p))}}.$$

Since the value of friction factor is calculated from above equations, it is possible to determine frictional pressure loss from Equation (2.1).

As shown in Equation (2.8), no analytical solutions are available for turbulent flow. Instead, correlations developed based on experimental tests have been presented for modelling the turbulent flow friction factor.

Although this method is the standard method in the O&G industry, in this study a newer and more accurate method developed by Kelessidis et al. (2006) and Founargiotakis et al. (2008) is applied to determine the pressure loss changes due to existence of fine particles in the drilling mud. This is discussed in detail in section 3.4 in the next chapter.

2.5.2 Cuttings transport

To understand the cuttings transport phenomena as a general concept, it is crucial to know about the key elements of the process. Assuming no chemical reaction between the solid and the liquid phase, a number of parameters affect the slurry transport (Doron & Barnea, 1993; Doron et al., 1987; Hyun et al., 2000; Kelessidis & Bandelis, 2004; Y. Li et al., 2007; Nguyen & Rahman, 1998):

- transporting media: pipe, or annulus;
- geometry of the transporting media: diameter sizes, roughness, inner pipe rotational speed, and eccentricity of the inner pipe in the annulus;
- conduit inclination: vertical, deviated, or horizontal;
- carrying fluid properties: density, and rheology;
- concentration of the solid in slurry;
- solid particle properties: density, shape, and size;
- solid/liquid interaction: slip velocity;
- solid/solid interaction in the bed layers;
- velocity (or flow rate) of the slurry;
- pressure and temperature; and
- time dependency of fluid flow: steady, transient.

Much research has been performed in studying cuttings transport in vertical O&G wells. This is probably because the collinear fluid velocity and the gravity force that act in opposite directions are easier to model and analyse. However, in directional

wells the gravitational force acts downward whereas the fluid velocity vector is aligned with the angle of the borehole wall. If the vertical component of the fluid flow cannot hold the cuttings in the flow stream the cuttings will fall out of suspension and collect on the low side of the borehole which may cause hole cleaning problems.

Improper hole cleaning problems may follow and cause (Y. Li et al., 2007; API RP 13D, 2010):

- reduced ROP,
- higher equivalent circulating densities (ECDs),
- increased fluid loss, formation fracture and loss of circulation,
- over-pull on connections,
- increased drag and torque,
- hole pack-off, and
- stuck pipe.

Cuttings bed formation in directional and horizontal wells is difficult to rectify because the fluid velocity near the bore-hole wall is very low and eccentric pipe rotation or special drilling tools are needed to deter the accumulation of cuttings or break up the consolidated cuttings pile (Ramadan et al., 2003; Ramadan et al., 2005). It is important to remember that when drilling with CT there is no tube rotation except at the bottom-hole assembly and bit via a down-hole motor and poor hole cleaning is more likely to occur if one or more fluid parameters are incorrect.

Figure 2.3 shows the general mechanisms of hole cleaning in a wellbore with only two controlling parameters (different annular velocities and well inclinations) and defines five zones (A to E) that corresponds to vertical, inclined and horizontal wellbores with different annular velocity. It shows that increasing the wellbore inclination away from a vertical trajectory exacerbates cuttings transportation even under high annular velocity for deviated and horizontal wells (zone C) as the cuttings concentration becomes higher along the lower side of the hole. Reducing the fluid velocity aggravates this situation even more. This figure only provides a general schematic grasp of cuttings movement, therefore for specific cases appropriate analysis needs to be conducted.

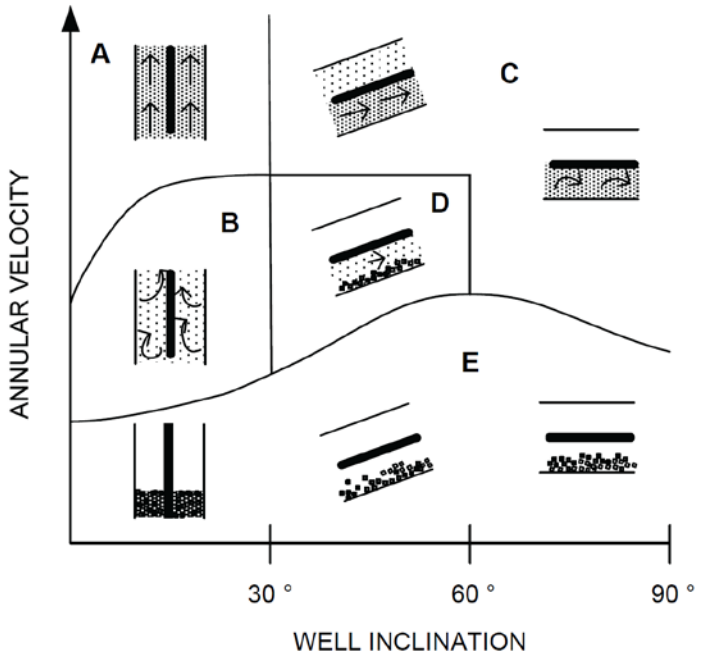

Key

A	Zone 1 - Efficient hole cleaning
B	Zone 2 - Slow cuttings removal
C	Zone 3 - Good hole cleaning with moving cuttings bed
D	Zone 4 - Some hole cleaning – cuttings bed formed
E	Zone 5 - No hole cleaning

Figure 2.3 The quality of cuttings transport against two controlling variables: annular velocity and well inclination (API RP 13D, 2010)

A directional well trajectory can be divided into three main categories section for which innumerable hole angle limits have been advanced. Arbitrarily:

- Vertical through low angle: 0°-30°,
- Critical angle: 30°-60°, and
- High angle through horizontal and up-dip: 60°-90° (API RP 13D, 2010).

Cuttings transport efficiency in vertical and low angle well geometries is typically modelled by using the difference between the upward annular fluid velocity and downward cuttings slip velocity. API RP 13D uses the procedure that was introduced by R. E. Walker and Mayes (1975) to find the net upward velocity which in mathematical terms is expressed by:

$$v_u = v_a - v_s \,. \tag{2.9}$$

where

v_a = annular fluid velocity which is determined directly from mud flow rate divided by the annular cross sectional area,

v_u = net upward cuttings velocity and it is less than the annular fluid velocity, and

v_s = difference between the above two velocities and is called slip velocity.

To analyse the cuttings transportation efficiency in near vertical wellbores a term called transport ratio, R_t, is defined:

$$R_t = \frac{v_u}{v_a} \tag{2.10}$$

In vertical holes cuttings are transported in suspension mode. However in directional and horizontal holes different cuttings transportation mechanisms occur and they are explained in the following section.

2.6 Patterns of cuttings transportation

Different flow profiles or patterns for cuttings movement are formed in the annulus of a well and they depend upon several controlling factors. The following profiles are depicted schematically in Figure 2.4 where a yellow background indicates the drill string and the white background shows the annulus between the string and walls of the bore-hole; the latter being represented by two black lines. They have been reported by different investigator (Ford et al., 1990; Hyun et al., 2000; Kelessidis & Bandelis, 2004; Nguyen & Rahman, 1998) as:

1. **Homogenous suspension** where all of the cuttings are dispersed uniformly throughout the annulus.
2. **Heterogeneous suspension** where the cuttings are in suspension but more occupy the lower side of the wellbore.
3. **Suspension and moving bed** where the cuttings are mainly transported on the lower side of the wellbore and an initial build-up of moving cuttings against the lower side of the borehole occurs.
4. **Moving bed** where all of the cuttings are moving but blanket the lower side of the wellbore.
5. **Moving and stationary beds** where a layer of cuttings against the lower side of the well is stationary and a layer of above the stationary cuttings is mobile.
6. **Dune movement**: this mode is the same as above but the cuttings are in cluster (see #6 in Figure 2.4). A cutting travels from downstream of the dune and after reaches to the front of the dune it settles down. This continuous particle movement causes the whole dune to move.

7. **Boycott movement** where in deviated wells especially at angles closer to vertical, the gravity effect forces the cuttings downward and the flow moves the cuttings upward. The cuttings close to the borehole wall slide downward due to a relatively lower localised fluid velocity. Cuttings closer to the centre of the annulus move upward relatively faster and cuttings between the two flow layers move at a median rate (Yassin et al., 1993). This phenomena was firstly mentioned by Boycott in 1920 when he realized that blood cells in inclined test tubes settle faster than in vertical ones (Boycott, 1920). The relative velocity of different layers of this mode are shown in #7 of Figure 2.4. Compared to the other profiles this one have not been mentioned much in the cuttings transportation literature in O&G industry. As an example, (Sharma, 1990) modelled the transportation of cuttings in the directional holes and realized that at certain flow velocities the particles close to the wall slide downward while the particles close to the main fluid stream transfer upward. In a specific case when the majority of the cuttings slide downward the profile is called sliding and this is a specific case of a general profile, i.e. Boycott profile. Sliding is a more common term in the O&G industry rather than the Boycott movement (Sifferman & Becker, 1992).
8. **Stationary bed** where especially in horizontal wells the fluid flow cannot carry the cuttings, all of them accumulate and no cuttings move.

Lower flow rates in the annulus space contribute to the formation of stationary layers which are not desirable and higher flow rates are required for improved cuttings transport without cuttings sag, settling and slumping. The only profiles which do not have any stationary sections are pattern #1-4 shown in Figure 2.4.

Higher flow rates are accompanied by higher pump pressures (all other variables unchanged) but a rig's or CTU's surface equipment may not be able to generate or accommodate such high pressures. Also higher pump pressures create higher down-hole ECDs which may exceed a formation's fracture gradient and high flow rates can create wash-outs in less consolidated formations.

As a boundary between unwanted scenarios #5-8 and acceptable scenarios #1-3 the minimum flow rate for scenario #4 is known as the Minimum Transportation Velocity (MTV) (Ford et al., 1990). Such a transition velocity reflects the minimum pump rate to prevent cuttings settlement for particular angled well bore trajectories. At mud flow velocities larger than MTV the cuttings transportation profile is moving

bed (mode #4) and below MTV some stationary particles accumulate at the lower side of the hole.

Ford et al. (1990) has performed set of experiments to determine the MTV and they showed the sensitivity of hole angle, inner tube rotation, fluid rheology and cuttings sizes. Figure 2.5 shows the MTV for particle range of 1.7-2mm where a non-rotating drill string is central in a cylindrical wellbore. In this figure the effect of the rheological properties are shown and it indicate that the water and high viscosity polymer fluids show better cuttings carrying capacity than the medium viscosity polymer fluids. In minex drilling applications the cuttings sizes covers a much wider range and majority of them are fine particles.

In O&G applications mixing of the cuttings while they are transported from the bottom of the hole to the surface is not as challenging as in minex. This is due to the diverse range of particle sizes and densities, they travel at different velocities to the surface. Since retrieval of quality cutting samples and the circulation of clean recycled drilling fluid (to allow accurate depth assignment and quantitative analyses) are crucial for a widespread adoption of MBHCTD the importance of excellent cuttings transport cannot be overstated. The depth of origin of the cuttings needs to be as trustworthy as the coring technique to avoid mixing otherwise the exact depth of the cuttings cannot be determined. This only occurs if the cuttings transport to the surface without any settlement in the annulus space. In addition if washout occurs the washed cuttings from the borehole wall will mix with the bit grinded cuttings. While this issue may be unlikely to happen across the hard rock formations, it can be the case when drilling at shallow depths into broken and fractured ground. Moreover, solid removal equipment at the surface needs to clean the mud completely in which when the mud recirculated to the wellbore does not contain any trace of solid particles, otherwise it may mislead the analysis. Therefore determination of MTV is of paramount importance in minex drilling to avoid mixing of cuttings particles and this is the main focus of this study.

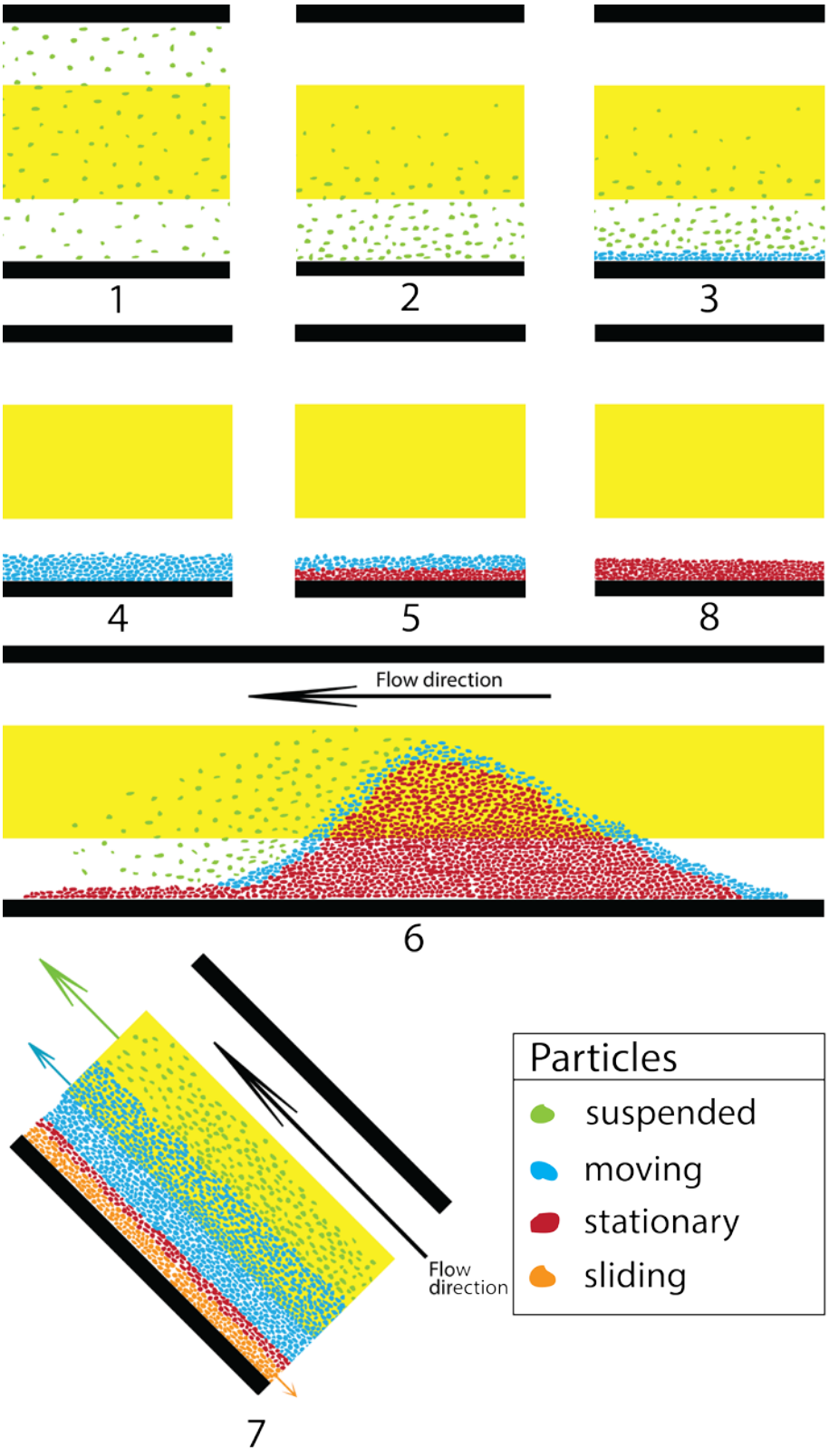

Modes of cuttings transportation

1. Homogenous suspension
2. Heterogeneous suspension
3. Suspension and moving bed
4. Moving bed
5. Moving/stationary beds
6. Dune movement
7. Boycott transportation
8. Stationary bed

Figure 2.4 Cuttings transportation profiles in the annulus space

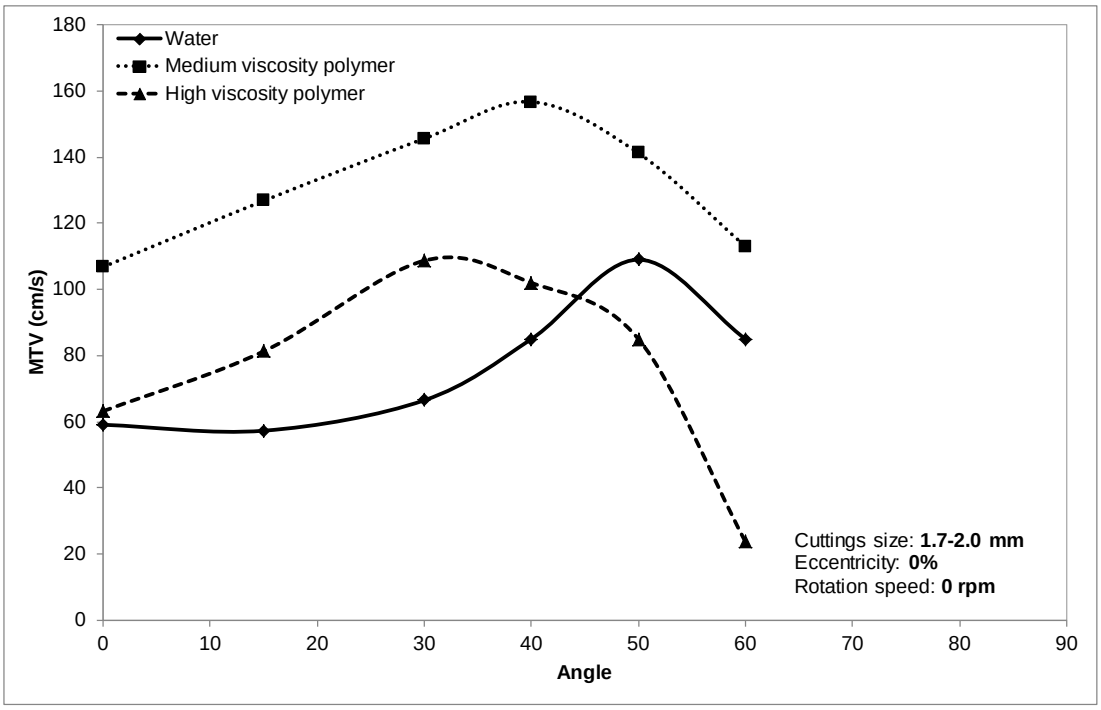

Figure 2.5 The effect of rheology on the MTV (Ford et al., 1990)

2.7 Factors controlling cuttings transportation

Formation of different transportation modes which was discussed in the previous section and efficient transportation of the cuttings depends not only on the annular velocity but also to the other factors. Investigators performed sensitivity analyses of controlling parameters in cuttings transportation and the followings are some of the reported outcomes:

2.7.1 Velocity or flow rate

This is inevitably the most important parameter because increasing the fluid flow velocity produces more energy to carry the cuttings (Doron & Barnea, 1993; Doron et al., 1987; Hyun et al., 2000; Kelessidis & Bandelis, 2004; Y. Li et al., 2007; Nguyen & Rahman, 1998).

2.7.2 Drilling fluid rheology

There is no single recommendation for the best type of the drilling fluid and its rheological properties that would be beneficial for cuttings transportation. Nguyen and Rahman (1998) in agreement with experimental work by Peden et al. (1990) reported that higher viscosity muds result in a better cuttings transport performance in horizontal wells. Also Tomren et al. (1986) mentioned that in a particular flow

regime, fluids with higher viscosity perform better in terms of cuttings transport. In many hard rock minex wells a high annulus pressure loss is not an issue and high viscosity fluids with high yield point (YP) to plastic viscosity (PV) ratio are recommended (API RP 13D, 2010). Yet, for MBHCTD the use of high viscosity fluids is not possible as the down-hole hammer and/or motor restrictions and high pressure losses as noted before are limiting factors.

However a contradictory view from Hyun et al. (2002) was that a less viscous fluid in turbulent flow regime resulted in better cuttings transport performances. Pilehvari et al. (1999) recommended that turbulent flow regime in horizontal and highly deviated wells, regardless of the viscosity of the fluid, will lead to good cuttings transport. Additionally, Leising and Walton (2002a) in their review of hole cleaning problems and solution in CTD suggested that using low viscosity fluid in turbulent flow provides effective enhancement in cutting transport than high viscosity fluids in laminar flow. Earlier Brown et al. (1989) and later Y. Li et al. (2007) had concluded that water is the best fluid for cuttings displacements in horizontal wells assuming that the pump would be able to provide the high flow rate required.

As noted in the previous section high pump rates are accompanied by high pressures which the rig or CTU and/or well design may not be able to accommodate. In cases where turbulent flow is not applicable, muds with strong suspension properties or high LSRV (low-shear-rate-viscosity) fluids are suggested (API RP 13D, 2010). With specific regard for MBHCTD a proposal by Leising and Walton (2002a) recommended the use of bio-polymers fluids instead of water because water does not have sufficient viscosity; especially as most CTUs cannot accept high pump pressures associated with high flow rate.

2.7.3 Drilling fluid density (mud weight)

Heavier weighted muds have an increased buoyancy factor relative to other less dense fluids which assists with an improved suspension of the cuttings. Accordingly Nguyen and Rahman (1998) stated that fluid density has a considerable effect on cuttings transport in horizontal wells and higher fluid densities can result in reduction of the bed thickness whereas Y. Li et al. (2007) showed that increasing the mud weight has a small to moderate decrease on cutting beds thickness. Kelessidis and

Bandelis (2004) suggest that increasing fluid velocity and mud weight is the best practice for efficient cuttings transport.

2.7.4 Cuttings density

In the O&G industry the density of sand, shale, limestone and dolomite drill solids usually ranges between 2.2-2.9SG (18.35-24.2ppg) whilst in the mineral industry ore bodies can provide drill cuttings such as gold with a density of 19.3SG (161ppg). Cuttings with higher densities will have faster slip velocities and can therefore be expected to sag, settle and slump faster than cuttings with lower densities.

2.7.5 Cuttings size

In minex drilling applications the cuttings sizes cover a much wider range than those from O&G wells and the majority are usually fine particles. Y. Li et al. (2007) concluded that particle diameter has a very small effect on bed thickness despite S. Walker and Li (2000) who earlier showed that the cuttings size has significant effects on the transportation. Others have advocated large cuttings transport is mainly driven by the fluid flow rate whereas pipe rotation and fluid rheology are the key factors in controlling small cuttings transport (Kelin et al., 2013).

2.7.6 Cuttings concentration

Increasing cuttings concentration in the drilling fluid will be dictated by the ROP. If the cuttings transport cannot clean the hole for a given ROP the cuttings will accumulate, overload the annulus, eventually pack-off and either cause loss circulation and/or stuck pipe.

2.7.7 Wellbore eccentricity

A drill string or CT would be said to be concentric and 0% eccentric if it is perfectly centred in the outer pipe or hole. Eccentricity affect the cutting transport efficiency negatively and higher pump rates are usually required to sustain or improve the removal of cuttings. In an experiment performed by Kelessidis et al. (2007) a fully suspended layer occurred at 0.77m/s (152ft/min) and 1.61m/s (317ft/min) for concentric and fully eccentric annulus geometry, respectively.

2.7.8 Drill string rotation

Drill string rotation mechanically agitates the cuttings and contributes to the cuttings carrying capacity of a drilling fluid. However, only the BHA and bit below the down-hole motor rotate in MBHCTD and the CT above the motor does not. Reciprocating motion of a drill string or CT is another option but it is not as effective as pipe rotation. Therefore, in CTD where the pipe rotation is not available, reciprocating motion and increasing flow rate would help (API RP 13D, 2010).

Wellbore rugosity as well as wellbore and tubular roughness is other parameters that affect the cuttings transportation. Wellbore rugosity is a qualitative description of the borehole wall roughness which reflects the change in borehole diameter with depth. The term usually refers to such changes recorded by wire line logs such as calliper logging measurements that have a small depth of investigation (Schlumberger, 2014). These two parameters have not received much attention as of the other parameters listed above about the cuttings transportation.

In this study, the aim is to identify the important factors which control the cuttings transportation in the annulus of MBH drilled with CT. To do this both numerical simulations and laboratory experimental studies have been conducted. Accordingly a summary of similar studies, mainly for O&G applications, are reviewed in the following two sections; especially as they were used as a guide.

2.8 Numerical simulation of cuttings transport

Doron et al. (1987) introduced two-layer modelling of slurry flow in a pipe. In this model if a solid bed formed it was either a stationary or a moving bed. The model as Figure 2.6 shows was later extended to a three-layer model that included a stationary bed at the bottom, a moving bed in between and a suspended layer at the top (Doron & Barnea, 1993).

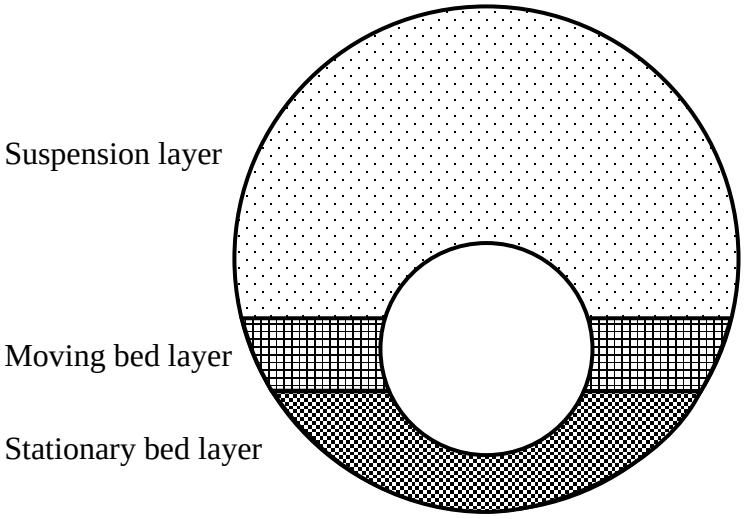

Figure 2.6 Cross section view of the annulus section with a 3-layer model (Nguyen & Rahman, 1998)

In this type of numerical simulation mass balance and momentum equations are solved to determine the height of each layer. In addition to these equations axillary equations such as turbulent diffusion, drag forces, gravitational force, lift forces, shear stresses between the layers, particle deposition rate and slip velocity are required to prepare a realistic model.

Such models then have been used for O&G applications by many investigators. One of the first applications was cuttings transportation in highly deviated holes by Nguyen and Rahman (1996). Ramadan et al. (2005) then developed a three-layer model to determine the transportation rate of the solid particles in deviated holes.

In the meantime Hyun et al. (2000) developed a cuttings transportation model for horizontal CTD. A summary of some numerical simulation studies carried out on the slurry transportation is given in Table 2.2.

Table 2.2 Some laboratory and numerical simulation studies and data on slurry flow in pipe and annulus space

reference	investigation method	V(m/s) or Q (l/s)	hole ID (mm)	inner pipe OD (mm)	particle specific gravity	particle size (mm)
(Doron et al., 1987)	num, lab, comp	0-3.5m/s	50	-----	1.24	3
(Nguyen & Rahman, 1998)	num, comp	0-1.22m/s	127	48	2.62	6.35
(Hyun et al., 2000)	num, comp	0-1.83m/s	127	48	2.62	6.35
(Kelessidis & Mpandelis, 2004)	lab	NA	70	40	2.59	2
(Ramadan et al., 2003)	num, lab	1.5-4.2l/s	70	-----	2.6	0.125-5.5
(Bandelis & Kelessidis, 2006)	lab	NA	NA	NA	NA	NA
(Y. Li et al., 2007)	num, comp	1.7-38l/s	203	114	2.6, 2.7	1-24
(Kelessidis et al., 2007)	lab	0-2.32m/s	70	50	NA	2
(Eesa & Barigou, 2009)	CFD, lab	0.025-0.125m/s	45	-----	1.02	2-9
(Al-Kayiem et al., 2010)	CFD	38-57l/s	250	127	2.57	2.54, 4.45, 7
(Xiao-le et al., 2010)	num	60, 80l/s	NA	NA	NA	NA

Abbreviations: num: numerical; comp: compared with others' models. In some cases where the inner pipe OD is shown as ---- it is meant that the experiments where performed for the pipe instead of the annulus.

Figure 2.7 shows the effect of annular velocity on the bed thicknesses, volumetric cuttings concentration and pressure loss in the annulus. From Nguyen and Rahman's (1996) 3-layer model for the cuttings transportation in the horizontal wells there is only a stationary layer of cuttings at the lower side of the wellbore when the flow rate is low. Increasing the flow rate agitates the upper part of the stationary layer and a moving layer forms on top of the stationary layer to give a 2-layer section. This occurs in section #1 in Figure 2.7.

Under further increasing fluid velocity the cuttings are lifted from the moving bed layer and move into suspension in the drilling fluid under an eddy diffusion mechanism (section #2 in Figure 2.7). This force is only enough to hold the suspended particles close to moving bed layer but as the flow energy is increased the eddy currents have more energy to lift and disperse the cuttings throughout the upper layer. Increasing the flow rate causes the erosion of the stationary layer (section #3 in Figure 2.7). At still higher flow rates only the moving bed layer and suspension layer exists and gradual increase in the flow rate erode the moving bed layer and increase the volume of particles in the suspension layer (section #4 in Figure 2.7). At section #5 all the particles are in the suspension layer.

Both sections #2 and 3 have three layers but the difference is that at the verge of boundary, stationary layer at the bottom moves as a block because the friction between the bottom layer of particles in this layer and the wellbore is less than the slip point friction force. Nguyen and Rahman (1996) called this point MTV based on the concept introduced by Ford et al. (1990) which in the Figure 2.7 is 1m/s (3.3ft/s).

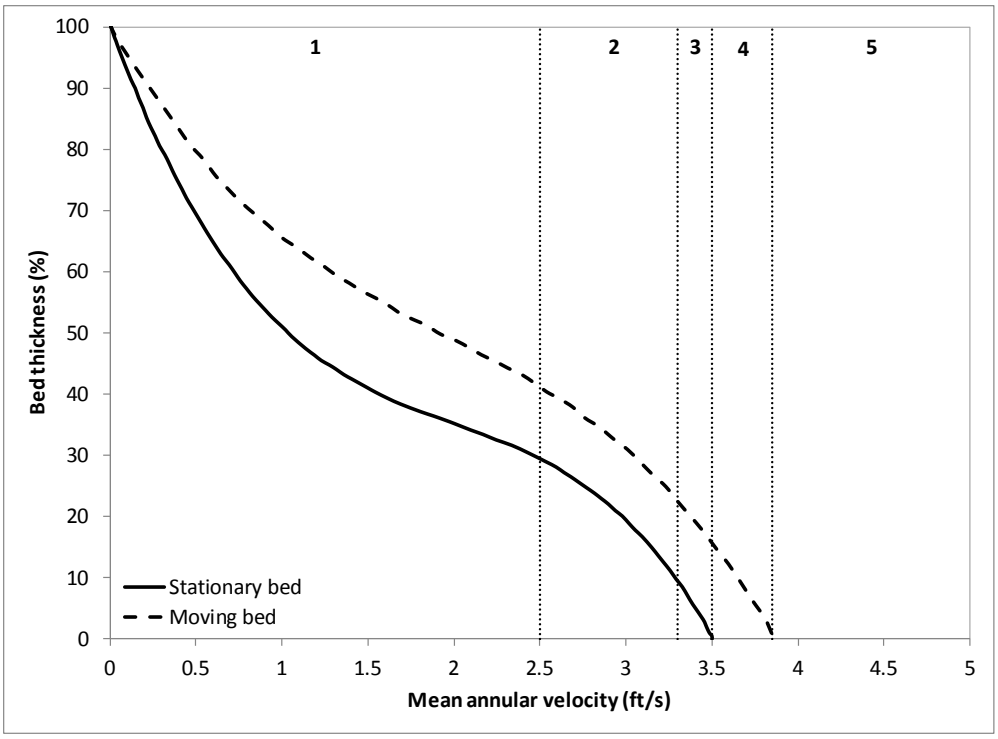

Figure 2.7 The effect of annular velocity on bed thickness, cutting concentration and pressure loss (Nguyen & Rahman, 1998)

2.8.1 Computational fluid dynamics studies

Computational fluid dynamics (CFD) has been used in many areas of science and even in the O&G industry but its application for the purpose of cuttings transportation has not been utilized very much.

For numerical simulation of layered models the governing equations such as mass, momentum and force balance equations are applied to each layer and each phase. In contrast, CFD requires the governing equations to be applied to small volumetric grids. Therefore CFD is a slower and more expensive method to apply to cuttings transport than layered modelling.

One of the first cuttings transport applications of CFD was probably introduced by Ali (2002). He conducted a sensitivity analysis of the effective parameters controlling the cuttings transportation in vertical and horizontal wells. The annulus configuration was 100m (328ft) section of 3.5in/12in (9cm/30.5cm), the drilling fluid density used was in the range of 8.34-15ppg (1.0-1.8SG) and the particles range was 0.1in-0.275in (2.5mm-7mm). Later, Al-Kayiem et al. (2010) used a CFD approach to model cuttings transportation in vertical and nearly vertical annuli that had widths of 5in /9.8in (127mm/250mm). They determined the sensitivity of different contributing factors in the cuttings transportation. For example Figure 2.8 shows the

sensitivity of cuttings sizes on the efficiency of the transportation. They found that smaller cuttings of about 0.1in (2.54mm) are easier to transport than larger cuttings, all other parameters unchanged. Approximately speaking the 0.1in (2.54mm) cuttings is close to the largest size cuttings considered in this study.

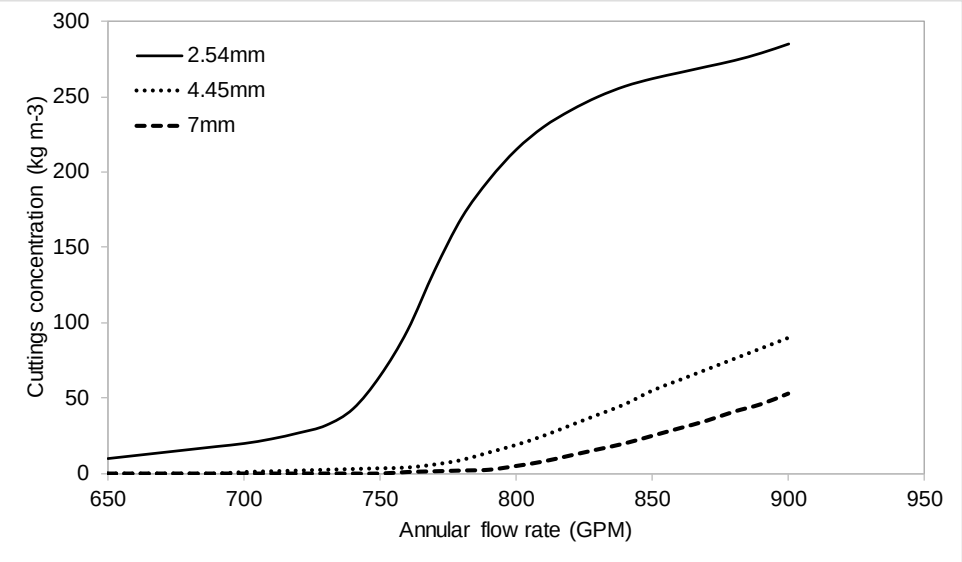

Figure 2.8 Cuttings transport efficiency at different cuttings sizes (Al-Kayiem et al., 2010)

Ali (2002) with water in turbulence and Al-Kayiem et al. (2010) with Power Law drilling mud in laminar flow have both used discrete phase model and steady state approach for their simulations but the use of large grid sizes did not permit an accurate determination of the local velocity of cuttings. They provided an efficiency of cuttings transportation without referring to the actual modes of transportations.

Osgouei et al. (2013) took a Lagrangian tracking approach for the solid particles in the water as a Newtonian drilling fluid in a horizontal configuration. The annular width was 1.85in/2.91in (47mm/74mm) and the inner pipe was located off-centre with an eccentricity of 0.623. In their model they presented the cuttings concentration in the annulus at different flow rates.

Slurry transportation along a pipe has been an area of research for many years. CFD has been one of the methods used with the aim being to transport the particles usually at high concentrations (up to 50% v/v) in mostly a suspension mode with high flow velocities (Lahiri & Ghanta, 2010a, 2010b; Nabil et al., 2013).

In such types of CFD simulations Eulerian-Eulerian approach is used where the solid phase is modelled as continuum, i.e. same as liquid. This is the approach used to investigate its suitability for the applications referred to this study.

The simulations of cuttings transportation related to O&G well drilling mainly consider both larger holes and annuli than those used in minex boreholes. In addition, mixing of the particles needs to be avoided in the annulus to avoid misleading interpretation of cuttings movement in the wellbore when it is for mining applications. To promote MBHCTD, the essential requirement of efficient cuttings transportation has been mentioned and the MTV needs to be known. In this study the MTV is determined by CFD numerical simulation using ANSYS Fluent version 14.0 software.

2.9 Experimental work

Performing physical simulations of cuttings transport in the laboratory with a flow loop is advantageous as it allows validation of numerically simulated models. Once a numerical simulator is validated against laboratory tests several sensitivity analyses can be performed in order to study the effect of various parameters for cuttings transportation.

Many fluid flow loops are designed to simulate single or multiphase flow behaviour through a conduit in which the continuous phase is either a liquid or gas. Compared to actual field trails, laboratory scale experiments for studying flow behaviour are very useful as they are less costly and time consuming. Also model parameters can be controlled in a more convenient way when trying to determine the impact of their changes. A typical flow loop consists mainly of a pump to circulate liquid, compressor to pressurize and circulate the gas, a flow rate measurement unit, and pressure transducers to measure the pressure.

Many fluid flow loops have been designed and used in the past. One of the more advanced multiphase fluid flow loops primarily for O&G applications was developed at Tulsa University in 1998 as a part of a US$5.9 million project. The Advanced Cuttings Transport Facilities (ACTF) is pictured below (Figure 2.9) includes a drilling section of 23m long that can be adjusted to inclinations from 0 to 90 degrees (TUFFP, 2012; TUDRP, 2012).

Figure 2.9 The drilling section of the ACTF at an inclination of 25° (Miska et al., 2004)

Figure 2.9 shows a view of the ACTF flow loop assembly. This set up is at a pilot scale and expensive to run for simple fluid flow studies. Other fluid flow loops have been developed at smaller scales, an example of which is shown in Figure 2.10 for CTD applications, where:

1. Annulus
2. Measuring section
3. Tank
4. Agitator
5. Centrifugal pump
6. Flow meter
7. Pressure transducer
8. PC and data acquisition system.

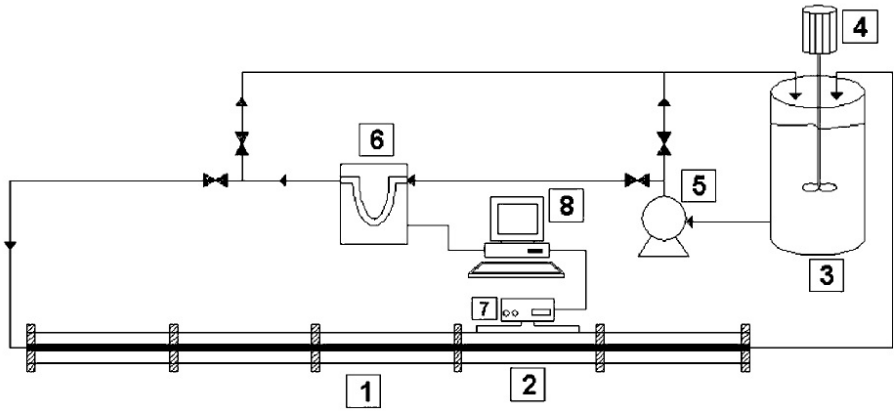

Figure 2.10 Schematic of a flow loop designed for O&G drilling applications (Kelessidis & Bandelis, 2004)

It is seen that all of the flow loops have a similar design concept but with certain capabilities for the required applications. Table 2.2 summarizes various literatures related to fluid flow and flow loop studies. These studies are those which modelled the transportation of the solid particles using a liquid, i.e. slurry transportation.

In Chapter 4 details are given for a new flow loop that was developed to enable MBH flow studies of fine to coarse cuttings for applications in minex drilling.

2.10 Summary

In this Chapter the adaptation and transformation of CTD technology from the O&G industry to minex is first discussed. A review of previous cuttings transportation investigations including numerical simulations and experimental studies is given and the differences with the current applications for hard rock drilling were noted.

Most of the available literature considers large annuli with relatively large cuttings sizes which are relevant to the O&G well drilling. However, this study aims at understanding wellbore cuttings transportation necessary for MBHCTD technology where the annulus is very small, and the cuttings cover a wider range of sizes.

Consequently both numerical simulations and laboratory experimental work has been carried out to such applications.

In the next chapter, the rheological properties and slurry behaviour in hard rock drilling will be discussed.

3 Rheological properties and slurry behaviour in hard rock drilling

As mentioned in the previous Chapter, the cuttings produced from impregnated diamond bit drilling are fairly fine powders. The effect of small size cuttings on the rheological properties of the drilling fluid is important and cannot be neglected. This aspect is investigated and presented in this Chapter through laboratory analyses of fluid rheological properties using drilled cuttings taken from a well at a mine site.

3.1 Introduction

The drilling fluid rheological properties need to be determined through laboratory tests in order to study the cuttings transport and pressure loss along the annulus. Existence of small size cuttings in hard rock drilling can affect drilling fluid rheological properties. For coarse cuttings, the viscosity of the slurry can be assumed to be very similar to the viscosity of the single fluid because the coarse particles do not affect the overall viscosity as much as fine cuttings (Doron & Barnea, 1996; Doron et al., 1987; Naganawa & Nomura, 2006; Xiao-le et al., 2010).

In oil and gas (O&G) well drilling, the concentration of the cuttings in the drilling fluid should be kept below 5% v/v (Albright et al., 2005; Kelessidis & Bandelis, 2004; Pigott, 1941). Also, the flow regime in the annulus section is ideally laminar and, in fact, coarser particles have been stated to dampen the turbulency of the flow (Fangary et al., 1997). Therefore, due to low cuttings concentration and low slurry velocities, the difference between the annular pressures exerted by the mud with and without cuttings is usually negligible. However, incorporation of small size hard rock cuttings (powder) in a drilling fluid can seriously affect its rheological properties. This is because smaller particles mix more readily – disperse and/or hydrate – with the drilling fluid and convert the single fluid into a cuttings slurry. As one consequence the pressure losses exhibited by the slurry increase.

For MBHCTD the pumping rate required to drive the down-hole motor is high and in a narrow annulus the slurry flow rate is high. Therefore the annular flow regime is usually transitional or turbulent.

In this study, rheological tests of drilling fluids with different concentrations of small size cuttings were carried out and the tests were followed by calculations of pressure losses.

3.2 Sample preparation procedure for rheological tests

Fine powder cuttings that were drilled whilst diamond coring at the Brukunga site in South Australia have been used in this study.

In order to produce dry samples from wet drilling muds several steps were undertaken in the laboratory. Different washing fluids were tested to find a cleaning fluid that provided the least change in cuttings size distribution between the wet to dry samples. The exact reproducible details of the cuttings sample preparation procedure are presented in Appendix A.

3.3 Rheological models of drilling fluid

In section 2.5.1 of Chapter 2 some of the commonly used rheological models were presented and it was explained that the Herschel-Bulkley (HB) model was chosen for the purpose of this study. For the three required unknown parameters Hemphill et al. (1993) developed a method to determine them from viscometer measurements. Their numerical iterative method was adopted as an API standard although in some cases it gives negative yield strengths.

Kelessidis et al. (2006) performed an extensive literature review of previous investigations in rheological models used in the O&G industry and proposed a golden search method to find the three unknown HB parameters. In their method yield stress value is limited between zero and the viscometer's minimum shear stress dial reading. The best value of yield stress in this range is calculated by using the golden search method. To analyse if the determined values fit accurately, different optimization methods are used such as the highest correlation coefficient, minimum sum of squared errors and best index value (BIV) closer to 1. Also, the following two middle values are calculated to start the optimization:

$$\tau_{y1} = \tau_{y\min} + 0.38197\left(\tau_{y\max} - \tau_{y\min}\right) \tag{3.1}$$

$$\tau_{y2} = \tau_{y\min} + 0.61803\left(\tau_{y\max} - \tau_{y\min}\right) \tag{3.2}$$

where,

$\tau_{y\min}$ and $\tau_{y\max}$ = lower and upper limit of the boundary, respectively, and

τ_{y1} and τ_{y2} = two middle values in the domain.

If τ_{y1} shows better fitting results than τ_{y2} then $\tau_{y\min}$ holds its previous value but $\tau_{y\max}$ is set to τ_{y2}. Alternatively, if τ_{y2} shows better fitting results than τ_{y1} then $\tau_{y\max}$ holds its previous value but $\tau_{y\min}$ is set to τ_{y1}. This process will continue until $\tau_{y\min}$ and $\tau_{y\max}$ converge on the same value. The resultant τ_y would be the best value to be considered for the yield stress.

For each τ_{y1} and τ_{y2}, the values of *n* and *k* are found using the following equation which is evaluated by taking logarithm of HB equation:

$$\log\left(\tau - \tau_y\right) = \log(k) + n\log(\gamma) \tag{3.3}$$

This equation indicates that the plot of $\log\left(\tau - \tau_y\right)$ versus $\log(\gamma)$ has an intersect and slope of $\log(k)$ and *n*, respectively.

The fitting function that was used in this study is BIV:

$$BIV = \frac{\sum_i \left(\hat{y}_i - \bar{y}\right)^2}{\sum_i \left(y_i - \bar{y}\right)^2} \tag{3.4}$$

Where, y_i s are the actual measured actual values of τ, $\hat{y}_i$ s are the predicted values of shear stresses and $\bar{y}$ is the average value of the measured parameters.

In O&G industry applications, only the fluid rheological properties are measured but the effects of cuttings on the rheological properties are not considered. The reason for this is that the cuttings are large in size and the flow regime is laminar as the flow velocity is low. But in this study the effect of cuttings on the rheological properties is observed and calculated because the cuttings produced in hard rock drilling using a diamond impregnated bit are of very small size and the annular flow velocity needs to be high to operate the downhole motor at high speed, which results in the flow regime being in a transition or turbulent.

The following section explains in detail the process of experiments conducted to determine the rheological properties of the muds used in this study.

3.3.1 Experimental rheology tests

In this section, the process of preparation of three different muds used in this study and the laboratory procedure to determine their rheological properties are explained. Also, the results are presented and discussed.

Mud preparation

Three mud systems with different compositions and properties were prepared for the purpose of this study; notably:

1. 22g Bentonite (Ausgel): and 3g low viscosity poly-anionic cellulose (AMC Pac L) in 1000ml tap water.
2. 1g regular viscosity poly-anionic cellulose (Ezee Pac R), 0.22g partially hydrolysed polyacrylamide (PHPA) (CR 650) and 2.17ml lubricant (Superlube) in 1000ml tap water.
3. 9ml Amine shale inhibitor (Shalehib NC), 2.7g Ezee PAC R and 3.56g PHPA (Clay Doctor) in 1000ml tap water.

The materials in the parenthesis are the trademarked names of products developed by Australian Mud Company (AMC); a wholly owned subsidiary of Imdex Limited.

A water based mud with a Marsh funnel viscosity (FV) within a range of 36-40sec/quart was proposed to have consistent practical viscosity. This is the medium viscosity range in the O&G well drilling. For this, 2 litres of water were poured in a beaker and then the proposed additives were added before measuring the funnel viscosity of the mud samples. The FV measured for the mud types #1, 2 and 3 were 39, 38 and 39sec/quart, respectively.

The pH of mud samples #1 and 2 was 8.9 and 8.26, respectively which is within the typical alkaline working pH range for water base drilling fluids. However, the pH of sample #3 was 4.8 (acidic) and therefore a few drops of caustic soda solution (NaOH) were added to increase the pH to 8.9.

Bentonite is a clay mineral that provides long lasting viscosity to these mud systems. Increasing its amount in the drilling mud also increases the gelation of the fluid and its resistance to flow (Bourgoyne et al., 1986).

Some polymers provide varying viscosity to the drilling fluid depending on the chain length of their monomer. If they consist of long chains (Pac R) they give higher viscosity whereas shorter chain polymers (Pac L) provide moderate viscosity. Additionally some polymers also give a mud varying degree of filtration control by

forming an impermeable filter cake against the surface of permeable sections in a borehole. Since most polymers are high performance synthetic additives a small amount of Pac/CMC on a weight-to-weight basis can provide a higher viscosity than native clays such as Bentonite (Mandal, 2012).

Partially hydrolysed polyacrylamide (PHPA) is a long-chain polymer that encapsulates particles in a drilling fluid. It prevents them from sticking together whilst simultaneously contributing to the viscosity. PHPA also acts as a “shale inhibitor” by preventing the hydration and/or dispersion (disintegration) of reactive drill solids (Mandal, 2012). However, it should remember that polymers shear degrade when being circulated through a rig’s surface equipment and around a wellbore and they need frequent replenishment to sustain their desired properties.

Lubricants reduce the frictional forces that drill strings experience and can provide easier movement of tubulars; especially in small diameter holes and/or directional wells. Shale inhibitors prevent shale and clay particles to interact with the mud. The Clay Doctor provides encapsulation properties without changing the viscosity (Mandal, 2012).

Each mud was contaminated with different 1-10% v/v concentration of cuttings. The rheology of seven samples for each mud was measured (21 samples in total) at ambient temperature and pressure with a 12 speed OFITE viscometer. The rheology results are shown in Table 3.1-a to c for the three muds, respectively.

Table 3.1 Dial reading results for mud samples

a: mud sample 1

	RPM	0%	1%	2%	3%	4%	5%	10%
rheology	600	27.8	27.9	27.3	29.5	29.6	30.7	41.3
	300	16.5	16.3	15.7	16.8	16.8	17.2	22.5
	200	12.7	12.7	12.4	12.9	12.9	13.2	16
	100	7	6.8	6.5	6.6	6.7	6.9	10.3
	60	4.8	4.7	4.5	4.5	4.4	4.7	7.1
	30	2.7	2.8	2.8	2.6	3	3.1	4.6
	20	2.4	2.5	2.4	2.3	2.7	2.8	4.1
	10	1.9	2	1.9	1.7	2.2	2.2	2.9
	6	1.8	1.9	1.7	1.5	2.1	2.1	2.6
	3	1.5	1.7	1.6	1.4	1.9	2	2.4
gelation	10min	1.3	1.6	1.9	1.8	2.7	2.8	10.2
	10sec	0.9	1.2	1	0.7	1.4	1.4	4.4

b: mud sample 2

	RPM	0%	1%	2%	3%	4%	5%	10%
rheology	600	13.1	12.1	12	12.8	13	14.4	19.8
	300	8.1	7.1	6.9	7.3	7.3	7.7	9.8
	200	6.2	5.3	5	5.2	5.3	5.5	6.7
	100	3.6	2.6	2.4	2.5	2.6	2.7	3.5
	60	2.2	1.8	1.7	1.8	1.8	1.7	2.4
	30	1.3	1.2	1.1	1	1	1.1	1.6
	20	1.2	0.8	0.7	0.8	0.8	0.8	1.3
	10	1	0.5	0.5	0.5	0.5	0.5	0.9
	6	0.8	0.4	0.4	0.5	0.5	0.4	0.6
	3	0.4	0.3	0.3	0.4	0.4	0.4	0.5
gelation	10min	0.1	0.1	0.1	0.2	0.2	0.2	2.2
	10sec	0.1	0.1	0.2	0.2	0.2	0.2	0.4

c: mud sample 3

	RPM	0%	1%	2%	3%	4%	5%	10%
rheology	600	28.7	29.2	28.9	30.1	31.3	32.9	49
	300	18.7	18.6	18.4	18.5	19.3	20.1	30.9
	200	14	14.1	13.7	13.6	14.4	15	23.3
	100	8.6	8.4	8.5	7.9	8.3	8.8	14.5
	60	6	5.6	5.8	5.3	5.5	5.9	10.4
	30	3.6	3.5	3.5	3	3.5	3.7	8
	20	2.7	2.7	2.8	2.2	2.7	3	5.9
	10	1.8	1.7	1.8	1.5	1.5	1.8	3.4
	6	1.4	1.3	1.4	1.2	1.1	1.4	2.4
	3	1	1.1	1.1	0.8	0.9	0.9	1.5
gelation	10min	0.4	0.3	0.4	0.5	0.3	0.5	0.9
	10sec	0.4	0.3	0.5	0.5	0.3	0.5	0.8

Lab data analysis

Taking a closer look at the data presented in Table 3.1-a to c indicates that at first there is a slight decrease in the dial readings due to an increase in cuttings

percentage. However, this trend quickly takes on an increasing trend. The initial decline observed is due to the small amount of cuttings in the mud which do not contribute much to plastic viscosity but partially break the clay-clay and clay-polymer interaction and gelation network in the mud. Further increasing the amount of solid causes more particle-particle frictional force, predominantly contributing to the plastic viscosity, which would cause the overall viscosity to increase.

Gelation of mud is related to the surface activity of the fine particles with the mud. Because mud 1 already has colloidal Bentonine particles it showed higher gelation compared to mud 2 and 3. However, mud 2 has PHPA and Superlube and mud 3 has shale inhibitor and PHPA, which partially prevent hydration and surface activity of the fine cuttings. This caused a flat gelation profile for mud 2 and 3 compared to a gradual increase in gelation for mud 1 from 0% to 5% cuttings concentration. As the cuttings concentration increased from 5% to 10% the gelation increased sharply for all the muds.

The HB model is applied to the measured laboratory data and the calculated rheological parameters are used in the next section to calculate system pressure drops as a function of changes in the cuttings concentration in three different muds. The golden search method was applied to determine the HB model constants (τ_y, K and n). Also, the BIV method was used to show the closeness of the fit. The results are shown in Table 3.2.

Table 3.2 Herschel-Bulkley parameters for all muds

	mud 1			mud 2			mud 3		
Cuttings Concentration	0%	5%	10%	0%	5%	10%	0%	5%	10%
$\tau_y(Pa)$	0.6369	0.887	1.0358	0.125	0.1478	0.2061	0.1312	0.1525	---
$n(-)$	0.8922	0.9864	0.898	0.7659	0.9858	0.9608	0.7053	0.7487	---
$k(Pa \cdot s^n)$	0.0286	0.0157	0.0395	0.033	0.0079	0.0125	0.1115	0.0935	---

In this Table the data corresponding to cuttings concentration of 10% v/v for mud #3 is not shown. This is due to the fact that by using the fitted curve the yield stress is estimated to be very low and not realistic. In real applications of hard rock drilling, the flow rate is very high, which corresponds to high shear rates. Therefore, the data used for pressure loss calculations in Section 3.4 corresponds to high shear rates where the curve shows a very good fit to the data and this ensures that it has no impact on presented results.

For example for 5% cuttings concentration in mud sample #3 the following equation shows the relationship between shear rate and shear stress:

$$\tau = 0.1525 + 0.0935\gamma^{0.7487} \tag{3.5}$$

Figure 3.1 shows the plots of shear rate - shear stress data and the best HB fit corresponding to mud sample #3 with three cuttings concentrations of 0%, 5% and 10% v/v. It is seen that at low shear rates the shear stress for 0% and 5% v/v cuttings are very close but are already separated from higher shear rates caused by the effect of increased cuttings content. This effect at a cuttings concentration of 10% v/v is very significant.

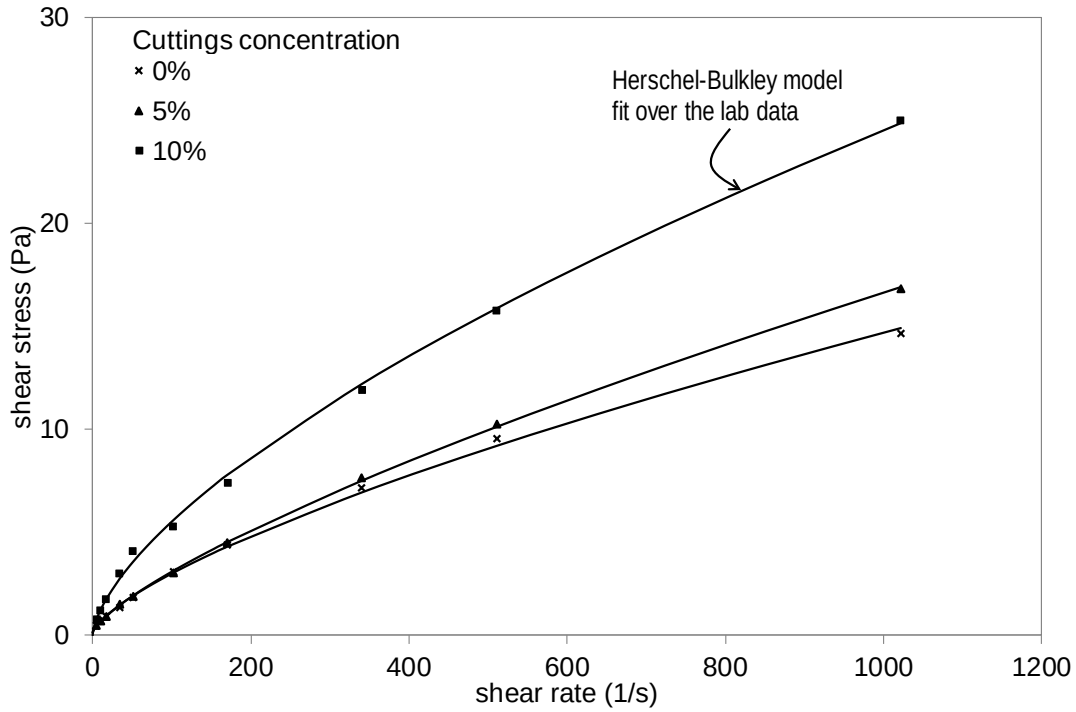

Figure 3.1 Herschel-Bulkley parameters for mud sample #3 at three different cuttings concentrations

Figure 3.2 and Figure 3.3 presents the shear rate - shear stress data corresponding to mud sample #1 and 2, respectively, with the same properties shown for mud #3 in Figure 3.1. It is seen from the figures that mud #3 have the highest rheological properties as it is shown higher shear stress at a constant shear rate comparing to the other muds and the less viscous mud is mud #2.

In Figure 3.3, which corresponds to mud #2, initially the rheological properties for 0% v/v are higher than 5% v/v, however, this trend changes at a shear rate of approximately $680\,s^{-1}$. Such decline occurs for mud #3 and 1 at lower concentrations but for mud #2 it continues to increase up to 5% v/v.

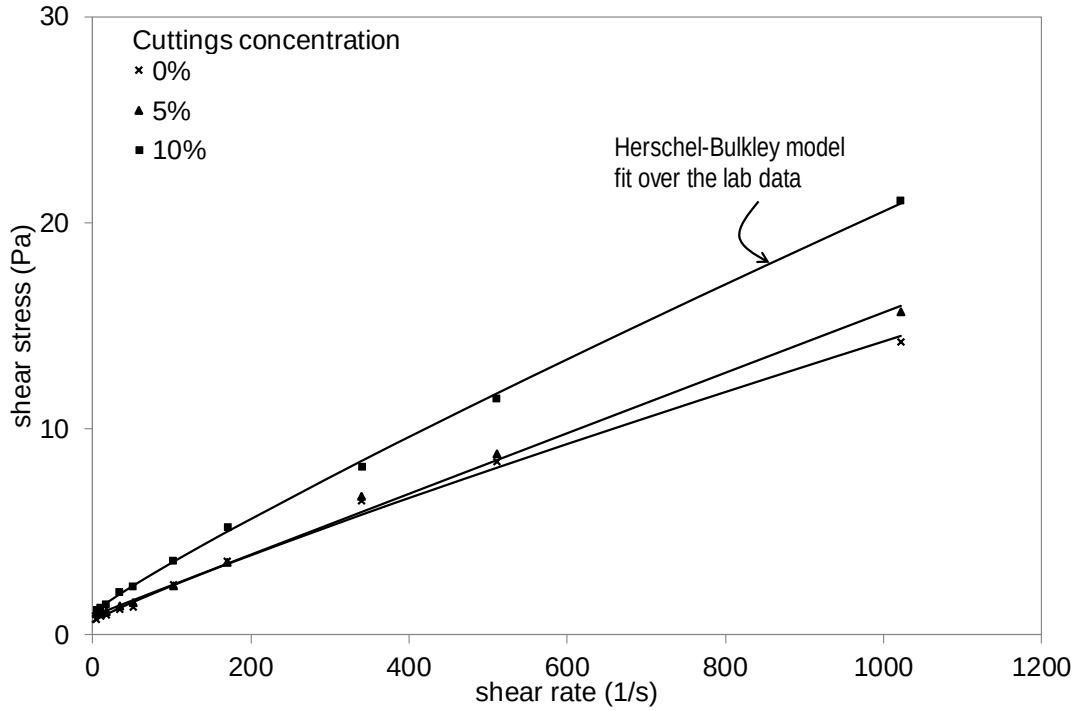

Figure 3.2 Herschel-Bulkley parameters for mud sample #1 at three different cuttings concentrations

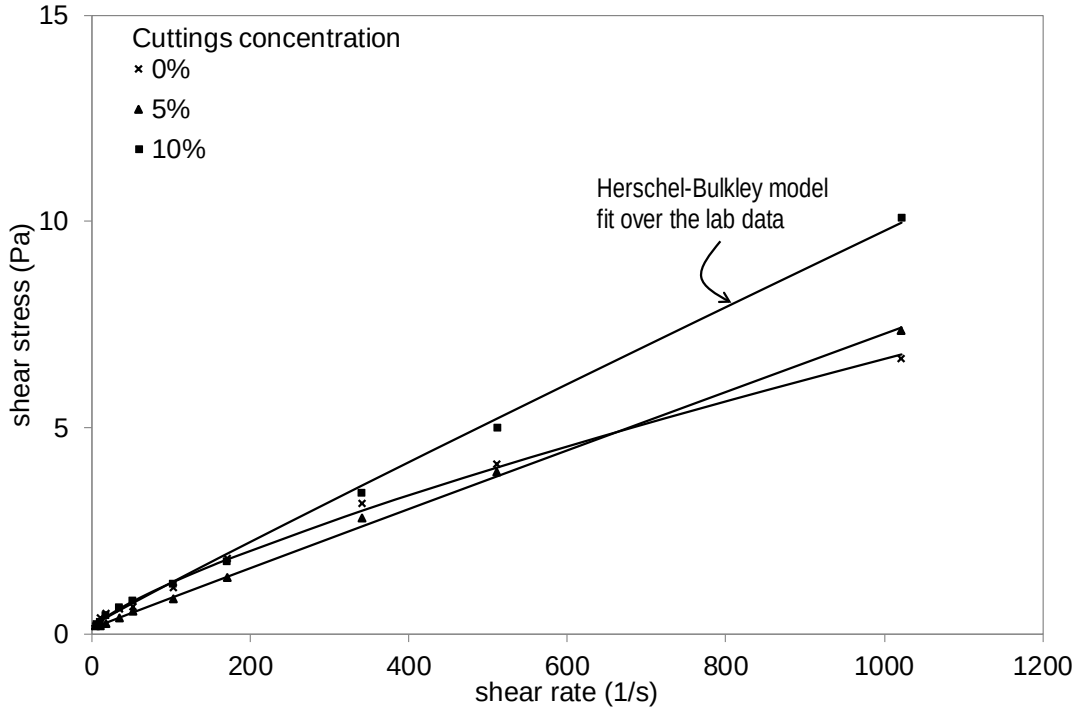

Figure 3.3 Herschel-Bulkley parameters for mud sample #2 at three different cuttings concentrations

While industry best practices endeavour to hold the cuttings concentrations at or less than a maximum 5% v/v in the mud, the calculations presented in the next section will indicate the pronounced effect of this volume of cuttings on a system's APLs.

3.4 Cuttings concentration effect on annular pressure losses

The API standard pressure loss calculation method has been introduced in section 2.5.1 of Chapter 2 however a more accurate method is used in this study to determine the pressure loss. Consequently, the pressure drop estimation formula considers two sets of equations. The rheology equations take into account the fluid properties whereas the field or equilibrium equations consider the effect of the shape of the flow channel (Kelessidis et al., 2006). For annulus space, the flow channel grid equations are complicated and therefore this study uses the common practice to approximate such geometry as an annulus section between two simple parallel planes (slot); especially when the annulus diameters ratio is greater than 0.3 (Bourgoyne et al., 1986; Fordham et al., 1991; Founargiotakis et al., 2008; Hanks, 1979; Kelessidis et al., 2011).

The developed models for pressure drop estimation consider different flow regimes (laminar, transition or turbulent), fluid rheology model (Bingham Plastic, Power Law or Herschel-Bulkley), pipe eccentricity and pipe rotation.

A vast amount of research has been performed to study annular fluid flow using analytical solutions, numerical simulations and experimental studies. Performing experimental simulations in the laboratory is essential to validate the results of analytical and numerical simulations. For example, Zamora et al. (2005) made a comparison of annulus pressure loss between the API standard model and field data. Laird (1957) proposed one of the initial fluid flow models that considered laminar flow of Bingham Plastic fluids for a concentric annulus geometry where he solved the governing fluid flow differential equations semi-analytically. Later on, other investigators (Hanks, 1979; Hussain & Sharif, 1997; Iyoho & Azar, 1981) improved the laminar fluid flow model with the help of analytical, semi-analytical and numerical methods in addition to laboratory experiments. However, no analytical solution for turbulent flow exists as unlike laminar flow it does not follow any specific streamlines and therefore analytical solutions cannot be easily developed for a turbulent flow. Instead, correlations developed based on experimental tests have been presented for modelling turbulent flows (Founargiotakis et al., 2008; Hartnett & Kostic, 1990; Sorgun et al., 2012).

In this study and to simulate CTD, the HB fluid rheological model is applied to a fluid carrying cuttings in a concentric annulus without pipe rotation.

Kelessidis et al. (2006) developed an analytical solution for laminar flow of HB rheological model in the annulus space considering slot approximation and proposed following equation:

$$q = \left(\frac{\Delta}{k}\right)^{m} \frac{2w(h/2)^{m+2}(1-\xi)^{m+1}}{(m+1)(m+2)}(\xi + m + 1) \tag{3.6}$$

Figure 3.4 presents a flowchart explaining the calculation steps to estimate the pressure loss based on Equation (3.6) on a trial and error basis. The only unknown in this solution is pressure loss per unit length ($\Delta = dP/dL$). However, the explicit formula for Δ is not available, so implicit solutions need to be used to find the results.

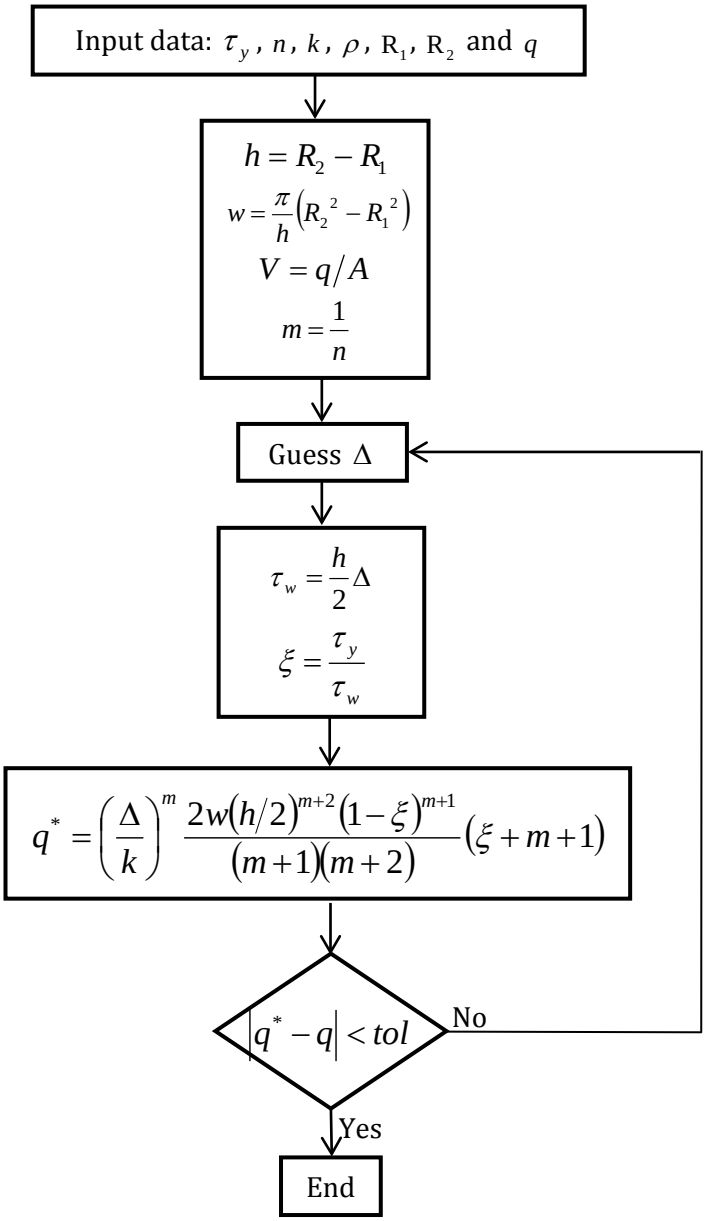

Figure 3.4 A flowchart to find the APL across a laminar flow regime for a HB fluid

Founargiotakis et al. (2008) proposed an empirical solution for annular pressure drop estimation of a HB fluid at the transition and turbulent flow. The key to the solution in their approach was to convert the HB parameters to local Power Law parameters (n' and k') and then to find the Metzner et al. (1955) Reynolds number. The flowchart explaining the steps to be taken in determining the pressure loss for a turbulent flow using this empirical solution is shown in Figure 3.5. Similar to the model presented in Figure 3.4, this is also an iterative calculation process. Also, the friction factor is calculated using an iterative approach which continues until the estimated flow rate converges on the original values presented by the user.

The transition is assumed to be a region instead of a single point from Metzner et al. (1955) who suggested to use the following limiting boundaries for the transition boundary:

$$\mathrm{Re}_1 = 3250 - 1150n' \tag{3.7}$$

$$\mathrm{Re}_2 = 4150 - 1150n' \tag{3.8}$$

Another trial and error method is used in Figure 3.6 to find the solution for the transition boundary based on these limits.

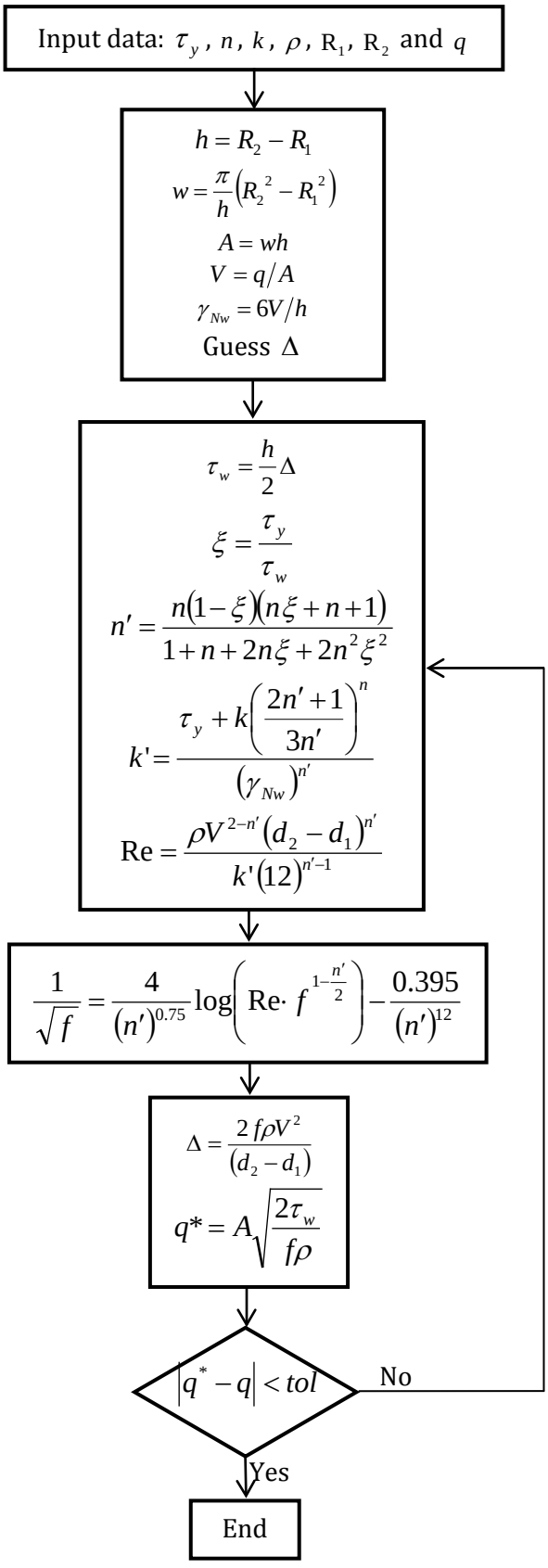

Figure 3.5 A flowchart to find the APL across a turbulent flow regime for a HB fluid

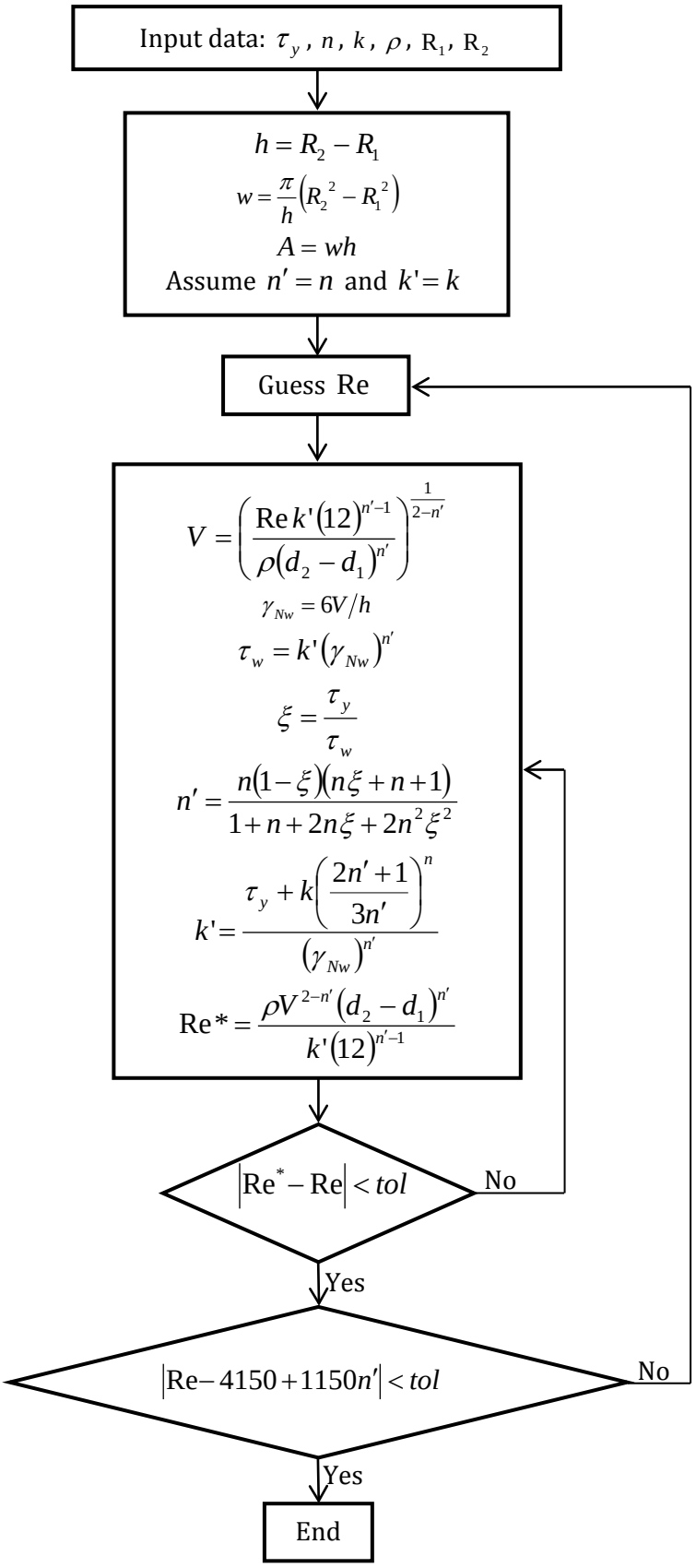

Figure 3.6 A flowchart to find the Reynolds number for the annular transition – turbulent flow boundary for a HB fluid

Here the following data were used to calculate the annular CT pressure loss:

- Hole diameter: 7cm (2.76in);
- CT OD: 5cm (1.97in);
- Mud density: 1010kg/m^3 (8.43ppg);
- Mud density with 5% v/v cuttings: 1094kg/m^3 (9.13ppg) because the slurry density is $(0.95\times1010)+(0.05\times2700)=1094$;
- Mud density with 10% v/v cuttings: 1179kg/m^3 (9.84ppg) because the slurry density is $(0.90\times1010)+(0.10\times2700)=1179$;
- Flow rate of 6l/s (95.1gpm) is by a downhole motor to turn the BHA which generates an approximate annular velocity of 3m/s (590ft/min); and
- Rheological parameters of mud #3.

To understand the effect of different annulus space hole size of 8cm (3.15in) was used while keeping the other parameters constant. For the flow rate of 6l/s, the velocity in the annulus (5cm/8cm) would be 1.96m/s (386ft/min).

Accordingly Figure 3.7 shows the effect of different cuttings concentrations on APL for two different annulus configurations. A clear inflexion point marked by a solid vertical line (LHS) indicates the change from laminar to transition flow regimes whereas a broken (RHS) vertical line marks the change from transition to turbulent flow regimes. However, for the 10% cuttings case with 5cm/8cm annulus configuration only the laminar-transition boundary line is visible within the presented range of velocity. At low flow velocities (shear rates) where the flow is laminar the annular pressure difference between 0% and 5% v/v cuttings concentrations in the mud is small but at higher velocities where the flow is turbulent the annular pressure difference becomes more pronounced. Specifically for the smaller annular volume (5cm/7cm) at 3m/s (590ft/min) velocity the pressure loss is 7058Pa/m (0.312psi/ft) and 8101Pa/m (0.358psi/ft) for 0% and 5% cuttings concentrations, respectively. This shows that an increase in the cuttings concentration from 0% to 5% v/v results in an increase in APL by 1043Pa/m (0.046psi/ft) or 14.8%. For a change in cuttings concentration from 0% to 10% v/v the increase in APL for transitional flow under the same velocity is 1952Pa/m (0.086psi/ft). Similarly for the larger annular volume (5cm/8cm) under a slower velocity of 1.96m/s (386ft/min) the pressure loss is 2207Pa/m (0.098psi/ft) and 2486Pa/m (0.110psi/ft) for 0% and 5% cuttings concentration, respectively. This shows that an increase in APL due to the increase in cuttings concentration is about

279Pa/m (0.012psi/ft) or 12.6%. For a change in cuttings concentration from 0% to 10% v/v the increase in APL under the same velocity is 628Pa/m (0.028psi/ft).

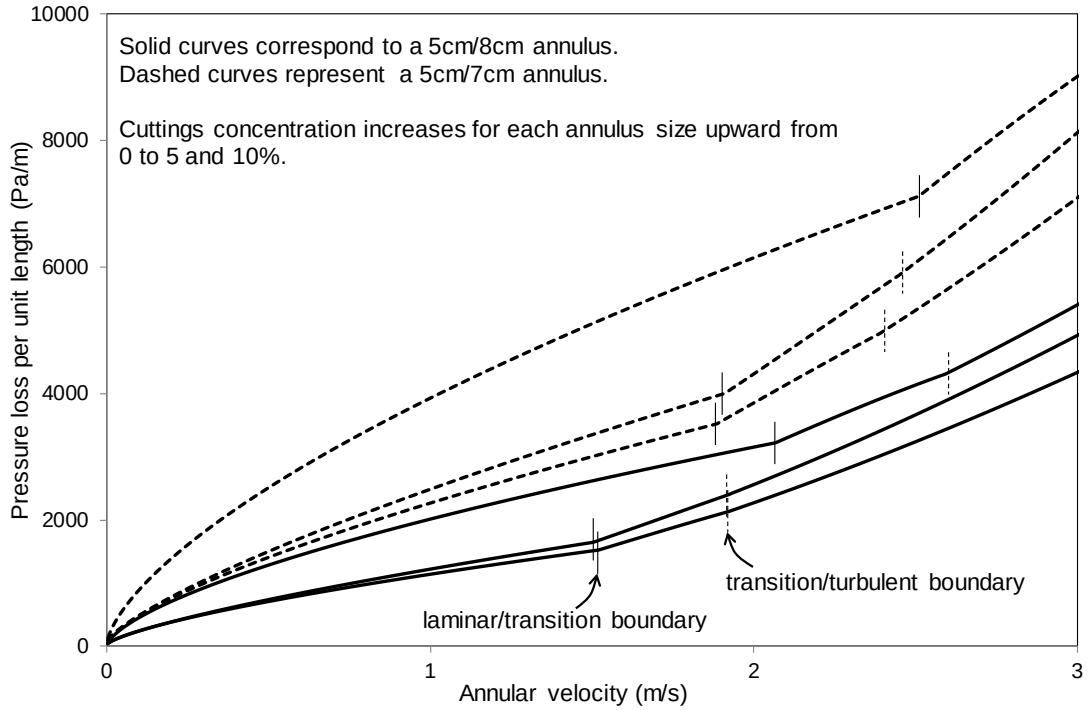

Figure 3.7 The effect of velocity on pressure loss for mud sample #3 with different concentration of the cuttings and different annulus sizes

Figure 3.8 and Figure 3.9 present the APL for mud #1 and 2, respectively, at the same conditions mentioned above for mud #3. It shows that for mud #2 which has the least viscosity compared to the other muds, the transitions occur at lower shear rates.

It is observed that for mud #2 at low velocities the APL for 0% v/v cuttings is higher than that of 5% v/v, however, the trends changes at around 0.7m/s. This is similar to observations in Figure 3.3 where for this mud the viscosity of 0% v/v was higher than that of 5% v/v at low shear rates.

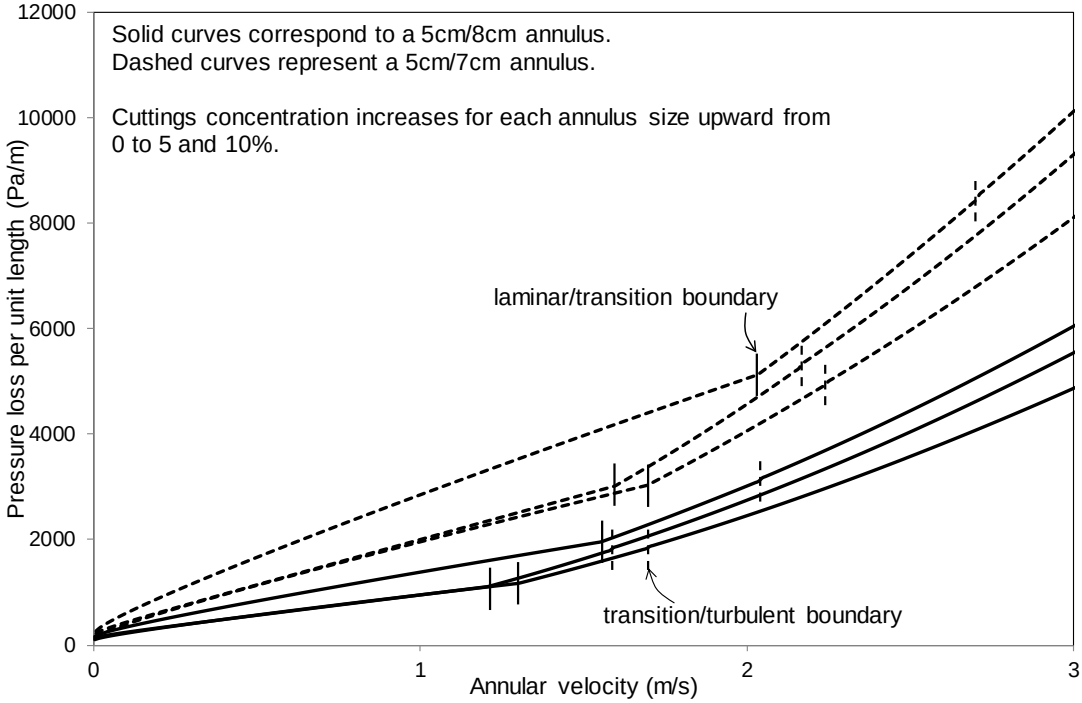

Figure 3.8 The effect of velocity on pressure loss for mud sample #1 with different concentration of the cuttings and different annulus sizes

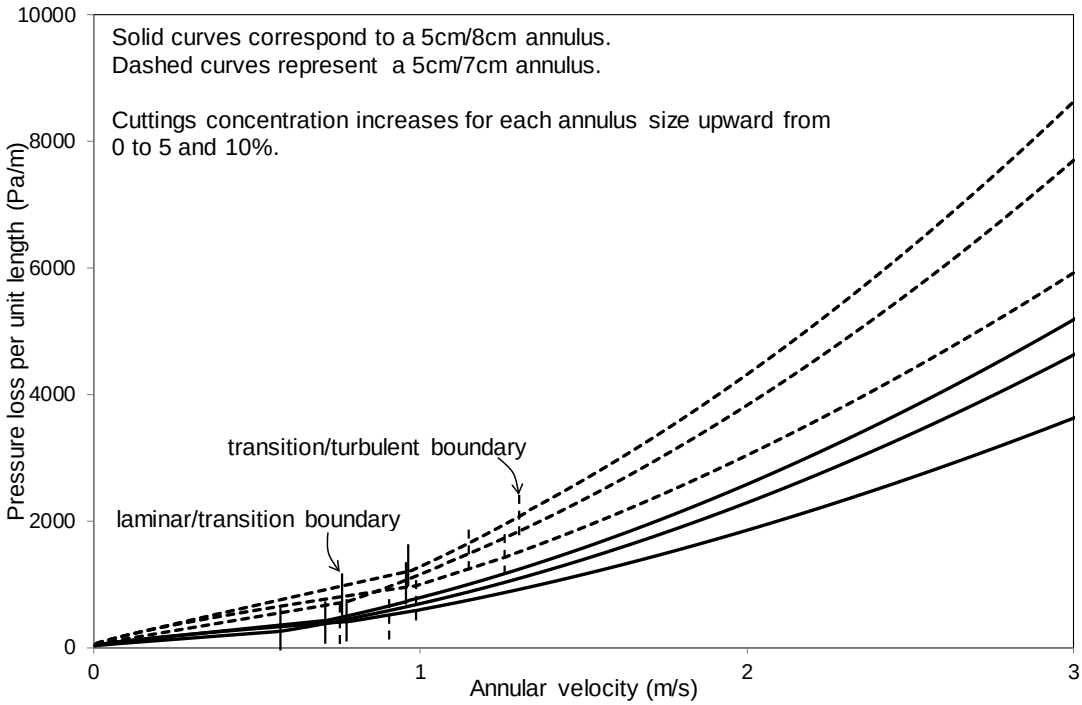

Figure 3.9 The effect of velocity on pressure loss for mud sample #2 with different concentration of the cuttings and different annulus sizes

The above results show that there is a significant impact from cuttings concentration on APL in MBHCTD due to the small annular volume (clearance), high slurry velocity, and specific rheological properties of the mud. The results of Figure 3.7 show that under a constant flow rate larger annular dimensions reduce the

pressure loss considerably. However, drilling a bigger hole needs more energy that has to be provided to drive a more powerful downhole motor. Hence, the motor needs more flow rate to provide the desirable rotation speed to drill the larger hole at an acceptable ROP. To achieve a faster ROP and therefore a cheaper operation different parameters need to be optimized; notably cuttings concentration, flow rate, APLs according to the CT rig system and MBH specifications.

3.5 Summary

The results presented in this Chapter indicated that in hard rock drilling MBHCTD the effect of small size cuttings on drilling mud rheological properties is noticeable and requires consideration at all times. This is somewhat contrary to the applications in the O&G industry where the effect of larger size cuttings on drilling fluid rheology is often negligible.

The laboratory experiments in this study indicate that the effect of cuttings is more pronounced at higher fluid velocities. Again this may be something that is not significant in O&G well drilling but consideration is certainly warranted for cuttings transportation in minex drilling.

The next Chapter discusses the results of experimental work for cuttings transport studies using a flow loop unit.

4 Experimental simulations of cuttings transport

In this chapter the results of experimental simulations are presented for cuttings transport in a flow loop specifically designed for CTD in mineral exploration (minex) applications. Cuttings samples obtained from a mine site were used for the purpose of this study. Also different drilling fluids were used to investigate the effect of the rheological properties on cuttings transport. A minimum annular transportation velocity to carry the cuttings to the surface was determined in different experiments.

4.1 Mini flow loop

Figure 4.1 shows two views of a small scale “mini” vertical flow loop which was set up for some preliminary qualitative investigations of cuttings transport in MBHCTD. The flow rate of fluid injected into the CT is controlled using a bypass line at the pump outlet. The red arrows in the figure show the direction of the flow. Increasing the flow rate enhances the transportation of cuttings through the annulus space but larger cuttings were seen (RHS of Figure 4.1) to accumulate at the bottom of the annulus while the smaller cuttings were carried out of the annulus. The observations are in agreement with the Stokes number concept which indicates that smaller cuttings follow and adapt themselves to the main flow stream easier than coarser cuttings.

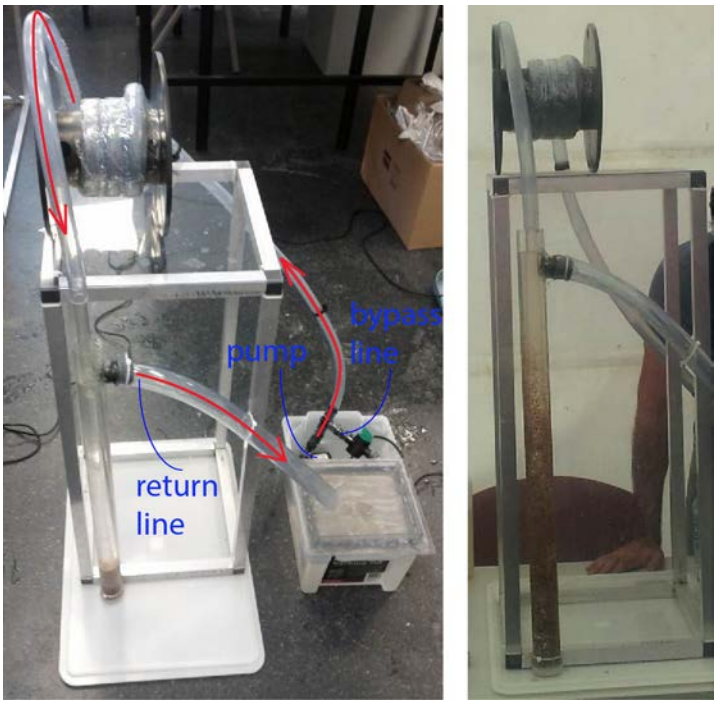

Figure 4.1 Mini flow loop designed for qualitative demonstration of cuttings transport in MBHCTD

The annulus configuration has a length of 65cm (25.6in) and is made of an inner plexiglass tube with the OD of 1.9cm (0.75in) and an outer plexiglass tube with an inside diameter of 4.2cm (1.65in). An aquarium pump is used to deliver water, as the drilling fluid, to the system at a fixed flow velocity of 0.17m/s (33.5ft/min). The tests were performed with two different sand particles sizes of 0.5 (0.2) and 3mm (0.12in). The cuttings were placed at the bottom of the annulus and the pump was then started to visualize whether the flow rate was sufficient to carry the cuttings upward. The results demonstrated that the finer cuttings were transported out of the annulus but the coarser cuttings remained in the annulus and they confirmed the validity of numerical simulations presented in Chapter 5.

4.2 Large scale flow loop

Figure 4.2 is a schematic diagram of a large scale slurry flow loop designed to study annular cuttings transport for MBHs in the laboratory but without scaling down the field parameters.

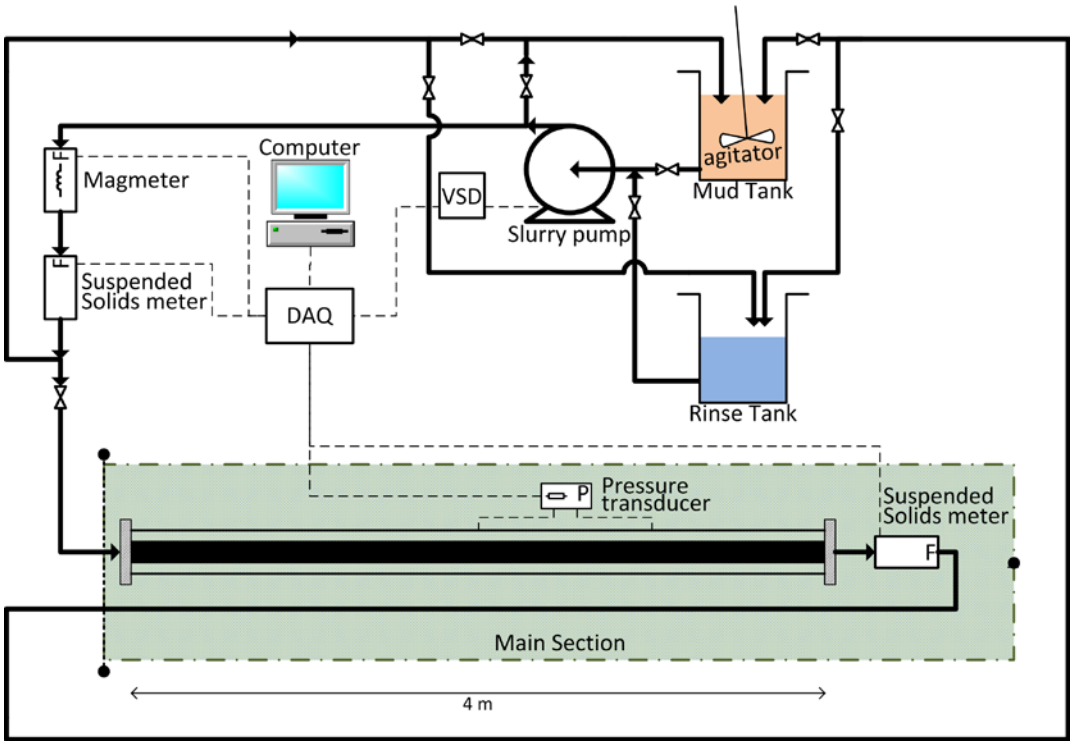

Figure 4.2 Schematic diagram of developed flow loop

Figure 4.3 and Figure 4.4 show different views of the flow loop. The large black tank is the slurry tank with a capacity of 1380 litres (8.68bbl) with a 1.5kW agitator (mixer with up to 1440rpm) set on top of it. Next to it is a white rinse tank with a capacity of 745 litres (4.68bbl) which contains the fluid used to clean the loop to prevent accumulation of the sludge and cuttings along the pipes and at the edges. Shown in blue and yellow colour is a 22kW centrifugal pump (RHS to the slurry tank) that has impellers which are coated with corrosion resistant materials to counter the erosive nature of cuttings.

The suction hoses that connect the pump to the tanks are 3in (76.2mm) whereas all other hose connectors and PVC pipes are 2in (50.8mm).

A Variable Speed Drive (VSD) is connected to the pump and it controls the output flow rate of the drilling fluid when its frequency is changed. The start/stop and frequency of the VSD are controlled by a digital output and analogue output respectively through the data acquisition (DAQ) system. The DAQ is installed inside the black box that is located on the table in front of the pump.

The main section of interest is the annulus configuration which is shown in an angled position in both figures. This section can be set at different angles from horizontal to vertical to test slurry flow behaviour at varying hole inclinations. The transparent outer pipe is useful to visually trace the cuttings flow path along the annulus space.

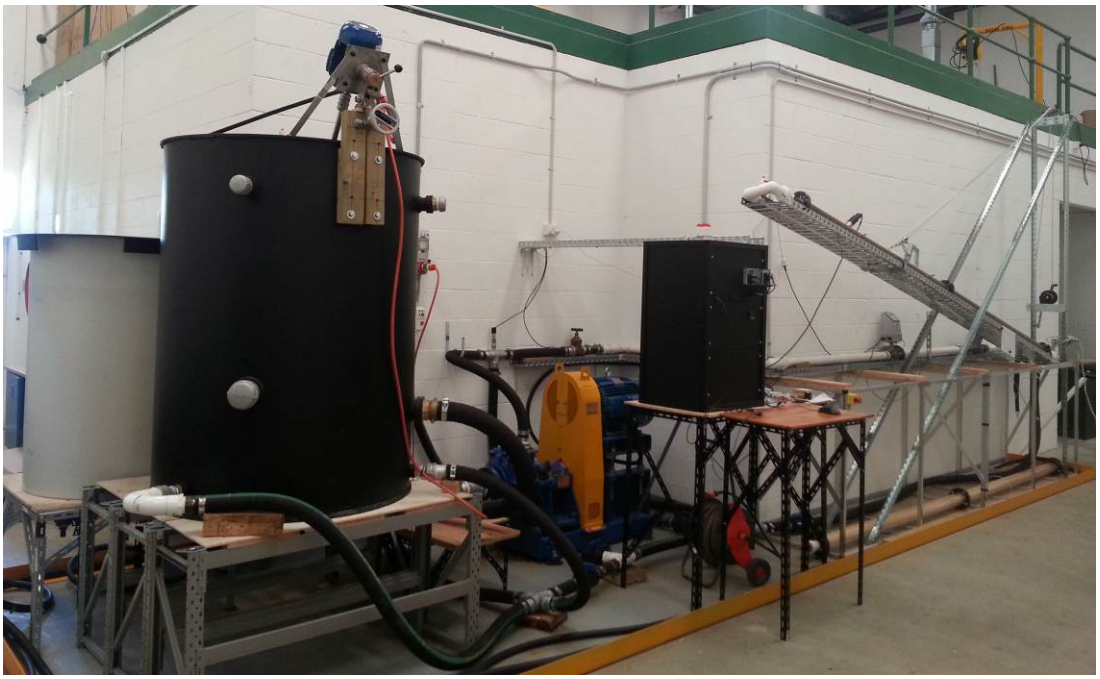

Figure 4.3 Flow loop; LHS view

Figure 4.4 Flow loop; RHS view

A magnetic flow meter (Magmeter), as shown in Figure 4.5, is used to measure the flow rate of the drilling fluid. This works according to Faraday's law of electromagnetic induction which states that when a conductive fluid passes through a magnetic field, a voltage proportional to the fluid speed is generated. This type of flow measurement instrument apparently provides high accuracy.

Figure 4.5 Magnetic flowmeter

Based upon the scattered light measurement principle two suspended solids meters (Figure 4.6) measures the amount of cuttings suspended in the fluid flow stream prior to and after the slurry has travelled in the annulus. It is therefore possible to calculate the amount of any cuttings that they may have settled in the annulus.


Figure 4.6 One of the two suspended solids meters

Currently two annulus configurations are available and both were with outer plexiglass pipes. One has an inner PVC pipe and the other has an inner actual CT pipe. The first configuration has two 2-meter transparent Cast Plexiglass tubes with an ID of 80mm (3.15in) and an inner PVC pipe with an OD of 2in (50.8mm). A see-through tube allows for the observation of the transportation patterns. The second annulus configuration has an actual concentric steel CT pipe with an OD of 1.5in (38.1mm) inside a Plexiglass pipe with an ID of 70mm (2.75in). Figure 4.7 shows this configuration.

The flow goes to the inner pipe (dashed line) and enters the annulus space through the burrowed small holes (which is shown with solid lines). At the end of the annulus section it then goes back to the inner pipe. The flow moves from the inner side of the steel pipe and then enters the annulus gap, the space between the outside of the steel

pipe and the inside of the Plexiglass pipe. Notably, following the holes inside of the steel tube is blocked so the flow can pass only through the drilled holes. Looking at Figure 4.7 note that the steel pipe outside the annulus is of the same diameter with the pipe inside. However, due to light refraction the former appears smaller than the latter.

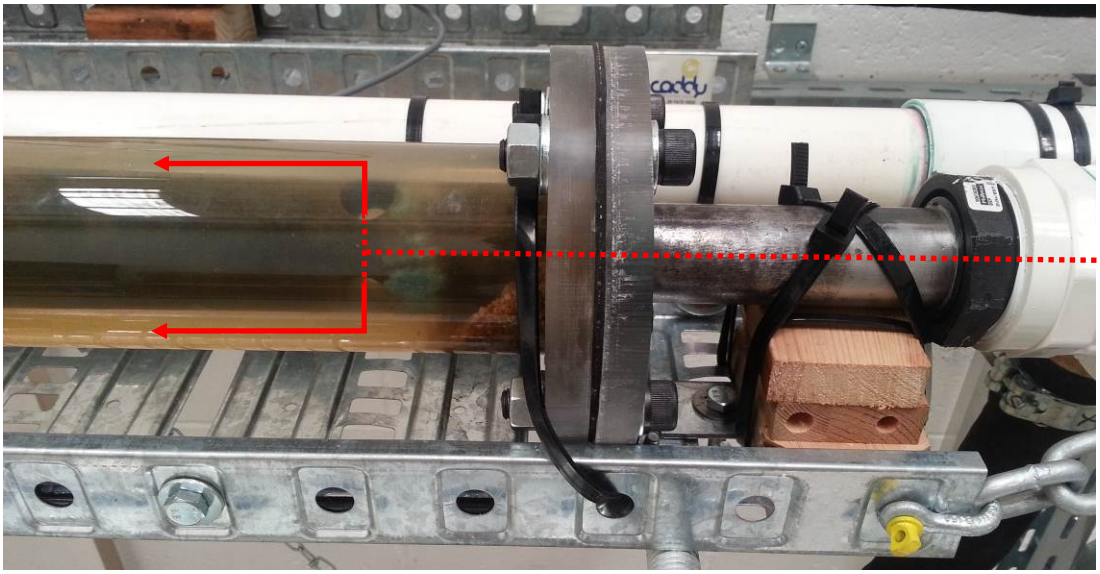

Figure 4.7 Second annular configuration of the annulus space with inner actual CT pipe and an outer transparent Plexigalss tube

A variable reluctance differential pressure transmitter measures the pressure difference between two points along the annulus space that are located one metre apart. The differential pressure range of the device is 14kPa (2.03psi). Figure 4.8 shows this pressure transmitter and the probes.

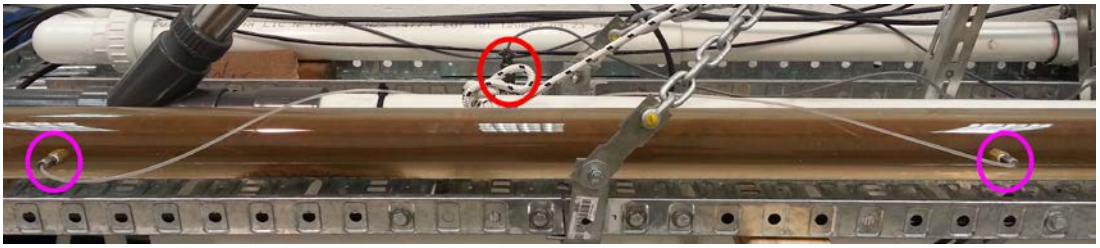

Figure 4.8 The pressure transmitter circled in red is connected to two probes (circled either side of the transmitter), one metre apart, in the annulus

National Instrument Labview software has been used to transmit and receive data to and from the DAQ. Figure 4.9 shows the front panel of the Labview interface designed for this study. It is only a graphical user interface (GUI) and without the block diagram showed in Figure 4.10 it cannot perform any task. In the block diagram the components are connected to perform the required tasks. For example one of the controls in the front panel is the Shut-Off Pressure, a threshold pressure

value to avoid over-pressurisation of the pump. This may happen if the return valve to the pump is closed and may cause bursting of the pipes if safety system is not applied. So in the block diagram a scheme is designed in a manner that when the pressure reaches to a certain user defined Shut-Off pressure value, it automatically turns off the pump. The data shown in the front panel are then stored in an Excel file for future access.

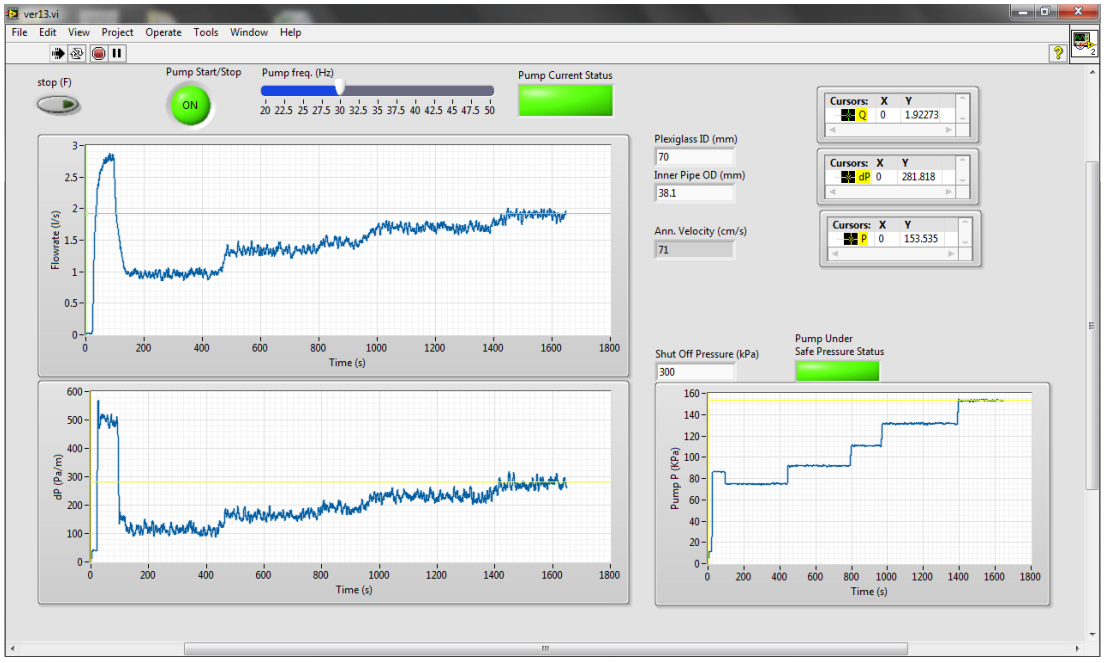

Figure 4.9 Designed Labview front panel

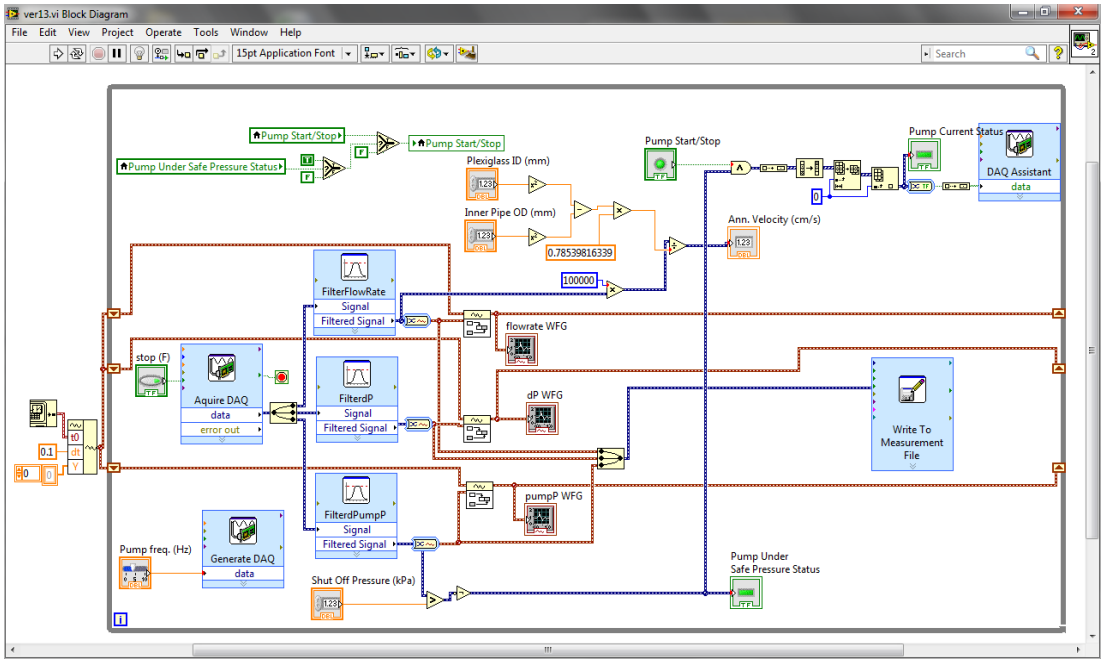

Figure 4.10 Designed Labview block diagram panel

4.2.1 Calibration of the sensors

Flow meter

The magnetic flow meter is installed along a straight section of the PVC pipes where the flow is expected to be uniformly smooth and it requires some time before reading the actual flow rate value. In Figure 4.11, it takes approximately 40 seconds for the Magmeter to obtain a stable reading after starting the pump. The start and stop refers to the pump status while the blue curve shows the measured flow rate by the Magmeter. "q_{ave}" is the average value of the measured flow rate once the flow is stabilized. The area bordered by the start and stop line, and the q_{ave} and the horizontal axis represents the accumulated transported volume of water which was calculated to be 264.45 litres. However, the actual transported volume of water is 269.44 litres measured volumetrically from the slurry tank. So the flow meter sensor was found to under-measure the flow rate by 1.86% and the discrepancy was deemed to be insignificant in terms of the results of this study.

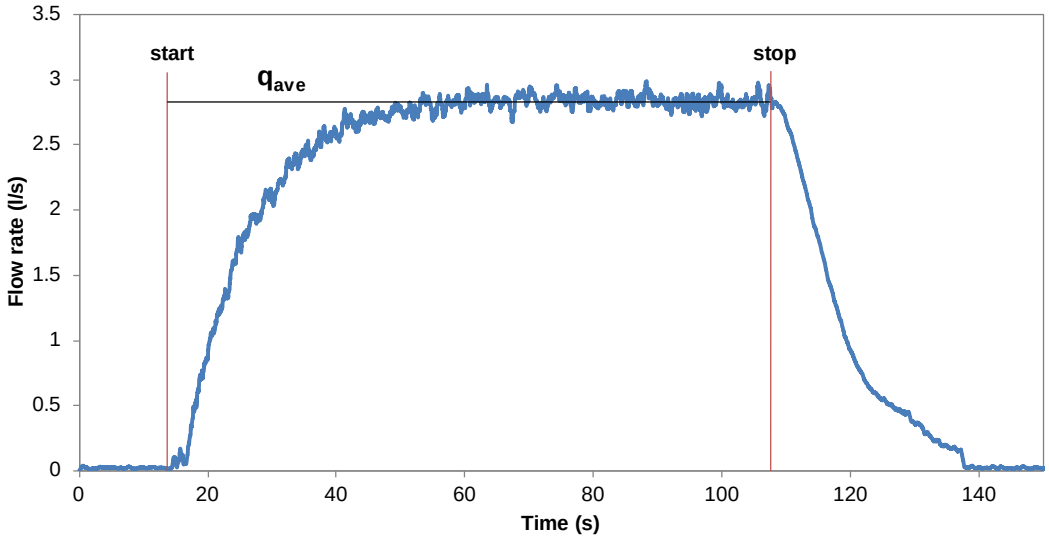

Figure 4.11 Magnetic flow meter calibration chart

Pressure sensor

The pressure sensor has two probes for adjustments of the lowest and highest pressure values. Ideally, when the differential pressure between the two probes of the sensor is zero and at its maximum (14kPa) the DAQ will receive 4mA and 20mA current, respectively.

4.2.2 Controlling parameters in the flow loop

The following parameters can be controlled in order to simulate the field scenarios more closely:

- Fluid: the properties of the drilling fluid (mud) such as weight and rheological properties in the mud tank.
- Cuttings: the properties of solid particles such as concentration, size, density and shape in the mud tank.
- Slurry flow rate: changing the frequency of the pump using a VSD controls the flow rate as described above. In order to reduce the flow rate, lower than the minimum rate of the VSD, a bypass valve is operated and controlled to return some of the flow back to the slurry tank. The flow rate is then measured using the Magmeter.
- Annulus configurations: can be altered by changing the inner and outer pipes.
- Hole inclination: can be changed to any angle between horizontal and vertical.

By changing the above controlling parameters, the pressure loss can be measured using pressure transducers. Also, the quantity of cuttings deposited in the annulus space can be measured from the difference between the solid concentrations as recorded at the two suspended solids meters.

4.3 Experimental procedures and results

The details of the cuttings collection for the tests in the flow loop are presented in Appendix A Section A.2. In this operation hammer drilling was used and the produced cuttings cover a wider range of sizes compared to the impregnated diamond bits.

4.3.1 Cuttings behaviour during the transport experiments

The mixed cuttings size has the original size distribution as those sourced from the mine site (see Appendix A Section A.2) which is shown in Figure 4.12.

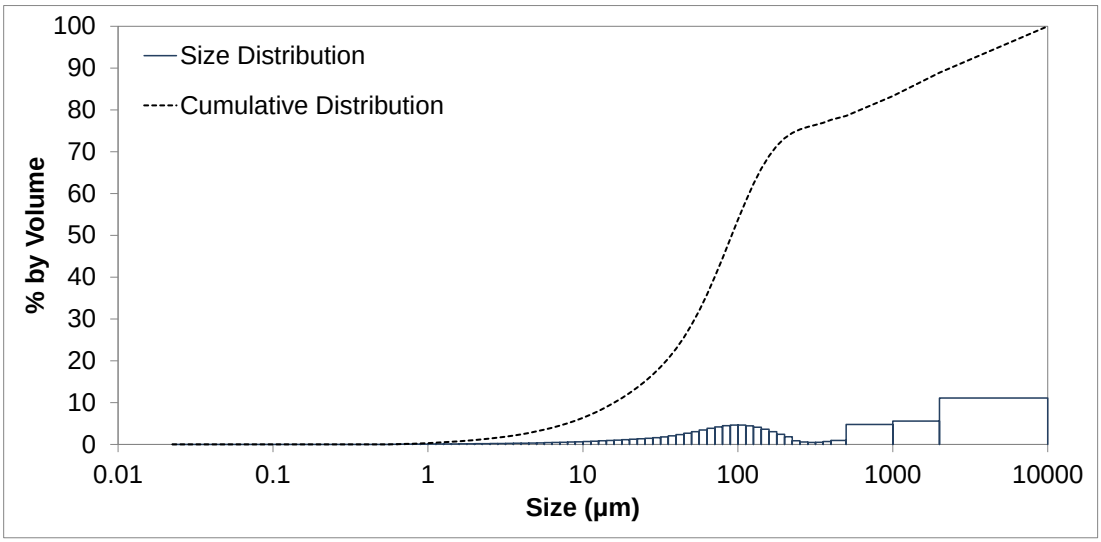

Figure 4.12 PSD of cuttings drilled up from the mine site

Three sieve sizes were used to separate the cuttings into three size categories as illustrated in Figure 4.13; notably groups #1, 2, and 3 as shown in Table 4.1. The sieve screen sizes were 0.425, 2.36, and 4.7mm (0.017, 0.093, and 0.185in). Only a small trace of other sizes can be seen in the cumulative size distributions for each of the three categories.

Table 4.1 Results after sieving the cuttings samples

Group	Cuttings size	Density (g/cc)	Amount	Percentage
1	<0.425mm	2.8	140kg	76%
2	0.425-2.36mm	2.75	24kg	13%
3	2.36-4.7mm	2.75	20kg	11%

As it is shown in Table 4.1, most of the cuttings are less than 0.425mm. The size distribution of the cuttings before sieving is shown in Figure 4.12. The data of 0.02 to 500 micrometre is measured by laser diffraction and the data of 0.5 to 10mm by wet screening. The size distribution graph is a histogram which presents the height of each block in percentage uninfluenced by the block area. In brief, the size of the block area has no relation with the amount of the mixture. For example, the 2-10mm range covers a sizable block area but the actual percentage only reveals 7.7%.

Since the recovered mixture samples from the well are not homogenous, the distribution shown in Figure 4.12 represents the accumulated weight average of the individual size analysis of each group in Table 4.1. Moreover, the average density of groups #1, 2 and 3 are 2.8, 2.75 and 2.75g/cc, respectively.

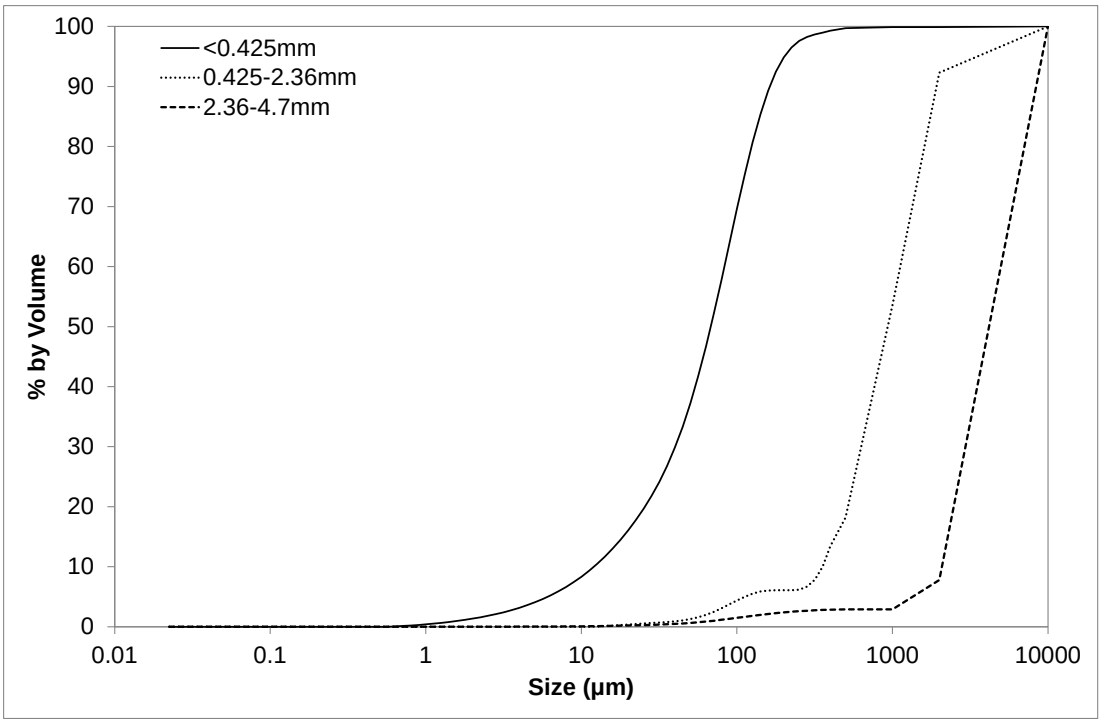

Figure 4.13 Cumulative particle size distribution used to perform the experiments

The drilling fluid is discarded after the experiment is performed for each cuttings size group. Each cuttings group was tested for a ten hour period during which time the test fluid and cuttings (slurry) were (was) agitated by the mixer in the mud tank and circulated/re-circulated throughout the system with the centrifugal pump.

Degraded (broken and eroded) cuttings were observed during the experiment for size groups #2 and 3 which initially had bigger particles. Figure 4.14 and Figure 4.15 show breakage of cuttings in size category #2 and 3 for particle sizes of 0.425-2.36mm and 2.36-4.7mm, respectively. Cumulative size distributions before and after the tests is shown with line graphs. The difference size distribution histogram is generated by subtracting after values from before values. In Figure 4.14 the cuttings in the range of 0.5-4.7mm are broken into smaller ones and are shown with negative values in the histogram and the amount of sizes smaller than 0.5mm increases.

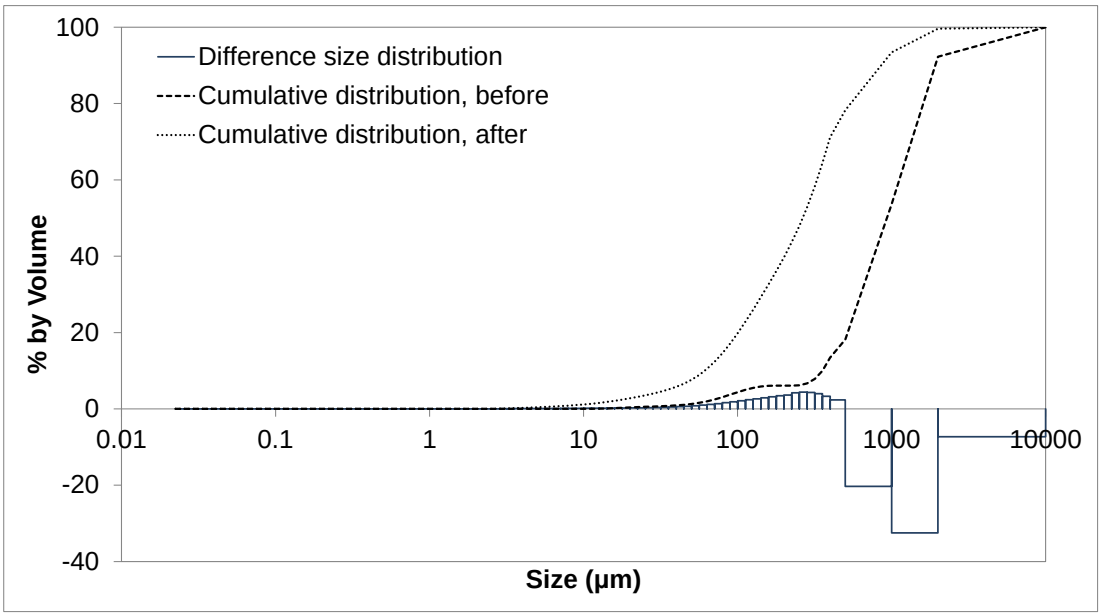

Figure 4.14 Breakage of cuttings in size category #2 (0.425-2.36mm cuttings)

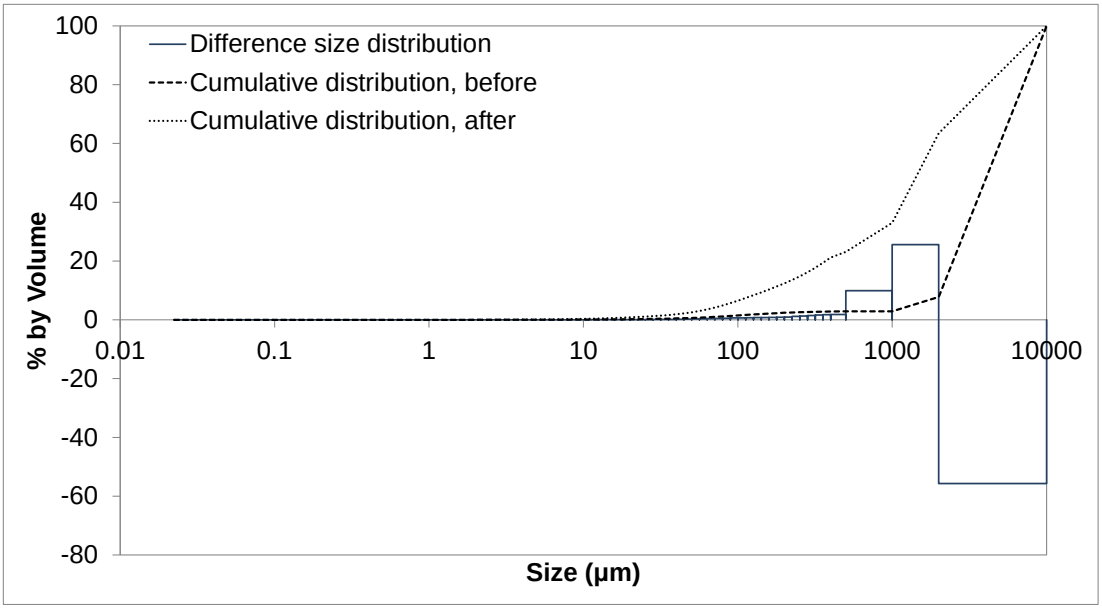

Figure 4.15 Breakage of particles in size category #3 (2.36-4.7mm cuttings)

The shear degradation and breakage of the cuttings verifies that cuttings erode mechanically at the surface (by mixer blades and pump impellers) and in the actual wellbore flow paths (by knocking and bruising each other). In the O&G industry it has long been known that if fine cuttings are not removed by solid control equipment ultra-fines will result from their re-circulation and the fluid rheology will be adversely affected.

The breakage phenomenon reveals that the cuttings are not durable in the process and reveal potential borehole instability issues during drilling this formation type. Investigation is required to further confirm this and validate against field

observations. This problem is initially dismissed in hard rock drilling however, the splintering of the particles prove otherwise.

4.3.2 Rheological properties of drilling fluids

For the sensitivity analysis of the rheological properties, 3 different drilling fluids (mud) were prepared. These drilling fluids for flow loop tests are different from the drilling fluids used in Chapter 3. The composition of the flow loop test fluids are:

1. Fluid #1: Water
2. Fluid #2: Water + 0.1% w/w of polymer (Corewell)
3. Fluid #3: Fluid #2 + 0.1% w/w of xanthan gum (Xan-Bore).

Corewell and Xan-Bore are both the trademarked names for product developed/purchased by the Australian Mud Company (AMC). Corewell is a multi-purpose crystalline polymer-based additive suitable for slim-hole drilling and solid separation enhancement. It also provides low viscosity to the drilling fluid system (Corewell, 2014). Xan-Bore, on the other hand, is a powder polymer-base additive which enhances hole cleaning and carrying capacity of the cuttings (Xan-Bore, 2014).

The rheological properties of the drilling fluids were discussed in Section 2.5.1 of Chapter 2. To measure the rheological properties of these fluids a 6 speed Fann V-G viscometer was used. Both Fluids #2 and 3 were tested twice and the results are shown in Table 4.2.

Table 4.2 Dial reading results for fluid samples

RPM	Fluid #2	Fluid #3
600	7.25	11.5
300	4.75	7.5
200	3.25	6
100	2	4
6	0	1
3	0	0.5

The data presented in Table 4.2 shows that the Fluid #2 follows a rheology model without yield stress opposite to Fluid #3 that shows a yield stress. Therefore, PL and HB models are proposed for Fluid #2 and 3, respectively. The procedure to calculate the HB parameters was mentioned in Section 3.3 of Chapter 3. However to determine the PL parameters, common logarithms are taken from both sides of PL equation as shown below:

$$\log(\tau) = \log(k) + n\log(\gamma).$$

The equation becomes a straight line and a linear trend-line needs to be fitted over the $\log(\tau)$ vs. $\log(\gamma)$ data.

The following equation is the Power Law model fitted over Fluid #2 data points:

$$\tau = 0.02423\gamma^{0.72934} \tag{4.1}$$

For Fluid #3 the following equation represents the HB model:

$$\tau = 0.0248 + 0.1042\gamma^{0.5798} \tag{4.2}$$

All of the values in Equation (4.1) and (4.2) are in SI units.

4.3.3 Experiment procedure

To prepare the slurry in the mud tank, first, one cubic meter tap water, as the basis of calculation, is poured into the tank. Secondly, the required additives are supplemented to prepare the drilling mud. Then based on the desired concentration of the solid particles, the needed amount is added to the drilling fluid to make the slurry. The next step is to run the pump and circulate the drilling fluid in the system.

To determine the MTV a sufficient flow rate has to be established to lift and carry all of the cuttings in suspension or in a moving state. The flow rate is then gradually reduced step-wise. For each step the system is allowed to stabilize until a steady state condition is reached. After observing a stationary section, the average values of the current and previous flow rate are recorded to calculate MTV. The velocity is simply determined by dividing the flow rate by the cross sectional area of the annulus space. This same process is then repeated for other hole inclinations.

There are some factors in the flow loop that can be controlled: annulus size, drilling mud, cuttings, slurry flow rate and hole inclination. After preparing the slurry in the tank the only controlling variables that can be changed are the flow rate and hole inclination. For every angle, the value of MTV needs to be found.

In usual O&G terminology 0° hole angle refers to a vertical well trajectory and 90° is assigned to horizontal well configurations and this terminology is applied in this reseach for consistency.

4.3.4 Experimental data

The data recorded in the experiment is shown in Table 4.3 showing the effects of three parameters such as cuttings size, mud type and hole inclination on the MTV. In these experiments the following conditions were fixed:

- Cuttings concentration was kept 1% v/v.

- The second annulus configuration had an actual steel CT with OD of 1.5in (38.1mm) and is concentrically placed inside a Plexiglass pipe with an inner diameter of 70mm.

Table 4.3 Data recorded showing the MTV in cm/s at different angles, cuttings sizes and drilling fluids

		Angle					
Cuttings size	**Fluid type**	**90°**	**75°**	**60°**	**45°**	**30°**	**15°**
2.36-4.7mm	**Fluid 1**	74	81	89	95	84	72
	Fluid 2	89	109	122	130	127	106
	Fluid 3	94	105	114	120	105	80
0.425-2.36mm	**Fluid 1**	87	91	100	88	85	70
	Fluid 2	80	94	110	120	114	102
	Fluid 3	97	102	115	118	113	78
<0.425mm	**Fluid 1**	70	75	76	74	66	45
	Fluid 2	40	60	62	60	60	40
	Fluid 3	40-	44	48	47	44	40-
Mixed cuttings	**Fluid 1**	76	82	89	91	83	66
	Fluid 2	53	70	83	87	83	65
	Fluid 3	59	67	75	80	73	50

The "40-" means that the MTV is less than 40cm/s (79ft/min) however the actual value was not possible to be recorded.

The mixed cuttings size in Table 4.3 has the size distribution shown in Figure 4.12. Notably, in two cases in Table 4.3 the MTVs are less than 40cm/s and it was not possible to measure the actual values. This is due to the fact that VSD was set at its practical minimum frequency value and the bypass line was fully open, therefore the annular flow rate was at its lowest value and at this point the annular velocity was 40cm/s and the cuttings were still at moving bed regime.

4.3.5 The effect of mud rheology on the minimum transportation velocity

The effect of mud rheological properties on the cuttings transportation was presented in Chapter 2 Section 2.7. Similar studies considered flow regime in the previous investigations, thus, to achieve the same accuracy, this study determines the MTVs' flow regime and also the Reynolds number.

The method presented in Chapter 3 section 3.4 determines the laminar-transition and transition-turbulent boundaries for all the fluids regardless of the cuttings. The outcomes are shown in Table 4.4. This also shows the Reynolds number and the equivalent velocity of that number. This will be an indication for easier determination of the flow regime of the measured MTV. As the viscosity of the

fluids increases from Fluid #1 to 3, the size of transition zone span remains constant with a value of 900; (3000 – 2099), (3311 – 2411) and (3489 – 2589). However, the onset of the boundaries increases as the fluids get more viscous. The equivalent velocity represents the velocity that is required to generate the boundary Reynolds number. It shows in the table that the onset of turbulent flow for water requires a very low value of fluid velocity (9cm/s). However, as the fluid increases in viscosity, higher velocity is required to generate transition or turbulent flow regimes. Compared to water, mud #2 necessitates higher velocity and mud #3 requires the highest to onset a non-laminar flow.

Table 4.4 Reynolds number and its equivalent velocity at the laminar-transition and transition-turbulent boundary for three muds

	Laminar to transition boundary		**Transition to turbulent boundary**	
	Re	**Equivalent velocity (cm/s)**	**Re**	**Equivalent velocity (cm/s)**
Fluid 1	2099	7	3000	9
Fluid 2	2411	49	3311	62
Fluid 3	2589	86	3489	105

The Reynolds number and flow regime of the results presented in Table 4.3 are shown in Table 4.5.

Table 4.5 Reynolds number and flow regime of the minimum transportation

Cuttings size	Fluid type		Angle					
			90°	75°	60°	45°	30°	15°
2.36-4.7mm	Fluid 1	MTV (cm/s)	74	81	89	95	84	72
		Re	23606	25839	28391	30304	26796	22968
		Flow regime	Tur	Tur	Tur	Tur	Tur	Tur
	Fluid 2	MTV (cm/s)	89	109	122	130	127	106
		Re	5190	6715	7749	8401	8155	6481
		Flow regime	Tur	Tur	Tur	Tur	Tur	Tur
	Fluid 3	MTV (cm/s)	94	105	114	120	105	80
		Re	2960	3466	3898	4194	3466	2350
		Flow regime	Tran	Tran	Tur	Tur	Tran	Lam
0.425-2.36mm	Fluid 1	MTV (cm/s)	87	91	100	88	85	70
		Re	27752	29029	31899	28071	27114	22329
		Flow regime	Tur	Tur	Tur	Tur	Tur	Tur
	Fluid 2	MTV (cm/s)	80	94	110	120	114	102
		Re	4533	5564	6794	7588	7109	6172
		Flow regime	Tur	Tur	Tur	Tur	Tur	Tur
	Fluid 3	MTV (cm/s)	97	102	115	118	113	78
		Re	3096	3326	3947	4095	3849	2267
		Flow regime	Tran	Tran	Tur	Tur	Tur	Lam
<0.425mm	Fluid 1	MTV (cm/s)	70	75	76	74	66	45
		Re	22329	23924	24244	23606	21053	14355
		Flow regime	Tur	Tur	Tur	Tur	Tur	Tur
	Fluid 2	MTV (cm/s)	40	60	62	60	60	40
		Re	1878	3145	3279	3145	3145	1878
		Flow regime	Lam	Tran	Tran	Tran	Tran	Lam
	Fluid 3	MTV (cm/s)	40-	44	48	47	44	40-
		Re		998	1131	1097	998	
		Flow regime	Lam	Lam	Lam	Lam	Lam	Lam
Mixed cuttings	Fluid 1	MTV (cm/s)	76	82	89	91	83	66
		Re	24244	26158	28391	29029	26476	21053
		Flow regime	Tur	Tur	Tur	Tur	Tur	Tur
	Fluid 2	MTV (cm/s)	53	70	83	87	83	65
		Re	2686	3825	4750	5043	4750	3481
		Flow regime	Tran	Tur	Tur	Tur	Tur	Tur
	Fluid 3	MTV (cm/s)	59	67	75	80	73	50
		Re	1520	1824	2143	2350	2062	1199
		Flow regime	Lam	Lam	Lam	Lam	Lam	Lam

Lam = laminar, Tran = transition, Tur = turbulent

For water all MTVs are in turbulent flow regime as it is calculated in Table 4.4. The minimum velocity that causes turbulent flow regime is 9cm/s. It is not the case for the other muds as they require higher velocity at the onset of turbulency.

Figure 4.16, Figure 4.17 and Figure 4.18 show the effect of mud rheology on MTV for different cuttings size categories, whereas the results of the mixture are

shown in Figure 4.19. It is noted that some of the MTV values for particles less than 0.425mm are not shown because their exact values were indiscernible. In all of the MTV profiles from horizontal (90°) inclination through to an angle of 45°, regardless of the sizes of the cuttings or fluid type, the MTV increases before decreasing at higher well bore inclinations. This observation coincides with the O&G industry's long time general awareness that wells with 'critical angle' inclinations between 30°-60° are the most difficult to keep clean (Ford et al., 1990; Martin et al., 1987) although J. Li and Walker (2001) have declared a 30° inclined wellbore is the hardest to clean.

For Group #3 (2.36-4.7mm) coarse cuttings, when the drilling fluid changed from water to Fluid #2, higher fluid velocity is required to avoid occurrence of stationary particles, even though Fluid #2 has higher fluid viscosity. Then when Fluid #3 is used, the minimum transportation velocity reduced from those values of Fluid #2. As the hole inclination increases the difference between Fluid #2 and 3 MTVs increases as well. In the second category of the particles, 0.42-2.36mm, the MTV profiles are getting closer to each other compared to 2.36-4.7mm particles especially for Fluid #2 and 3. However, at 30°-60° inclinations, while Fluid #2 and 3 results are close to each other, their values are higher than that of water MTV values.

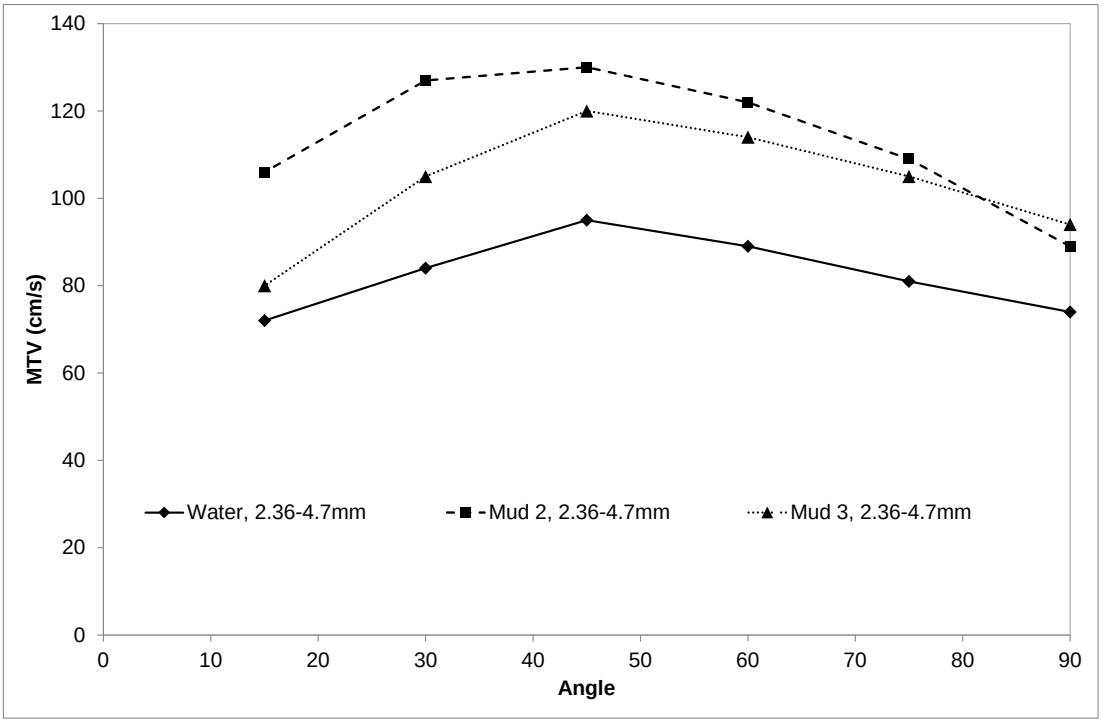

Figure 4.16 Effect of mud rheological properties on the MTV for 2.36-4.7mm particles

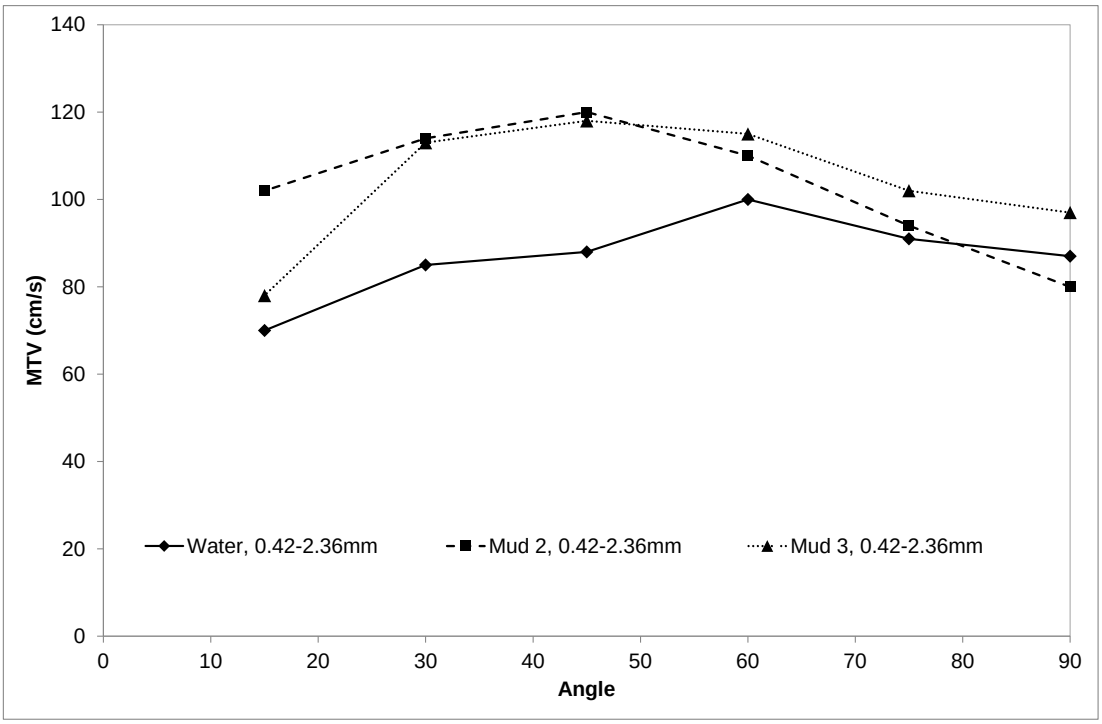

Figure 4.17 Effect of mud rheological properties on the MTV for 0.42-2.36mm particles

So far the understanding from Figure 4.16 and Figure 4.17 is that the viscous drilling fluids required higher MTV than water to clean the cuttings. However the results of finer particles, less than 0.42mm, which is shown in Figure 4.18, contradict the aforementioned statement. As the drilling fluid gets more viscous, the transportation efficiency is enhanced. The reason is that if fluid viscosity is able to suspend the cuttings while transporting them, then less flow energy is needed to move them at the lower side of the wellbore. Based on Stocks number smaller particles follow the fluid streamline better than coarser ones. Therefore, coarser particles settle down faster comparing to finer particles. Water does not have the viscosity to suspend them and therefore higher turbulency is the means to transport the cuttings. However the more viscous the drilling fluid is, the higher the lifting capacity is, especially when the particles are smaller.

It is also obvious that for finer particles the MTV profiles are more flattened especially at the middle compared to larger ones.

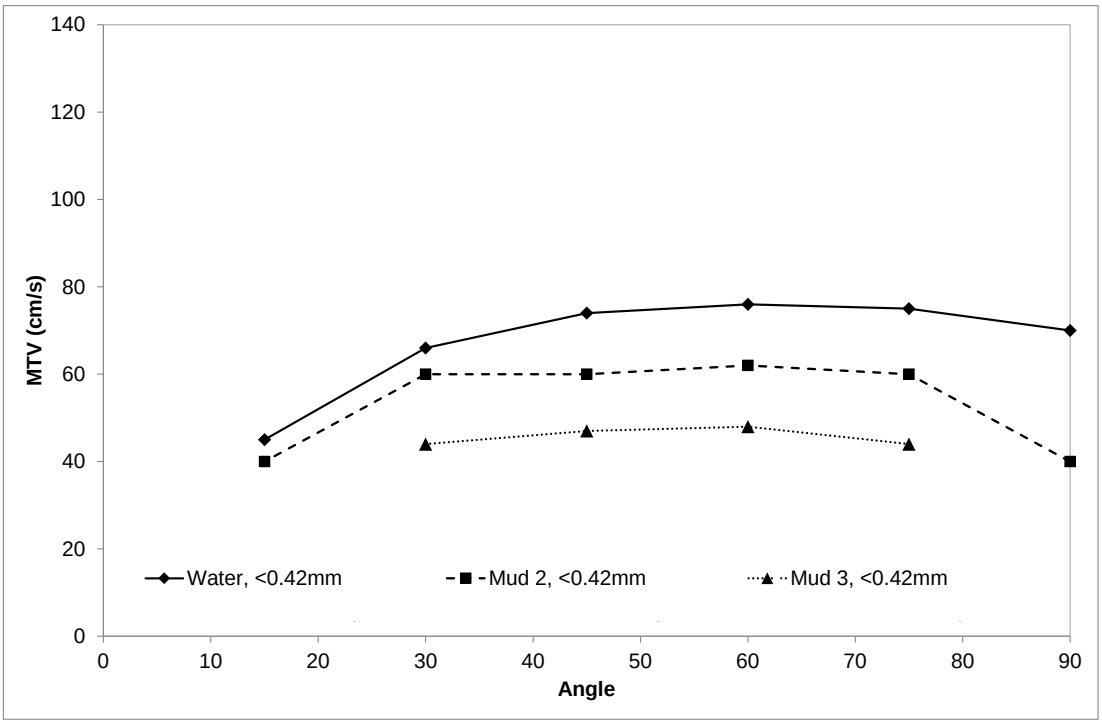

Figure 4.18 Effect of mud rheological properties on the MTV for particles less than 0.42mm size

The trend in the mixture of particles is the same as fine particles; however, the profiles are closer to each other than in finer particles.

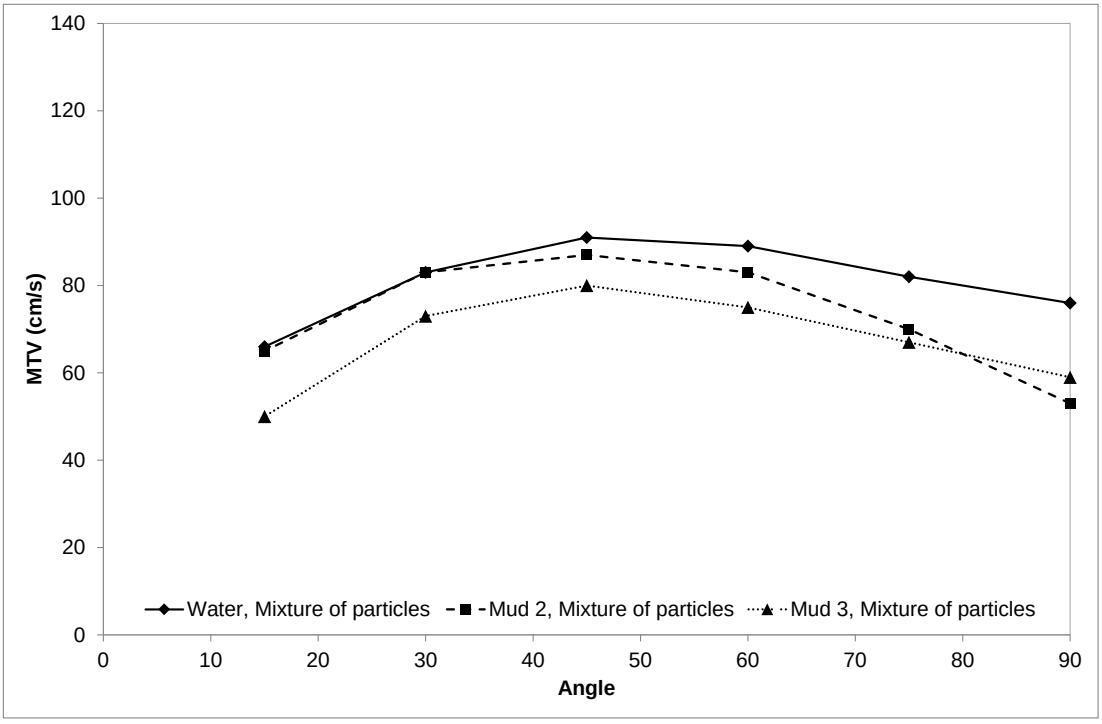

Figure 4.19 Effect of mud rheological properties on the MTV for mixture of particles

To understand the rheological effect on cuttings carrying capacity, knowing the type of drilling fluid is of paramount importance. In oil industry the choice is obvious, that is not to use water as the drilling fluid. In minex, however, water is a good choice since downhole hammer and motor/turbine function better with it than a

viscous drilling fluid. Ignoring water, the results show that among Fluid #2 and 3, Fluid #3 performs better since it has higher viscosity and higher low-shear-rate-viscosity, even Fluid #2 shows higher Reynolds number and in turn higher turbulency. In some cases while Fluid #2 MTVs occur in turbulent flow, Fluid #3 MTVs happens in either transition or laminar flow. This shows that the turbulent flow is not the main regime of flow to control the cuttings transportation. This finding is not in agreement with Leising and Walton (2002a) investigation as they stated that in CTD, using low viscosity fluid in turbulent flow enhances the cuttings transportation than high viscosity fluids in laminar flow.

Including the water, for bigger cuttings (greater than 0.42mm), the statement mentioned by Brown et al. (1989) and Y. Li et al. (2007) complies with the finding in this study that water is the best fluid for cuttings transportation in horizontal wells. However, this statement disproves the case of finer particles. Brown et al. (1989) and Y. Li et al. (2007) investigations were oil industry-based and the cuttings sizes that they usually dealt with were large. However in minex the majority of particles are fine and therefore the generalization of the findings in oil applications to hard rock drillings is not acceptable.

4.3.6 The effect of cuttings size on the minimum transportation velocity

Figure 4.20, Figure 4.21 and Figure 4.22 show the individual effect of the four different cuttings categories on the MTVs for the three different fluids and various hole angles. While the drilling fluid is water, all the MTV trends are close to each other. However, for finer particles, with sizes less than 420 microns, the required velocity to carry the cuttings in moving bed mode is lower. In contrast, the profiles for higher viscosity fluids are more parted. For Fluid #2, as the cuttings become smaller the required MTV turns significantly lower. And for Fluid #3, cuttings sizes of 0.42-2.36mm and 2.36-4.7mm follow exactly the same profile. Smaller cuttings, on the other hand, have a considerably lower MTV values. In all of the cases the mixture profile is between category size #1 and 2. In the mixture, finer particles are carried at low velocities, opposite to the coarser particles that are transported at higher velocities. Thus, the controlling factor is the concentration of coarse particles in the mixture.

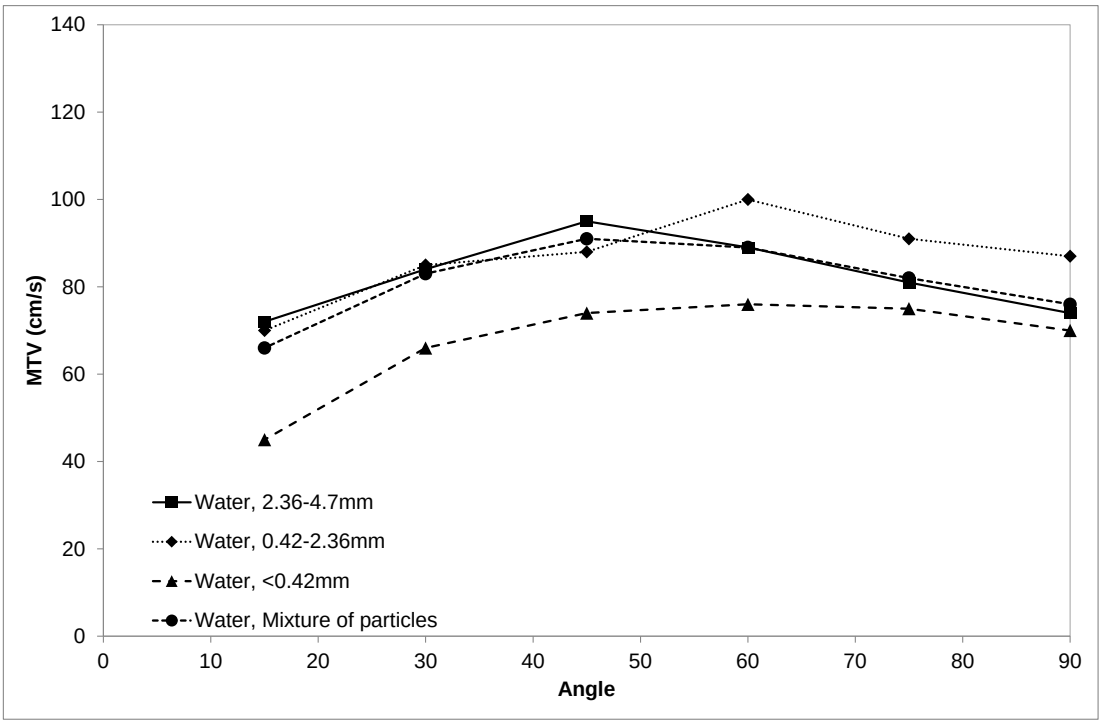

Figure 4.20 Effect of cuttings size on the MTV for water as a drilling fluid

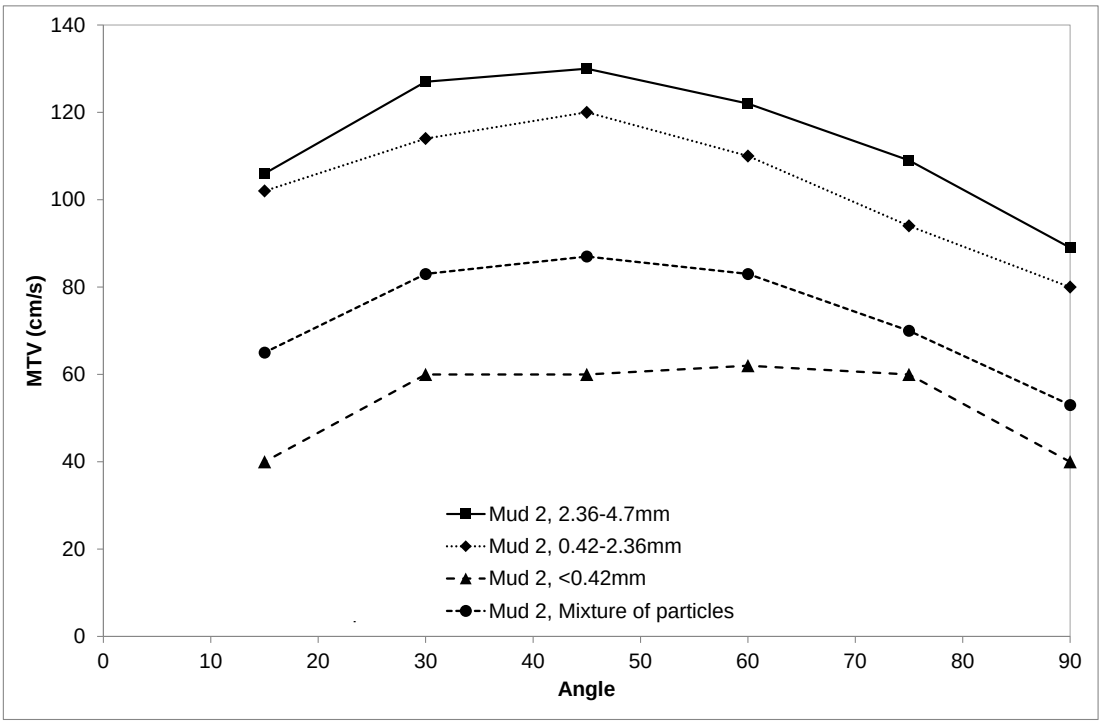

Figure 4.21 Effect of cuttings size on the MTV for mud #2 as a drilling fluid

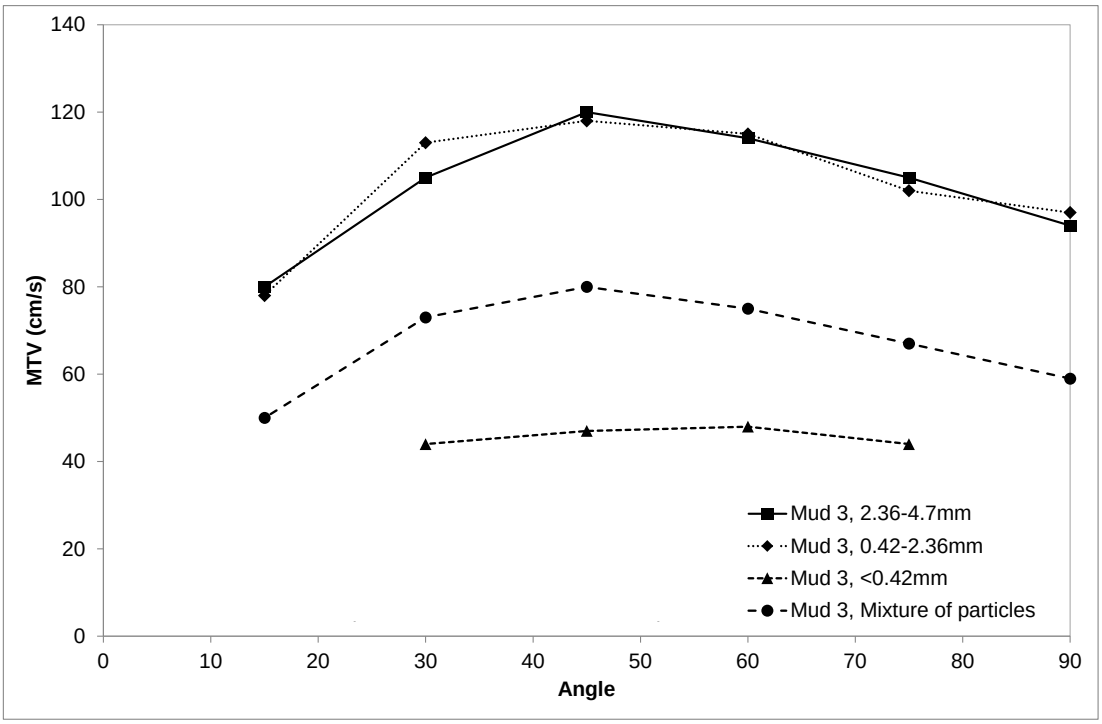

Figure 4.22 Effect of cuttings size on the MTV for mud #3 as a drilling fluid

4.3.7 Experimental observations

As explained before experiments are done at different borehole angles for both water and drilling fluids for different flow rates. The initial flow rate was high enough to transport all the cuttings in the annulus in no-stationary-particle pattern. The annular flow rate was then reduced step-wise until the initiation of stationary particles inside the annulus. At this point, for water, a dune movement profile is observed (Figure 4.23) whereas for the Fluids #2 and 3 a stationary/moving bed profile is formed (Figure 4.24). The moving particles are not perceived in the figure, however, the moving layer only exists as a small portion on top of the stationary section. In conclusion, for water, at velocities just above the MTV the cuttings are in moving beds and below that the cuttings display a dune movement profile. For Fluids #2 and 3, at velocities just above MTV the cutting are in moving bed profile but at lower velocities the cuttings will be transported in moving/stationary pattern.

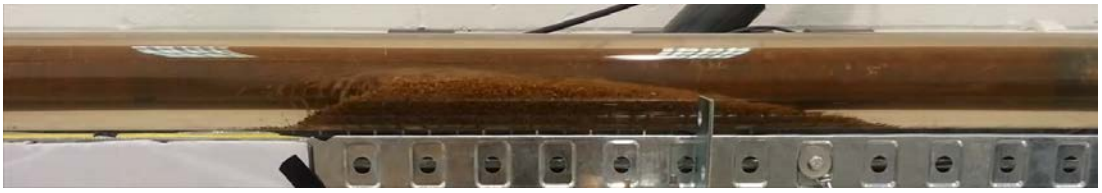

Figure 4.23 Dune movement of cuttings in Fluid #1 (water)

Figure 4.24 Stationary/moving bed of cuttings in Fluid #2

For a given drilling fluid and cuttings, there are two forces acting on the cuttings in the deviated holes that characterize the cuttings movement in the annulus space. One is the fluid velocity which its mean vector direction is always coinciding with the annulus space. Another factor is the gravitational force with its direction being always downward. At horizontal configuration, these two vectors have an angle of 90° apart and the gravity only holds the cuttings at the lower side of the wellbore. When the inclination increases the gravitation effect is divided into two components, one perpendicular to the main stream and another one acting in opposite direction to the flow velocity. This means that at a certain angle, if the pump shuts off and the mud viscosity is not adequate to hold the cuttings in suspension, then the latter force component can slide the cuttings downward. This is very important in mud design because if the rheological properties of the mud cannot hold the cuttings in suspension then problems such as pipe sticking may occur. This problem is mitigated in CTD because pump shut off happens less likely compared to conventional drilling operation.

In this study when circulation of Fluid #1 (water) was stopped, downward sliding of cuttings or Boycott movement in the annulus was seen for inclinations as low as 75°. However, for the more viscous Fluid #2 the Boycott transportation was delayed and started at an angle of 30° when the suspension of the cuttings from the gel strengths in the mud was countered by gravity settling across the annular gap on the low side of the inclined hole.

Another observation recorded during the experiments involved Group #1 cuttings (< 0.425mm) after the MTVs for water is recorded and the pump shuts down. This causes cuttings to settle down at the lower side of the annulus while the hole configuration is horizontal. After Corewell is added to the slurry in the tank to prepare mud #2 slurry, which takes 30 minutes, the pump starts again to determine the MTVs for mud #2. It is observed, it requires a high flow rate to wash out the layer of cuttings settled at the lower side of the annulus because they become sludge. To wash that zone a velocity of about 150cm/s is required, which is much larger than

40cm/s MTV of the current condition. This problem is less prominent with larger cuttings in the wellbore because high flow rate is not required to erode this bed. Since the majority of the cuttings are fine particles in mineral application, settlement of the cuttings should be avoided, otherwise, the same problem will occur and cleaning the layer of settled cuttings will require high flow rate. In CTD, for the reason that the pump shuts down less frequently than normal oil drilling, care in operation highly needs to be taken into consideration to avoid any problem.

4.4 Summary

In this chapter the detailed specifications of a designed flow loop were presented. The experimental results showed that although many parameters applied here are relevant to both sectors of the drilling industry, an overall different understanding for cuttings transportation in O&G and minex MBHCTD wells is required.

Even there is no unique answer to the rheological effect on cuttings transportation in O&G industry, the findings in this study does not follow any of the trends reported in O&G application. In conclusion, the type of mud and its rheology cannot give a generalized answer to the cuttings transportation efficiency and it needs to be in conjunction with the cuttings size.

In the next Chapter results will be presented for this study's numerical simulations of cuttings transport correspond to this Chapter's flow loop experiments.

5 Numerical simulation

In this chapter the developed numerical model for the simulation of annular cuttings transportation is presented. The governing mass and momentum balance equations for an Eulerian Granular (EG) model are introduced and the constitutive equations required to solve the model through a computational fluid dynamics approach are presented.

The developed model is used to simulate the cuttings transport in the flow loop and to make sensitivity analysis in vertical holes. The simulation is also applied in directional wells to determine the MTV and cuttings movement profile.

5.1 Introduction

Computational fluid dynamics (CFD) is the solution of fluid flow and heat transfer problems by solving the mass, momentum, heat and other governing equations with a computer simulation (Versteeg & Malalasekera, 2007). Different approaches are available to model slurry flow; that is, in this case, a mixture of solid particles (cuttings) in a drilling fluid which shows multiphase flow.

The fluid is usually treated as a continuum using the Navier-Stokes equation and therefore the Eulerian approach is applied. On the other hand, the solid particles can be treated with either an Eulerian approach by assuming them as a continuum or a Lagrangian approach where the path lines of the individual particles are tracked.

In the latter method the conservation equations are solved for the fluid as a continuous phase and the particles trajectories are determined with the equation of motion. However, the Lagrangian approach was not chosen as the cuttings distribution and their average velocity as a continuum, which are important parameters in this study, can be modelled using the Eulerian approach.

The Eulerian-Eulerian (assuming both fluid and solid as continuum) approach can be performed with one of the following methods:

- **Volume of Fluid (VOF)**: is a surface tracking technique for immiscible fluids which is not suitable for slurry modelling.

- **Mixture** model: where a mixture momentum equation with a relative velocity to describe the dispersed solid phase is required.
- **Eulerian** model: for which one continuity and one momentum equation are required for each phase that in turn increases the computational process compared to the VOF and Mixture models (Ansys, 2011).

In this study the Eulerian-Eulerian model was used for simulation purposes but as the second phase is solid it is also called Eulerian Granular (EG) model. In this model instead of tracking and focusing on the individual particles an average value for them is used instead.

5.2 Developed model

5.2.1 Governing equations

In the Eulerian model, for each phase, one continuity and one momentum equation is expressed. The continuity equation for phase q when the heat and mass transfer do not occur between phases is expressed as:

$$\frac{\partial}{\partial t}\left(\alpha_q \rho_q\right)+\nabla\cdot\left(\alpha_q \rho_q \vec{\mathrm{u}}_q\right)=0 \quad , \tag{5.1}$$

and the momentum equation is:

$$\begin{aligned}&\frac{\partial}{\partial t}\left(\alpha_q \rho_q \vec{\mathrm{u}}_q\right)+\nabla\cdot\left(\alpha_q \rho_q \vec{\mathrm{u}}_q \vec{\mathrm{u}}_q\right)=-\alpha_q \nabla p+\nabla\overline{\overline{\tau}}_q+\alpha_q \rho_q \vec{g}\\&+\left(\vec{F}_q+\vec{F}_{lift,q}+\vec{F}_{vm,q}\right)+\sum_{p=1}^{n}\left[K_{pq}\left(\vec{v}_p-\vec{v}_q\right)\right]\end{aligned} \quad . \tag{5.2}$$

where,

α = volume fraction,

q = phase,

ρ = density,

$\vec{\mathrm{u}}$ = velocity,

p = static pressure,

$\overline{\overline{\tau}}_q$ = q^{th} phase stress-strain tensor,

$\vec{F}_q$ = external body force,

$\vec{F}_{lift}$ = lift force,

$\vec{F}_{vm}$ = virtual mass force,

K_{pq} = interphase momentum exchange coefficient, and

n = number of phases,

This equation is for the liquid phase and for the solid phase a solid pressure term ($-\nabla p_s$) would be added to the right hand side of the equation.

The left hand side of the momentum equation is the rate of increase of the mixture momentum and the right hand side is the sum of different kind of forces applied on the mixture (Ansys, 2011). The sum of the volume fraction of all the phases is 1.

$$\sum_{q=1}^{n} \alpha_q = 1 \tag{5.3}$$

5.2.2 Constitutive equations

The following sections explain the required extra constitutive equations that are combined with the governing equations to solve the problem.

Turbulent models

k-ε and *k*-ω are the two commonly used turbulent models. *k* is the turbulent kinetic energy, ω is the specific dissipation rate, and ε is the rate of dissipation. *k*-ε performs better at the free steam and *k*-ω shows better results at near the wall. Shear-Stress Transport (SST) *k*-ω model uses the advantages of both *k*-ω and *k*-ε by applying *k*-ω near the wall and *k*-ε away from the wall (Ansys, 2011). In this study, in vertical annular flow *k*-ε is used and in directional wellbore conditions SST *k*-ω is applied.

For a vertical configuration the *k*-ε dispersed turbulence model is used in preference to a mixture model because the secondary solid phase cuttings are in dilute concentration in the slurry. The following equations characterize the modified *k*-ε turbulent model for the continuous phase in a multiphase slurry flow:

$$\begin{aligned}
&\frac{\partial}{\partial t}\left(\alpha_q \rho_q k_q\right) + \nabla \cdot \left(\alpha_q \rho_q \vec{u}_q k_q\right) = \nabla \cdot \left(\alpha_q \frac{\mu_{t,q}}{\sigma_k} \nabla k_q\right) \\
&+ \alpha_q G_{k,q} - \alpha_q \rho_q \varepsilon_q + \alpha_q \rho_q \Pi_{k_q} \\
&\frac{\partial}{\partial t}\left(\alpha_q \rho_q \varepsilon_q\right) + \nabla \cdot \left(\alpha_q \rho_q \vec{u}_q \varepsilon_q\right) = \nabla \cdot \left(\alpha_q \frac{\mu_{t,q}}{\sigma_\varepsilon} \nabla \varepsilon_q\right) \\
&+ \alpha_q \frac{\varepsilon_q}{k_q}\left(C_{1\varepsilon} G_{k,q} - C_{2\varepsilon} \rho_q \varepsilon_q\right) + \alpha_q \rho_q \Pi_{\varepsilon_q}
\end{aligned} \tag{5.4}$$

The parameters in these equations are defined as:

$$\Pi_{k_q} = \sum_{p=1}^{M} \frac{K_{pq}}{\alpha_q \rho_q} \left(k_{pq} - 2k_q + \vec{u}_{pq} \cdot \vec{u}_{dr} \right),$$

$$\Pi_{\varepsilon_q} = C_{3\varepsilon} \frac{\varepsilon_q}{k_q} \Pi_{k_q}, \text{ and}$$

$$\mu_{t,q} = C_\mu \rho_q \frac{k_q^{\,2}}{\varepsilon_q}.$$

where

μ_t = turbulent viscosity,

G_k = production of turbulent kinetic energy,

Cs = constants,

σ_k and σ_ε = turbulent Prandtl numbers for k and ε,

Π = influence of the dispersed phase on the continuous phase,

M = number of secondary phases,

k_{pq} = covariance of the velocities of the continuous phase q and the dispersed phase p,

k_q = turbulent kinetic energy for phase q,

$\vec{u}_{pq}$ = relative velocity, and

$\vec{u}_{dr}$ = drift velocity.

Constants and turbulent Prandtl numbers values are:

$C_{1\varepsilon} = 1.44$, $C_{2\varepsilon} = 1.92$, $C_{3\varepsilon} = 1.2$, $C_\mu = 0.09$, $\sigma_k = 1.0$, $\sigma_\varepsilon = 1.3$.

Extra equations are required based on the Tchen-theory to determine the turbulent quantities in the dispersed phase (Ansys, 2011).

The main equations used for SST k-ω are:

$$\begin{aligned} \frac{\partial}{\partial t}(\rho k) + \frac{\partial}{\partial x_i}(\rho k u_i) &= \frac{\partial}{\partial x_j}\left(\Gamma_k \frac{\partial k}{\partial x_j} \right) + \tilde{G}_k - Y_k + S_k \\ \frac{\partial}{\partial t}(\rho \omega) + \frac{\partial}{\partial x_j}(\rho \omega u_j) &= \frac{\partial}{\partial x_j}\left(\Gamma_\omega \frac{\partial \omega}{\partial x_j} \right) + G_\omega - Y_\omega + D_\omega + S_\omega \end{aligned} \tag{5.5}$$

where,

$\tilde{G}_k$ = generation of k cause by mean velocity gradient and is calculated form G_k,

G_ω = generation of ω,

Γ_k and Γ_ω = effective diffusivity of *k* and ω, respectively,

Y_k and Y_ω = dissipation of *k* and ω caused by turbulence,

D_ω = cross-diffusion term,

S_k and S_ω = source terms.

All of these terms have their own definition and equations. The full list of these equations is presented in the ANSYS Fluent Theory Guide (2011).

Solid viscosity

In the EG approach a granular viscosity needs to be specified because the solid cuttings are treated as fluid. Solid viscosity consists of two components, shear and bulk viscosities, whose sources are the momentum exchange of the particles.

The granular shear viscosity (μ_s) by itself comprises of three subcomponents: collisional ($\mu_{s,col}$), kinetic ($\mu_{s,kin}$) and frictional ($\mu_{s,f}$) viscosities.

$$\mu_s = \mu_{s,col} + \mu_{s,kin} + \mu_{s,f} \tag{5.6}$$

Collisional component is determined with the following equation:

$$\mu_{s,col} = \frac{4}{5}\alpha_s{}^2 \rho_s d_s g_{0,ss}(1+e_{ss})\left(\frac{\theta_s}{\pi}\right)^{1/2} \tag{5.7}$$

where,

$g_{0,ss}$ = radial distribution function which will be explained later,

e_{ss} = solid particles restitution coefficient which is the ratio of their speeds after to before collision, and

θ = granular temperature.

The kinetic component of solid shear viscosity can be determined either with Syamlal et al. (1993) or Gidaspow et al. (1992) models. In this study Gidaspow et al. (1992) model is used in the form of:

$$\mu_{s,kin} = \frac{10\rho_s d_s\sqrt{\theta_s\pi}}{96 g_{0,ss}(1+e_{ss})}\left[1+\frac{4}{5}\alpha_s g_{0,ss}(1+e_{ss})\right]^2. \tag{5.8}$$

The frictional component which arises due to the friction between the solid particles is neglected because it is only dominant when the solid concentration is close to the packing limit and the actual cuttings content of the slurry is very dilute; ideally less than 5% v/v and 1% v/v in the flow loop experiments conducted during this study.

Granular bulk viscosity (λ_s) expresses the resistance of particles to expansion and compression which determines with Lun et al. (1984) model:

$$\lambda_s = \frac{4}{3}\alpha_s \rho_s d_s g_{0,ss}(1+e_{ss})\left(\frac{\theta_s}{\pi}\right)^{1/2} \tag{5.9}$$

Radial distribution

Radial distribution shows the probability of a particle colliding with another nearby. For *N* number of solid phases the following equation developed by Lun et al. (1984) is used:

$$g_{0,ll} = \left[1-\left(\frac{\alpha_s}{\alpha_{s,\max}}\right)^{\frac{1}{3}}\right]^{-1} + \frac{1}{2}d_l \sum_{k=1}^{N}\frac{\alpha_k}{d_k} \tag{5.10}$$

$$\alpha_s = \sum_{k=1}^{M}\alpha_k$$

where,

d = average diameter of the particles,

α_s = total volume fraction of the solid phase, and

$\alpha_{s,\max}$ = packing limit.

Particle pressure

When the solid volume fraction is less than the packing limit then this term is used in the granular momentum equation as ∇p_s. It consists of two terms one of which is due to kinetic energy and another one due to the collision of particles. The following equation developed by Lun et al. (1984) is used to determine particle pressure:

$$p_s = \alpha_s \rho_s \theta_s + 2\rho_s(1+e_{ss})\alpha_s{}^2 g_{0,ss}\theta_s \tag{5.11}$$

Granular temperature

Granular temperature is a measure of the internal energy stored within the particles after they collide with each other. It is proportional to the kinetic energy of the random and fluctuating velocity of the particles. Based on the kinetic theory, the transport equation is:

$$\frac{3}{2}\left[\frac{\partial}{\partial t}\left(\alpha_s\rho_s\theta_s\right)+\nabla\cdot\left(\alpha_s\rho_s\vec{v}_s\theta_s\right)\right]=\left(-p_s\bar{\bar{I}}+\bar{\bar{\tau}}_s\right):\nabla\vec{v}_s \\ +\nabla\cdot\left(k_{\theta_s}\nabla\theta_s\right)-\gamma_{\theta_s}+\phi_{ls} \quad (5.12)$$

The terms are explained in the following form:

Rate of change of kinetic term + convective term = generation of energy by solid stress tensor + diffusion of energy + collisional dissipation of energy + energy exchange between liquid phase *l* and solid phase *s*.

The following equations developed by Gidaspow et al. (1992) are applied to complement Equation (5.12):

$$k_{\theta_s}=\frac{150\rho_s d_s\sqrt{\theta\pi}}{384(1+e_{ss})2g_{0,ss}}\left[1+\frac{6}{5}\alpha_s g_{0,ss}(1+e_{ss})\right]^2+2\rho_s\alpha_s{}^2 d_s(1+e_{ss})g_{0,ss}\theta_s\sqrt{\frac{\theta_s}{\pi}}$$

$$\gamma_{\theta_s}=\frac{12\left(1-e_{ss}{}^2\right)g_{0,ss}}{d_s\sqrt{\pi}}\rho_s\alpha_s{}^2\theta_s{}^{3/2} \quad (5.13)$$

$$\phi_{ls}=-3K_{ls}\theta_s$$

Interactions between the phases

As there are both liquid and cuttings phases in the flow the interphase exchange coefficients (K_{pq}) between the phases is necessary. To determine the fluid-solid exchange coefficient, the liquid phase is assumed to be the continuous phase and the drag between the liquid and solid particles is measured. Among all the available models, Gidaspow et al. (1992) model, which is a combination of two other models, is used because it is the more suitable model for slurry flows and covers a wider range of solid concentrations. When the fluid concentration is more than 0.8, Wen and Yu (1966) model is applied and otherwise Ergun (1952) equation is utilized:

For $\alpha_l > 0.8$:

$$K_{sl}=\frac{3}{4}C_D\frac{\alpha_s\alpha_l\rho_l\left|\vec{v}_s-\vec{v}_l\right|}{d_s}\alpha_l{}^{-2.65}$$

$$C_D=\frac{24}{\alpha_l\,\mathrm{Re}_s}\left[1+0.15(\alpha_l\,\mathrm{Re}_s)^{0.687}\right] \quad (5.14)$$

$$\mathrm{Re}_s=\frac{\rho_l d_s\left|\vec{v}_s-\vec{v}_l\right|}{\mu_l}$$

For $\alpha_l < 0.8$:

$$K_{sl} = 150\frac{\alpha_s(1-\alpha_l)\mu_l}{\alpha_l d_s^{\,2}} + 1.75\frac{\rho_l \alpha_s \left|\vec{v}_s - \vec{v}_l\right|}{d_s}$$

Particle-particle and particle-wall restitution coefficients are equal to 0.9 and 0.2 , respectively.

5.3 Simulation procedure

Figure 5.1 shows the procedure used to perform a numerical simulation in this study. The first step is to design and built a representative three dimensional (3D) model with a geometry builder software; in this study, ANSYS "DesignModeler". The inner and outer diameters and the length of the annulus section are applied to build the geometry. In addition, the inclination of the borehole needs to be set. To reduce the amount of computation, a plane of symmetry divides the annulus into two equal haves vertically along the flow direction.

Then, the mesh needs to be applied in ANSYS Meshing. To account for near wall treatment and having smaller mesh sizes near the walls, two inflation methods are applied to the inner and outer walls. Figure 5.2 shows the meshing applied to the half of an annulus section since the plane of symmetry divided it in half. All of the annular boundaries are named in this module and they are used in the ANSYS Fluent module to provide the boundary conditions. These boundaries are the:

- Velocity inlet, where the velocity of the slurry entering the annulus is characterized.
- Pressure outlet, where the slurry exits from the annulus under a zero gauge pressure.
- Inner wall, which indicates the outer wall of a drill string or CT.
- Outer wall, which indicates the borehole wall.
- Plane of symmetry, which limits duplication of the other half of the wellbore by the ANSYS Fluent software and reduces the computational time.

Computation of the simulation is performed in ANSYS Fluent version 14.0. In this module the flow regime needs to be determined first. It is derived from the APL calculation as presented earlier in Section 3.4. If the flow regime is laminar the laminar flow model is chosen and if it is turbulent either *k-ε* or SST *k-ω* models are used. For the multiphase model the Eulerian approach has been selected and consequently any kind of fluid and solid (cuttings) materials needs to be defined as a

fluid. The ANSYS Fluent software accepts both the Power Law and Herschel-Bulkley as fluid rheological models and the values for their required parameters also need to be input.

When the solid is selected as a granular model its properties and the models to define solid viscosity, radial distribution, particle pressure, granular temperature and interactions between the phases are selected. The boundary conditions are assigned to each boundary and for each phase.

Finally the type of the solution method is chosen and then the solution is initialized. A steady state solution approach is used first to check whether it is possible to reach a converged and sensible result. Otherwise the transient model is used. The time step size should be chosen carefully to avoid divergence.

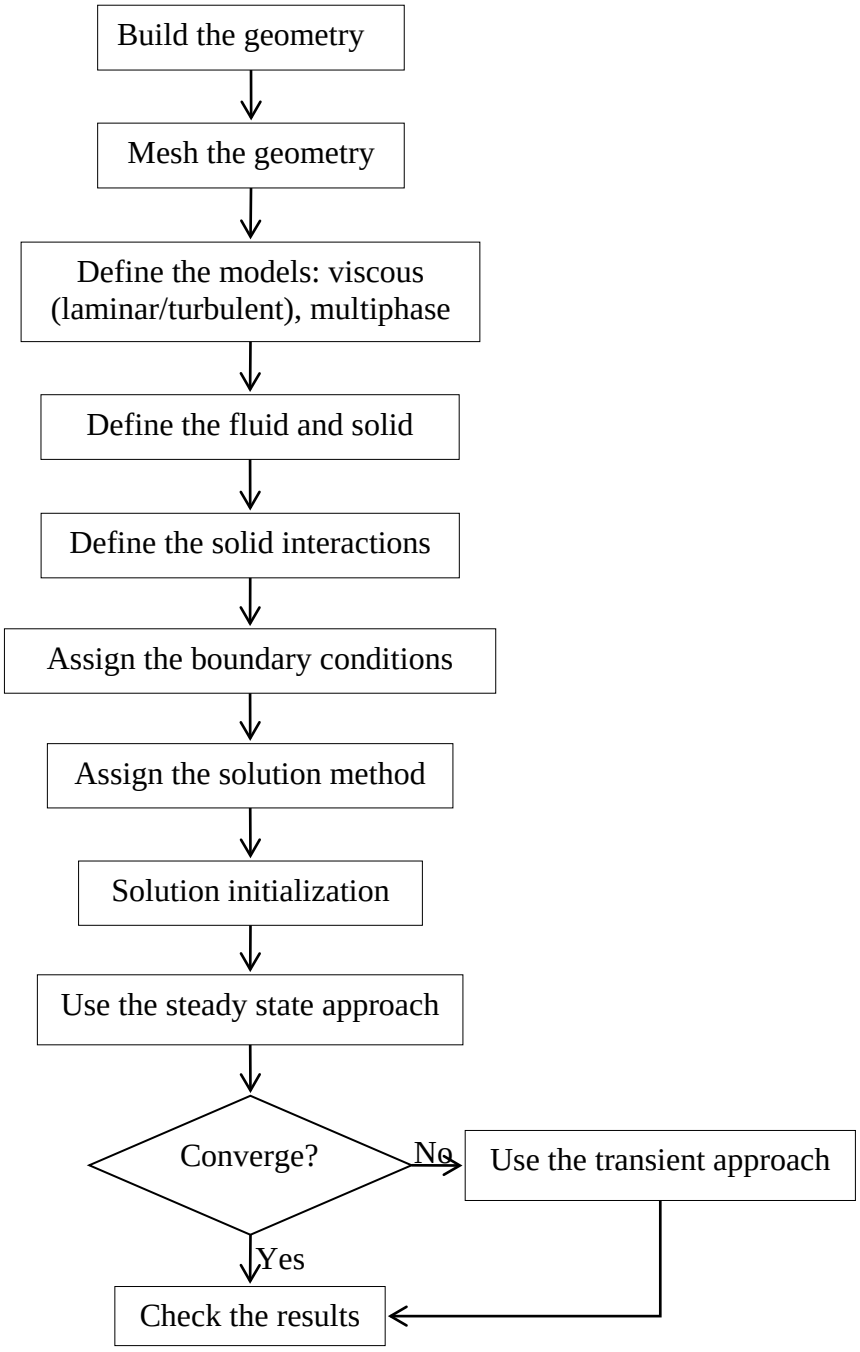

Figure 5.1 The flowchart for numerical simulation

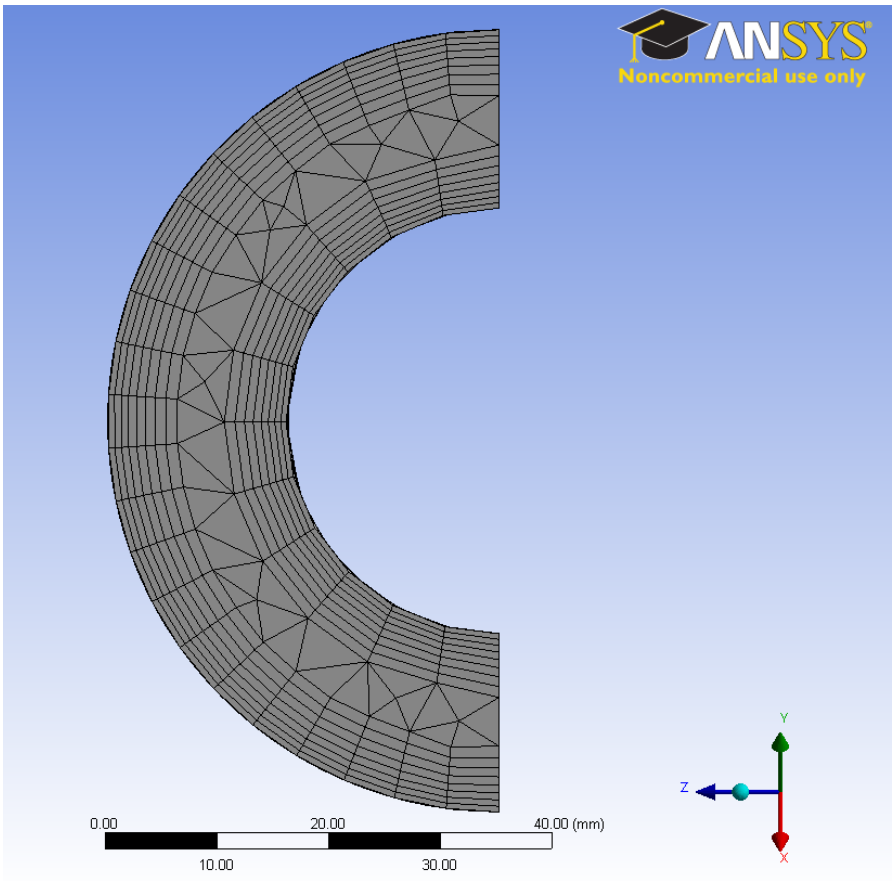

Figure 5.2 Meshing applied to the face of annulus which the plane of symmetry divides it into half

When the turbulent model is used, there are two parameters that need to be determined in order to characterize the turbulency; notably, turbulent intensity and turbulent length scale. Turbulent intensity (I) is the ratio of velocity fluctuation to inlet velocity and is calculated using the following equation:

$$I = 0.16\,\mathrm{Re}^{-1/8}. \tag{5.15}$$

The turbulent length scale (l) is a parameter that characterizes the size of large eddies. The following equation is used to determine the turbulent length scale:

$$l = 0.07 d_{hyd} \tag{5.16}$$

In this equation d_{hyd} is the hydraulic diameter of the flow medium.

Another parameter that is needed to be determined is granular temperature (θ):

$$\theta = \frac{1}{3}u'^{2}$$
$$u' = UI \tag{5.17}$$

Where, u' is the velocity fluctuation and U is the free stream velocity (Saxena, 2013).

5.4 Numerical simulation results

The developed model was used for both vertical and directional boreholes. It is initially used to model vertical wells and then applied to simulate directional wells. The results are presented in the following sections.

5.4.1 Vertical wells

Mini flow loop

Initial numerical simulations were performed to determine the APL in MBHCTD vertical boreholes. To achieve an accurate and reliable model the developed model needs to be validated against experimental results. A simple mini flow loop was designed and used for slurry transport simulations in the laboratory. The annular section was simulated to determine if water velocity could carry the particles out of the annulus. The annulus dimensions were 1.9cm/4.2cm (0.74in/1.65in) with a length of 65cm (25.6in) and the sand particles occupy 10cm of the bottom section of the annulus. The simulation were performed with two different sand particles sizes of 0.5 (0.2) and 3mm (0.12in). The cuttings have a density of 2600kg/m^3 (21.7ppg) and when the pump started, the water with a velocity of 0.16m/s (31.5ft/min) flowed from the bottom of the annulus to the top. These conditions were simulated with a transient model in ANSYS Fluent 14. After the hole and tubular geometry was input in ANSYS, a mesh was applied to the profile.

Figure 5.3 shows the experiment observation for comparison against the numerical simulation results. As is seen in the left picture of Figure 5.3, all the cuttings of 0.5mm (0.02in) are transported out of the annulus after a certain time and only the water phase remains. An identical result was obtained through numerical simulation. However, for 3mm (0.12in) particle sizes, all the cuttings remained at the bottom of the annulus as the results of both laboratory and numerical simulations show in the right picture of Figure 5.3.

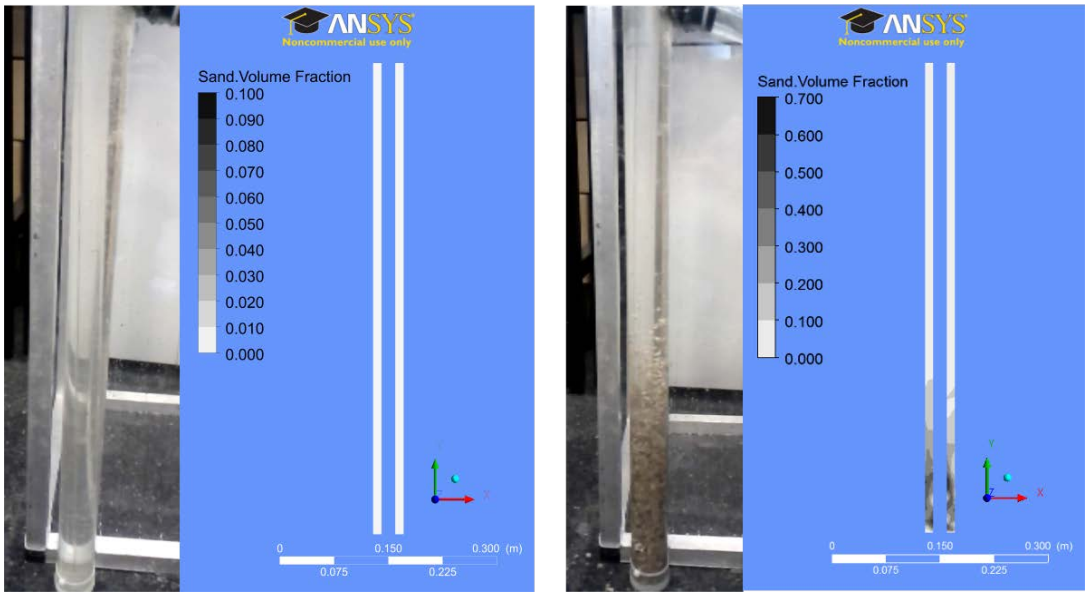

Figure 5.3 Comparison of cuttings transport modelled physically using a vertical mini flow loop and simulated numerically using CFD for two cuttings sizes of 0.5mm (left) and 3mm (right)

Sensitivity analysis for vertical flow modelling

The CFD model that was validated by the mini flow loop experiments was used in this section to determine the APL with the same sized cuttings that were used to examine their effect on the rheological properties of the drilling muds (see Chapter 3).

Figure A.1 shows that the size of the majority (≈ 60%) of the cuttings is finer than 20 microns. In addition, the cuttings concentration was kept under 5% v/v in the annulus for the simulations performed in this study (Albright et al., 2005; Kelessidis & Bandelis, 2004).

When the fluid first enters the annulus the flow is uniform; that is, a constant flow velocity exists in the entrance cross section. However, due to the no-slip condition at the wall and viscous shearing forces of the fluid, the velocity at the wall tends toward zero. This leads to higher velocities away from the wall to satisfy mass conservation. The distance from the entrance to the occurrence of fully developed flow is called hydrodynamic entrance region (Cengel & Cimbala, 2006). When the pressure loss in a pipe section is determined the entrance effect needs to be included in the analysis to avoid any miscalculation. The entrance length for the turbulent flow can be approximated by the following equation:

$$L_{\text{entrance, turbulent}} \approx 10 d_{hyd} \,. \tag{5.18}$$

In the above equation d_{hyd} is the hydraulic diameter. Assuming an annular configuration of 5cm/8cm (1.97in/3.15in), the entrance length would be 30cm

(11.8in) and therefore the length of the pipe needs to be longer. The pipe length used in the numerical model was 1m. For this annulus configuration the number of mesh elements was 14520. In this case the k-ε turbulent model was applied.

The results of sensitivity analysis of different parameters are shown in Figure 5.4 to Figure 5.6. As noted before, high annular velocities and turbulent flow arise because a high pump rate is needed to turn the downhole motor/turbine for rotary CTD. It is quite obvious that increasing fluid velocity increases the pressure loss because more energy would be required to pump the fluid with higher velocity.

As it is seen from Figure 5.4, adding 5% v/v cuttings particles to the water shifts the clean water curve upward in the pressure loss chart consistently for both annulus configurations. Existence of cuttings increases the pressure loss because the cuttings lose momentum when they hit each other and the borehole or CT walls. Also, more gravitational forces is applied to the cuttings causing them to settle out from suspension. In addition, narrower annular configurations show higher pressure loss for a constant velocity.

Figure 5.5 shows the effect of cuttings density on the APL. Based on the concept of momentum loss, cuttings with higher densities lose more momentum due to hitting each other and the borehole or CT walls and in addition they experience higher gravitational forces. These are the reasons resulting in higher APL for denser particles.

Figure 5.6 shows the effect of cuttings sizes on the APL for two velocities. Based on the Stokes number concept, smaller cuttings follow the fluid path much easier than larger cuttings. It is the case that larger cuttings dampen the flow especially at lower annular velocities. For instance the APL difference between 1 and 2000 microns cuttings with a slurry mixture velocity of 3m/s (590ft/min) is 61Pa/m (0.0027psi/ft); however the difference for mixture velocity of 1m/s (197ft/min) is 279Pa/m (0.012psi/ft), as seen in Figure 5.6.

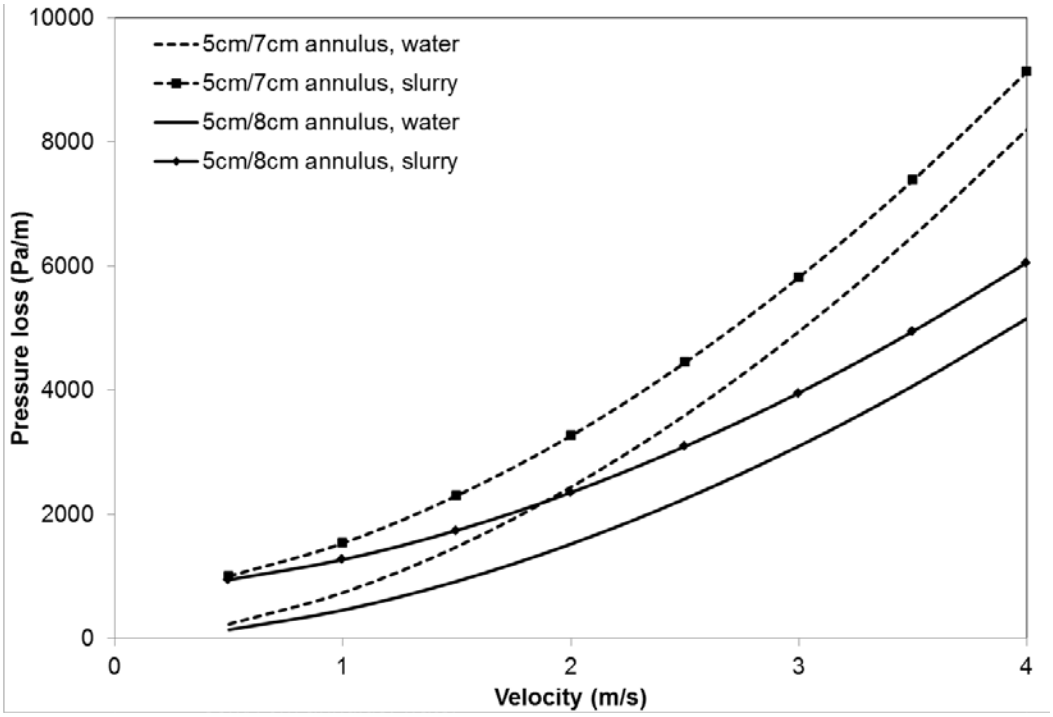

Figure 5.4 Effect of annulus dimension, annular velocity and cuttings on APL. Cuttings size = 20μm; cuttings concentration in slurry = 5% v/v; cuttings density = 2600kg/m^3

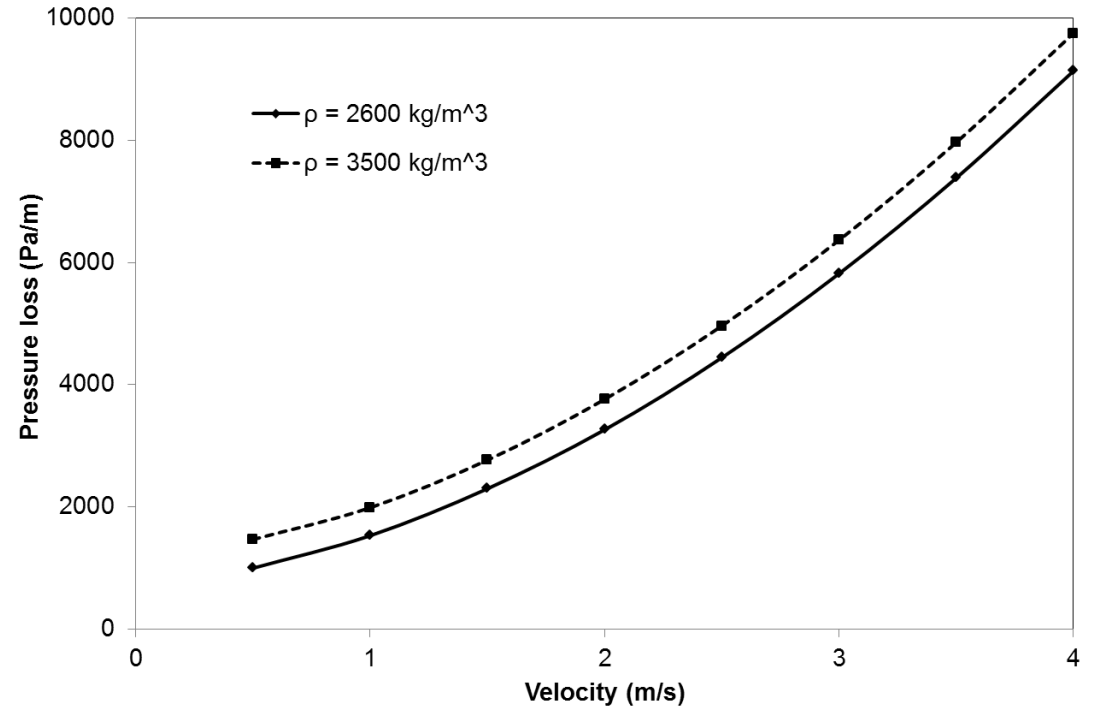

Figure 5.5 Effect of cuttings density on APL. Cuttings size = 20μm; cuttings concentration = 5% v/v; annulus = 5cm/7cm

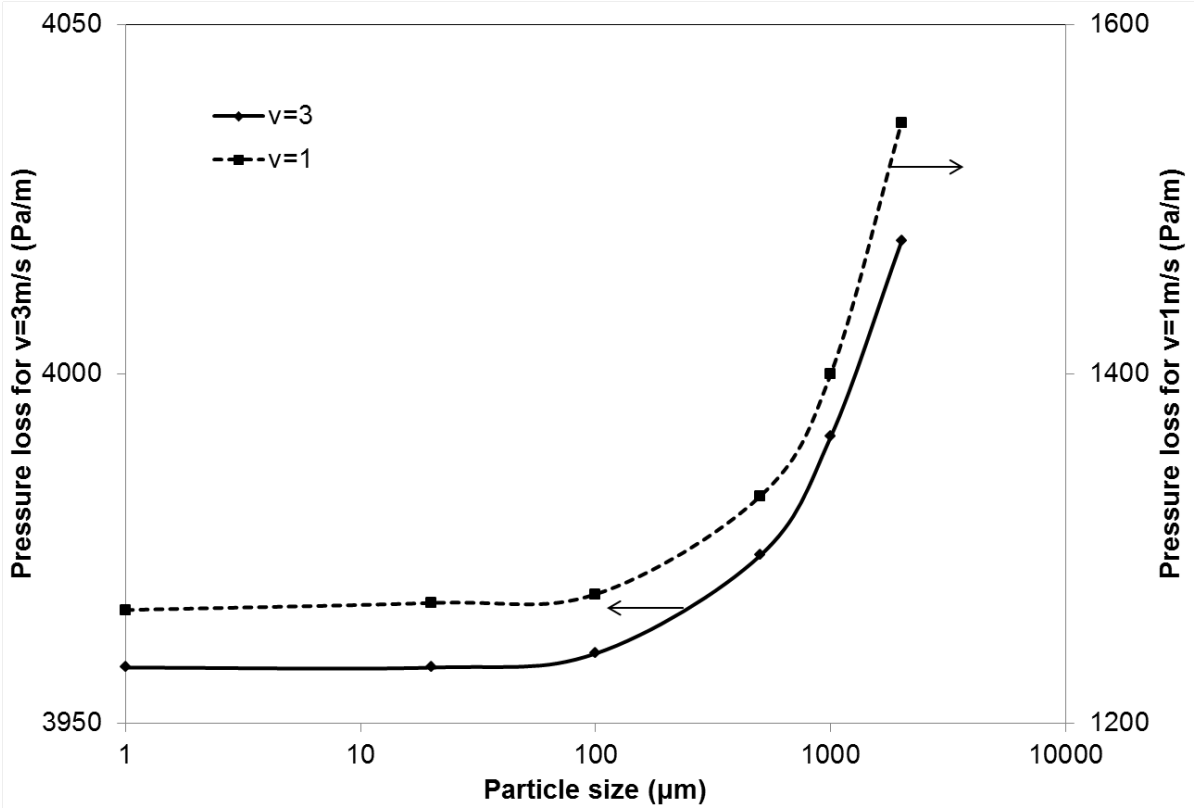

Figure 5.6 Effect of cuttings size on APL. Cuttings density = 2600kg/m^3; cuttings concentration = 5% v/v; annulus = 5cm/8cm

5.4.2 Directional wells and minimum transportation velocity (MTV)

In directional wells the cuttings need to be in the moving bed regime to avoid them from mixing. Therefore the flow rate needs to be chosen in such a way to put them into this mode and to validate the numerical model with the experimental results the corresponding flow loop set up specifications were modelled in the simulation.

The inner and outer diameters are 38.1 (1.5) and 70mm (2.76in), respectively and the length of the simulated annulus is 4m (13.12ft). The experimental data on the flow loop was recorded and the annular flow was observed at a “viewing window” which was 3m (9.84ft) from the entrance to the annulus (1m (3.28ft) from the exit from the annulus).

Wall roughness height is another parameter that needs consideration since the cuttings are in contact with the pipes especially the plexiglass tube. The wall roughness height for the plexiglass and rusted coiled tube steel tubes are 0.001mm and 1mm, respectively (Engineering ToolBox, 2014).

The Phase Coupled SIMPLE solution method was chosen to solve the equations of momentum. The discretisation method for gradient was chosen to be the least squares cell based method and the first order upwind method was applied to the other

parameters such as momentum, volume fraction, granular temperature, turbulent kinetic energy and specific dissipation rate. Initially the Under-relaxation factors were set at their default values which caused the simulation to diverge. To solve this issue the under-relaxation factors were reduced and in turn the simulation converged. This has been the main problem in the continuity residuals.

The residuals show the convergence in the calculation of each variable. In the transient mode for each time step, the calculation continues until all the residuals reach the convergence criteria or the number of iterations at each time step reaches a limiting number. For example, the convergence criterion for the continuity equation is set to 10^{-4}. Figure 5.7 shows an example of the residuals for a transient model where the changes in the residual values are a function of changing the iterations. The time value is 5.6sec and the maximum number of iterations per time step was 150. The parameters monitored to determine the residuals are shown as a legend in the top left hand side of the figure.

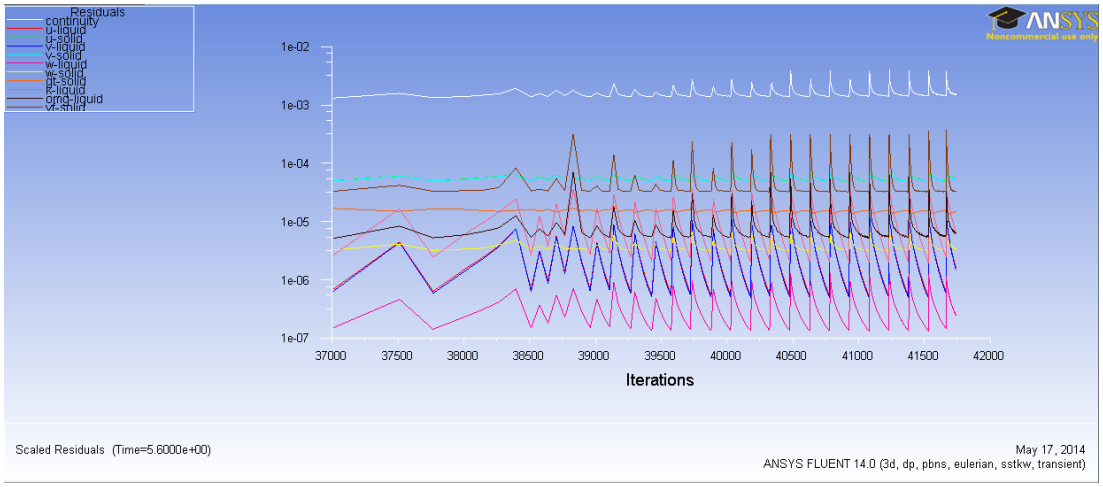

Figure 5.7 An example of monitoring the residuals in a transient calculation

The coding used in this study to determine the characteristics of the simulation was:

Mud type - Mud flow velocity - Cuttings size - Cuttings density - Cuttings concentration - Borehole inclination

As an example “Mud2-1.3m/s-2.6mm-2.75g/cc-1%-45°” means that mud #2 was pumped at a velocity of 1.3m/s carried cuttings with an average diameter of 2.6mm and density of 2.75g/cc at a concentration of 1% v/v along an annulus that was inclined to 45°.

In the above simulations it was found that the steady state mode does not converge so the transient mode was applied. The proper determination of the time

step plays a key role in convergence of the model. If it is too high it causes the model to diverge and if it is too low it takes it long time to converge.

The numerical simulations were carried out based on the laboratory experiments performed in the flow loop. As the cuttings sizes were reduced by attrition during the flow loop experiments the original and final cuttings sizes were used respectively for mud #1 and mud #3. When mud #2 is used an average value of the original and final cuttings sizes was applied.

The initial case that the CFD simulation has been performed was

Mud2-1.3m/s-2.6mm-2.75g/cc-1%-45°.

The SST k-ω turbulent model was used because the cuttings are more attached to the wall and this model is more representative of such situations. The time step size was chosen to be 0.02sec and the simulation continued for 10sec for the cuttings to reach the end of the annulus space. The computer that has been used for this study had an Intel Xeon CPU with 6 cores at 3.47GHz and 12 GB RAM. It took 5 days to complete this simulation.

A scalar cuttings velocity was defined to account for cuttings movement in the direction of the flow in the annulus space:

$$u_{\text{Flow Direction}} = u_y \sin\theta + u_x \cos\theta \tag{5.19}$$

where,

u_x and u_y = flow velocity in the x and y directions, respectively,

$u_{\text{Flow Direction}}$ = velocity in the flow direction, and

θ = hole inclination.

The same parameter called velocity magnitude is available in ANSYS but it does not account for the direction of the cuttings movement (i.e. in or opposite to the direction of the flow). Therefore the parameter was re-defined to consider the direction of the velocity magnitude.

Figure 5.8 shows the cuttings volume fraction (left) and cuttings velocity in the flow direction in the annulus. The white area between the two coloured strips is the inner pipe diameter. The + sign in the middle of the image indicates the viewing window (as described and defined earlier). The cuttings volume fraction is shown as a fraction (not % v/v) and it shows that the cuttings are accumulated at the bottom of the annulus due to the gravitational force.

The right hand image in Figure 5.8 shows that the velocity of the cuttings near the lower wall is zero and this is in agreement with the experimental results. Although the velocity of the slurry near the low side wall due to the no-slip condition is zero, the static condition is extended more away from the wall. The cuttings concentration along the top side of the annulus is not an absolute zero but it is infinitesimal and therefore the cuttings velocity is calculated.

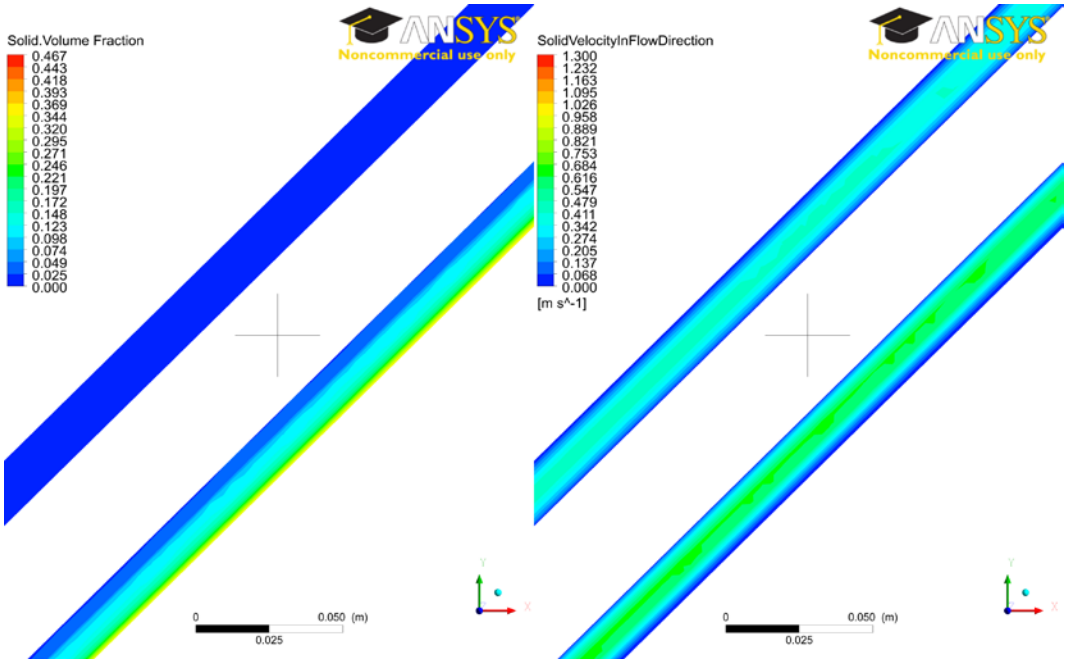

Figure 5.8 Cuttings volume fraction (left) and cuttings velocity in the direction of the annulus (right) on the plane of symmetry 3m away from the entrance for Mud2-1.3m/s-2.6mm-2.75g/cc-1%-45°

Figure 5.9 shows the results at the cross section of the annulus at the viewing window. The left hand side image shows the cuttings concentration distribution throughout the annulus. It shows a concentration of 34.6% v/v at the bottom of the borehole. Due to the viscosity of the drilling fluid some of the cuttings are held with the mud in the lower half of the annulus. On the right hand side the cuttings velocity along the annulus are shown. Although the entrance fluid velocity is 1.3m/s (256ft/min), the maximum cuttings velocity is 0.71m/s (138ft/min). This is due to the gravitational force acting on the cuttings and frictional force between the moving cuttings.

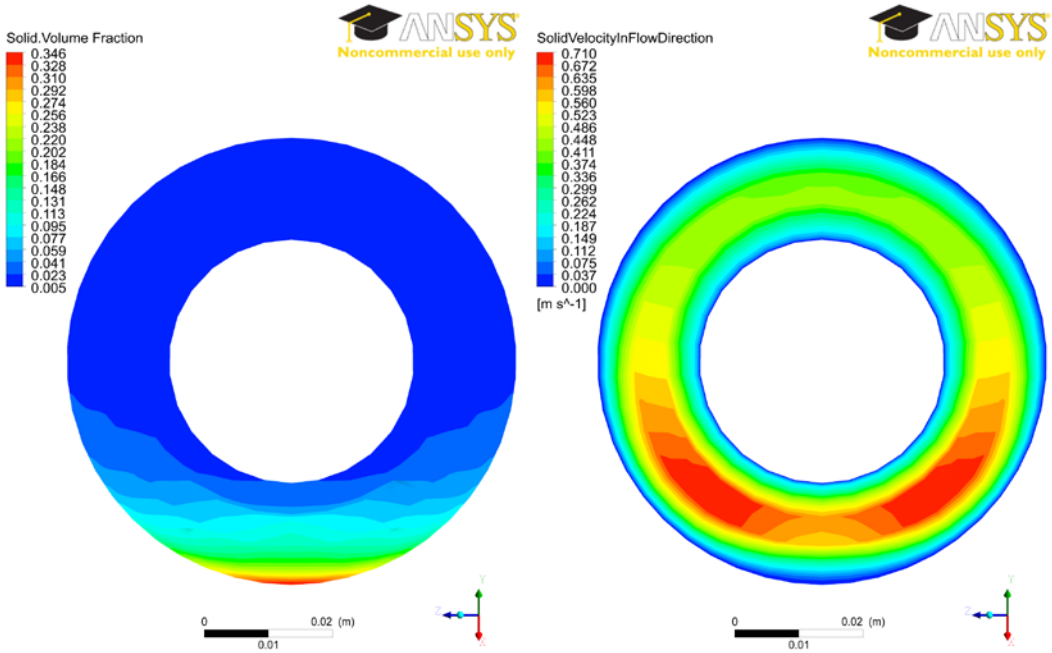

Figure 5.9 Cuttings volume fraction (left) and cuttings velocity in the direction of the annulus (right) on a cross section of the annulus 3m away from the entrance for Mud2-1.3m/s-2.6mm-2.75g/cc-1%-45°

Figure 5.10 shows the mud velocity in the annulus direction alongside the cuttings concentration. If the cuttings were not present in the mud the maximum flow occurred at the centre of the annulus and was uniformly distributed in the upper and lower sides of the annulus. However, because the cuttings occupy part of the lower side of the annulus the maximum mud velocity shifted to the upper side of the annulus and reached up to 1.9m/s (374ft/min). The mud velocity close to the cuttings in the lower side of the annulus is much slower than the entrance velocity of 1.3m/s (256ft/min) and this is due to the dampening of the flow by the cuttings.

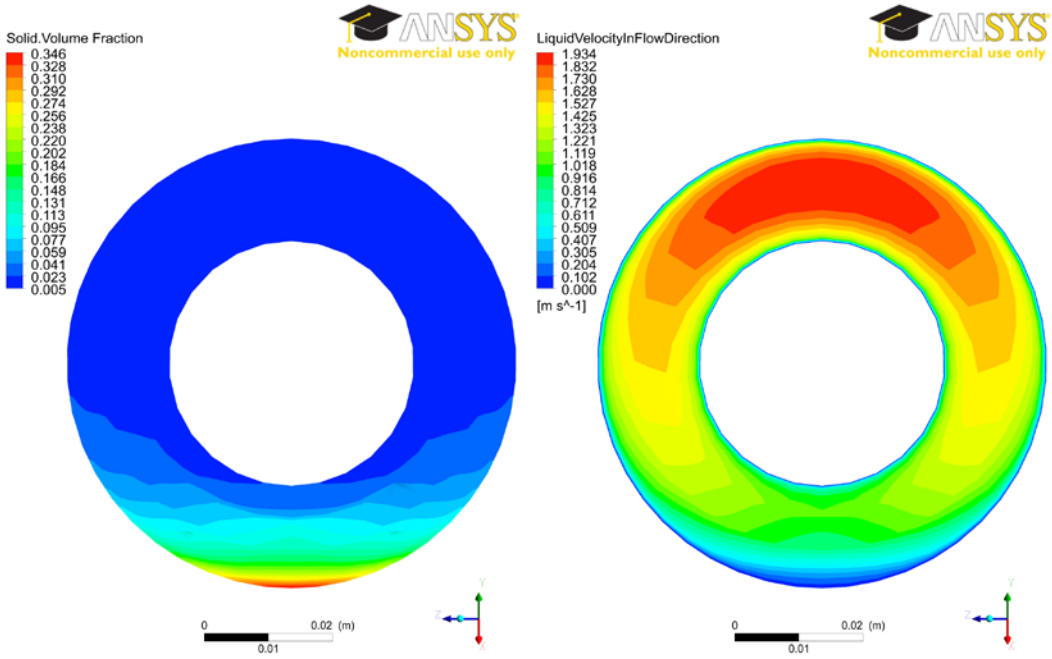

Figure 5.10 Cuttings volume fraction (left) and fluid velocity in the direction of the annulus (right) on a cross section of the annulus 3m away from the entrance for Mud2-1.3m/s-2.6mm-2.75g/cc-1%-45°

To check the effect of the flow rate the simulations were repeated at a higher flow velocity of 1.5m/s (295ft/min) and the results are shown in Figure 5.11. By comparison with Figure 5.9 that corresponds to a 1.3m/s (256ft/min) flow velocity significant change in the maximum cuttings volume fraction on the low side of the annulus can be seen as a results of a wider distribution of cuttings throughout the annulus. In addition the cuttings velocity in the annulus direction indicates that the velocity near the lower side of the wall is not so close to zero anymore and that the cuttings are transported in moving bed regime. Moreover, the maximum cuttings velocity is higher due to the overall increase in slurry velocity.

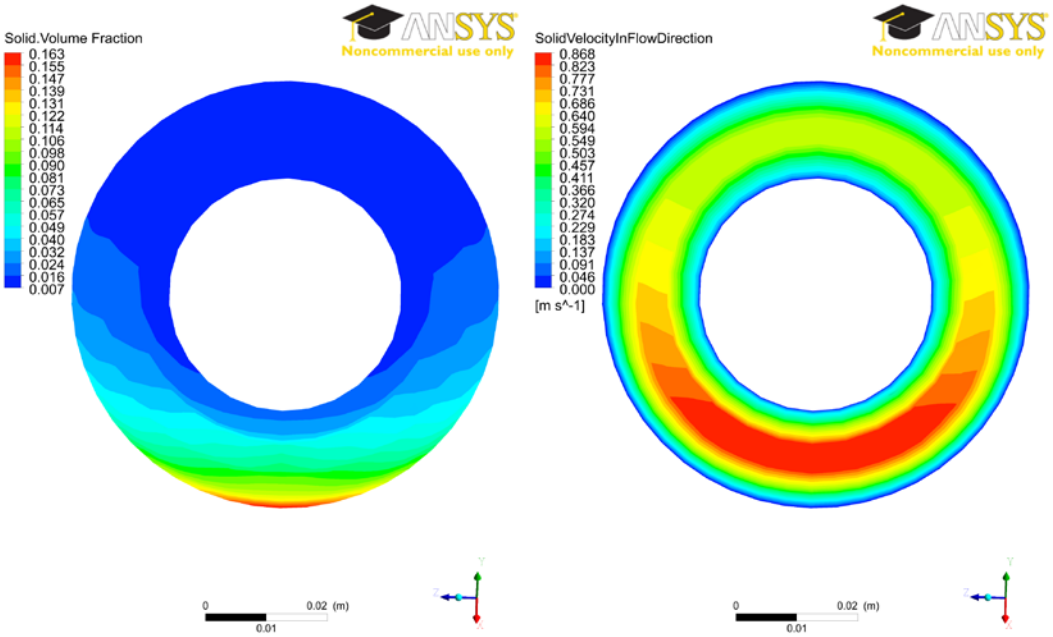

Figure 5.11 Cuttings volume fraction (left) and cuttings velocity in the direction of the annulus (right) on a cross section of the annulus 3m away from the entrance for Mud2-1.5m/s-2.6mm-2.75g/cc-1%-45°

To study the effect of mud rheology, mud #1 (i.e. water) was numerically simulated in the same way as previous cases at its MTV with the specifications:

Mud1-0.7m/s-0.068mm-2.8g/cc-1%-75°.

Here, the viscosity of the mud is less than the other two previous cases. The results of simulations presented in Figure 5.12 and Figure 5.13, indicates that the cuttings are settled at the bottom of the annulus because water does not have carrying capacity to hold the cuttings. The velocity of the cuttings near the wall confirms that it is nearly zero. At the MTV for both cases it can be seen that the viscous drilling fluid has a higher capacity to hold the cuttings even if the cuttings are larger.

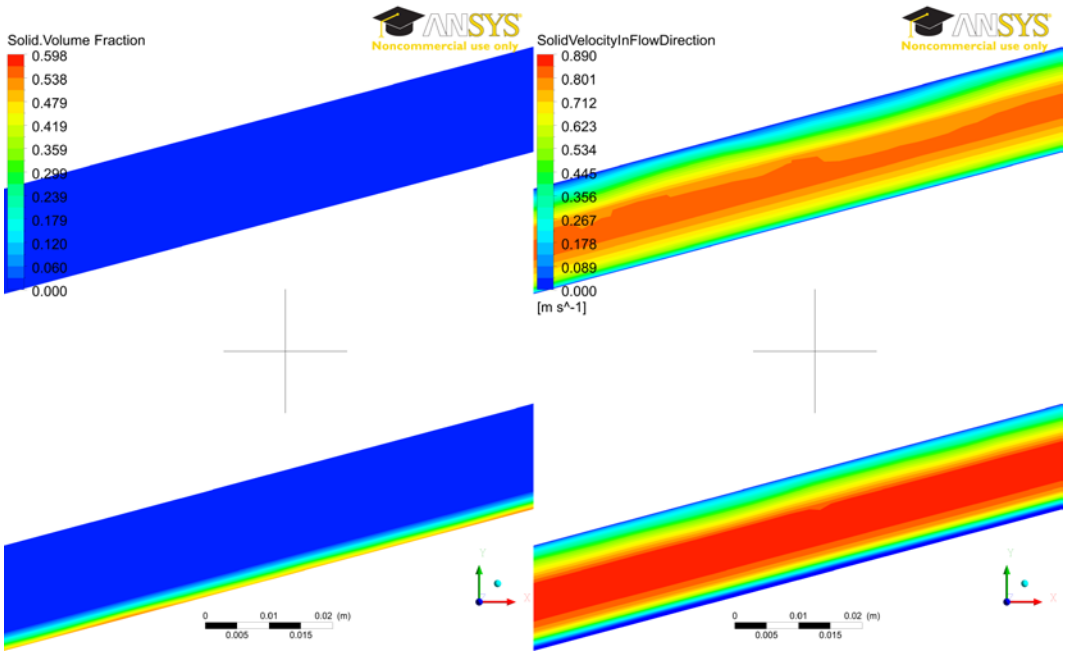

Figure 5.12 Cuttings volume fraction (left) and cuttings velocity in the direction of the annulus (right) on the symmetry plane 3m away from the entrance while for Mud1-0.7m/s-0.068mm-2.8g/cc-1%-75°

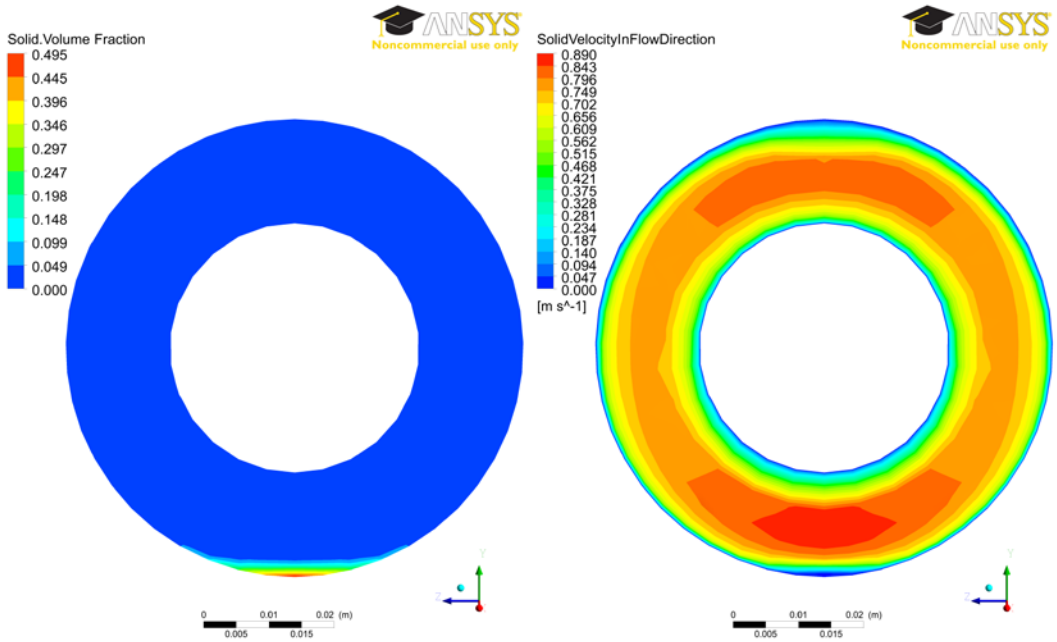

Figure 5.13 Cuttings volume fraction (left) and cuttings velocity in the direction of the annulus (right) on a cross section of the annulus 3m away from the entrance for Mud1-0.7m/s-0.068mm-2.8g/cc-1%-75°

The results of simulations corresponding to an increase in flow velocity from 0.7m/s (138ft/min) to 0.9m/s (177ft/min) is shown in Figure 5.14. Comparing Figure 5.13 and Figure 5.14 shows that the maximum cuttings concentration reduces from 49.5% v/v to 44% v/v and the maximum velocity increases from 0.89m/s (175ft/min) to 1.156m/s (228ft/min). The velocity of the cuttings near the wall is not zero and this shows that the cuttings are in moving bed.

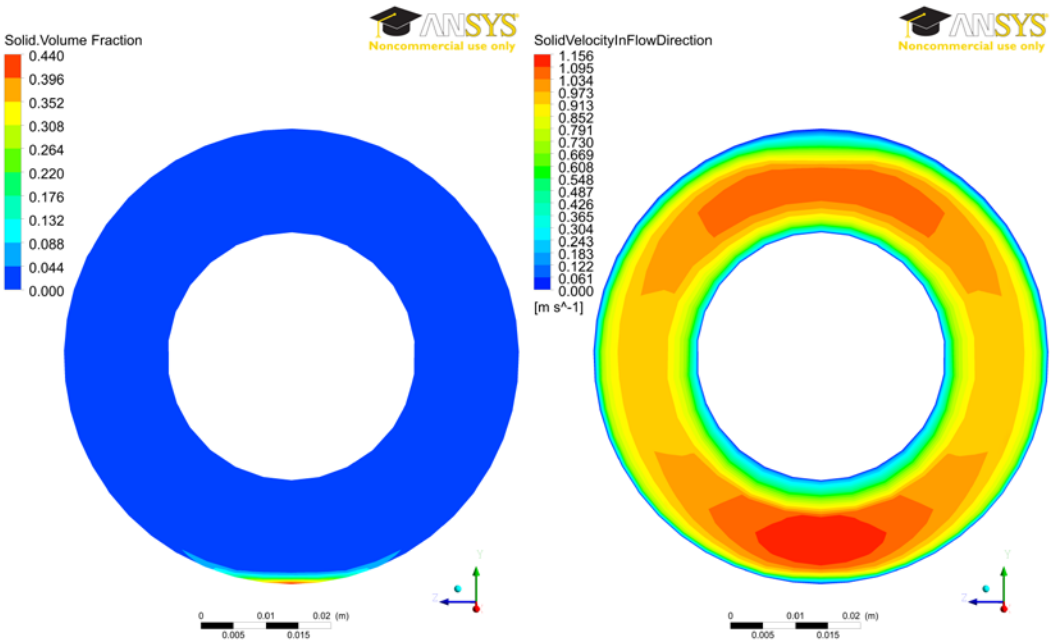

Figure 5.14 Cuttings volume fraction (left) and cuttings velocity in the direction of the annulus (right) on a cross section of the annulus 3m away from the entrance for Mud1-0.9m/s-0.068mm-2.8g/cc-1%-75°

For a better visualisation of the cuttings velocity near the low side of the wellbore the software images were magnified for both 0.7m/s (138ft/min) and 0.9m/s (177ft/min) fluid flow velocities as shown in Figure 5.15. In addition the scale of the velocity in the flow direction was limited to 0.0-0.2m/s (0.0-39ft/min) and the velocities above this range are shown in white colour. It is clearly visible that at 0.7m/s flow velocity the cuttings near the lower wall has zero velocity whereas at 0.9m/s the cuttings near the lower wall show velocities higher than zero.

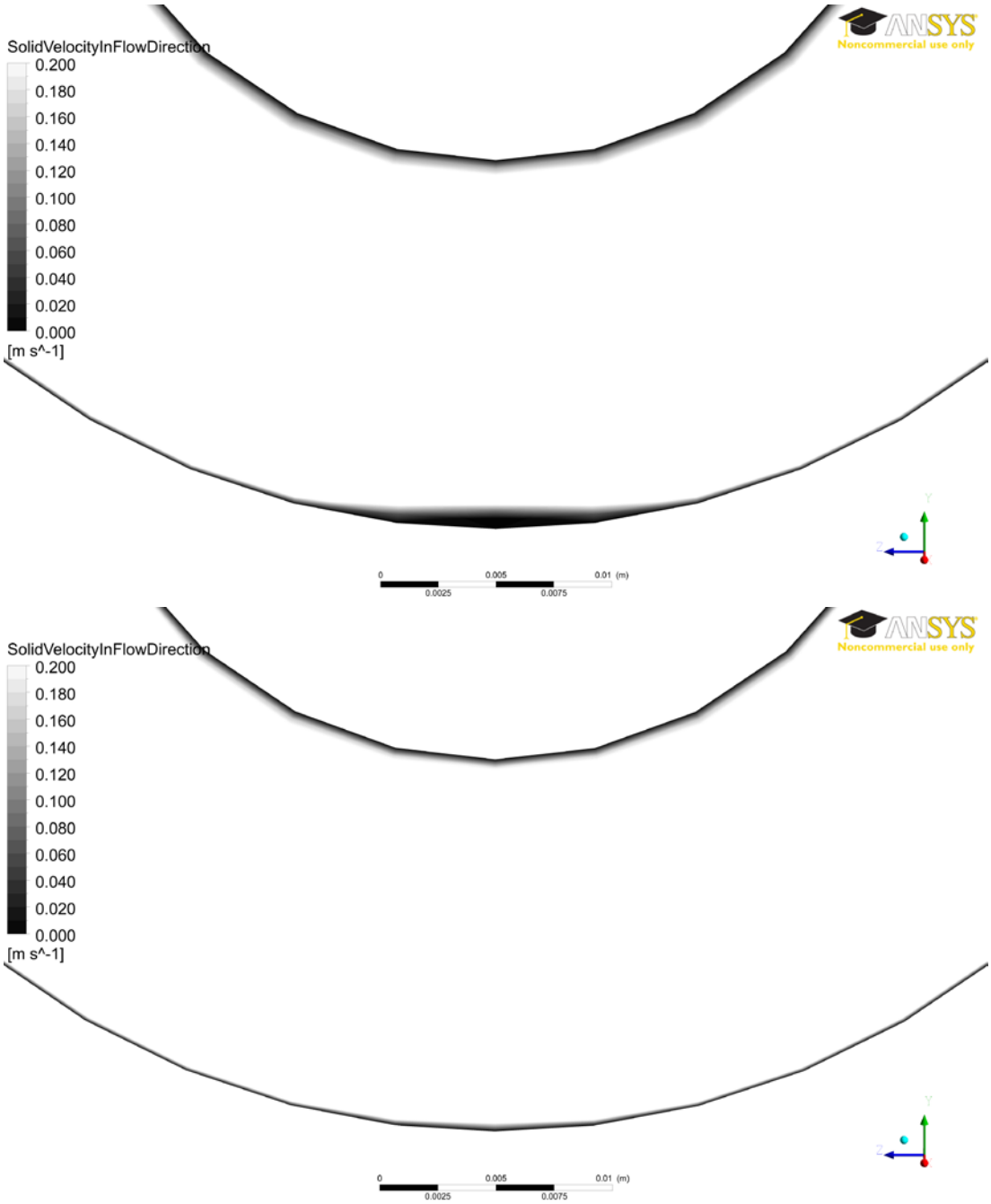

Figure 5.15 Cuttings velocity in the flow direction for Mud1-0.7m/s-0.068mm-1%-75° (top) and Mud1-0.9m/s-0.068mm-2.8g/cc-1%-75° (bottom)

Comparing this case with the previous case shows that at the velocity corresponding to the MTV, even the cuttings were much finer the water was not able to hold the cuttings in suspension and all of them lay at the bottom of the annulus. However, while the drilling fluid has higher viscosity (mud #2) and even the cuttings are bigger they distributed more along the annulus space and by increasing the velocity this distribution dramatically increased.

Boycott movement

In directional O&G wells downward cuttings bed movement has been described simply as downward slumping or sliding. However a more exact term is Boycott movement which was not frequently discussed. To study Boycott movement numerical simulations were made with the parameters:

Mud3-0.7m/s-1.557mm-2.75g/cc-1%-15°.

Mud #3 follows a HB rheological model and the MTV for this case is 0.8m/s (157ft/min). For these parameters a Reynolds number of 1942 is calculated and the flow regime is laminar. The results of simulations at different time steps from 0 to 8 seconds are shown in Figure 5.16 and were validated with experimental data.

With a MTV the expectation is that the cuttings stay mostly static near the wall and with a decrease in flow velocity from 0.8m/s to 0.7m/s the cuttings to slide downward and initiate a Boycott movement. This behaviour is clearly visible at t=8sec where the particles move downward.

The developed numerical simulation model is able to simulate and validate the experimental results and therefore it can be used as a reliable tool to perform the sensitivity analysis of other cases. The effect of change in cuttings size, mud rheological properties, hole inclination and flow regime were considered in the Chapter 4 (see Section 4.3). Therefore here the sensitivity analysis is done for cuttings density and cuttings concentration to see their effects on cuttings transportation behaviour.

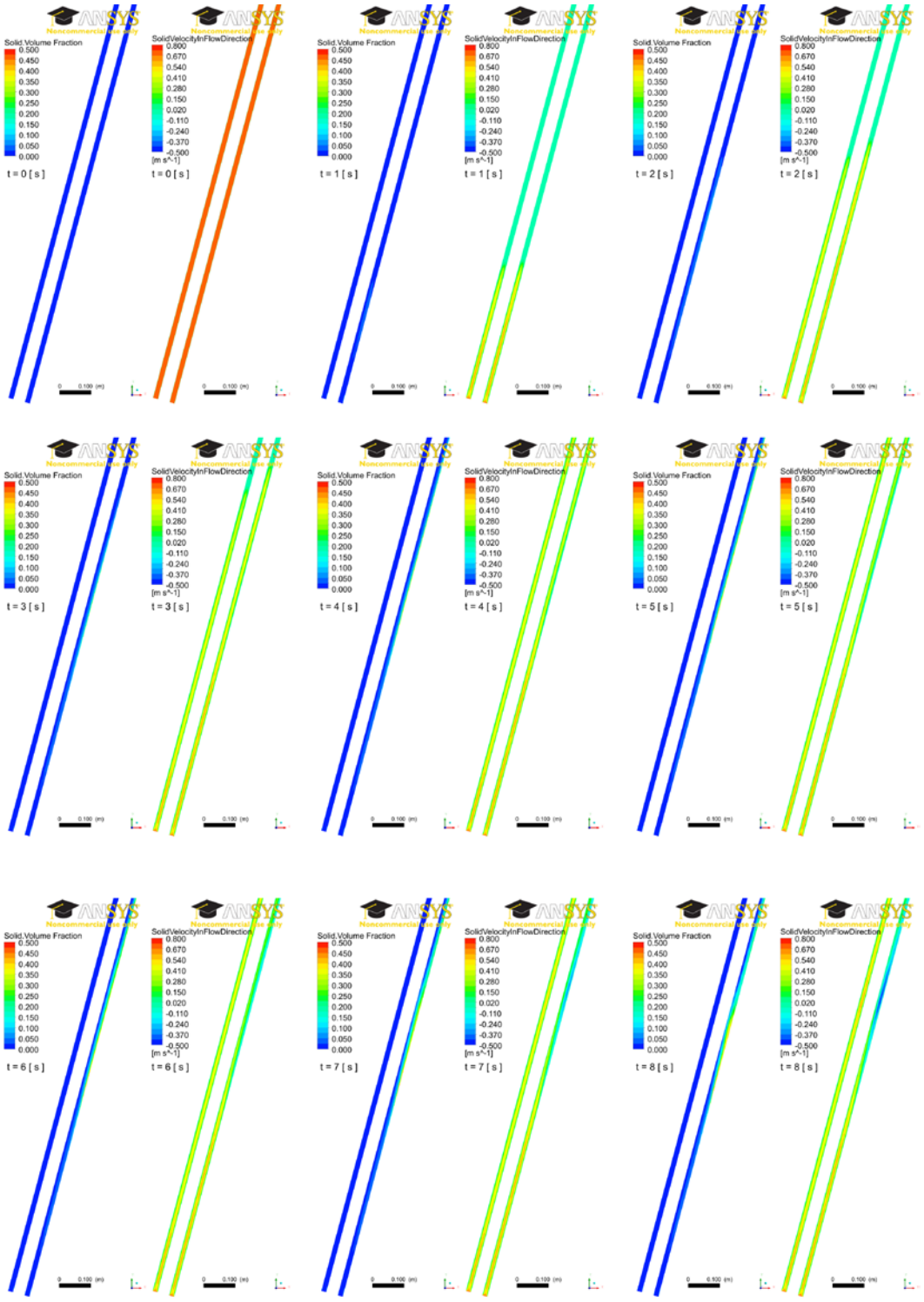

Figure 5.16 Boycott movement observed for Mud3-0.7m/s-1.557mm-2.75g/cc-1%-15° while the MTV is 0.8m/s

The effect of cuttings density

To determine the effect of density on the cuttings movement

Mud1-0.7m/s-0.068mm-2.8g/cc-1%-75°

was simulated with particle density being increased from 2.8g/cc (23.36ppg) to 5.0g/cc (41.7ppg) and the results are shown in Figure 5.17. The results indicate that

the cuttings exhibit Boycott movement and are sliding downward because their velocity is negative. The MTV in this case is more than the previous case and therefore to be able to carry all the cuttings upward a higher flow rate is required.

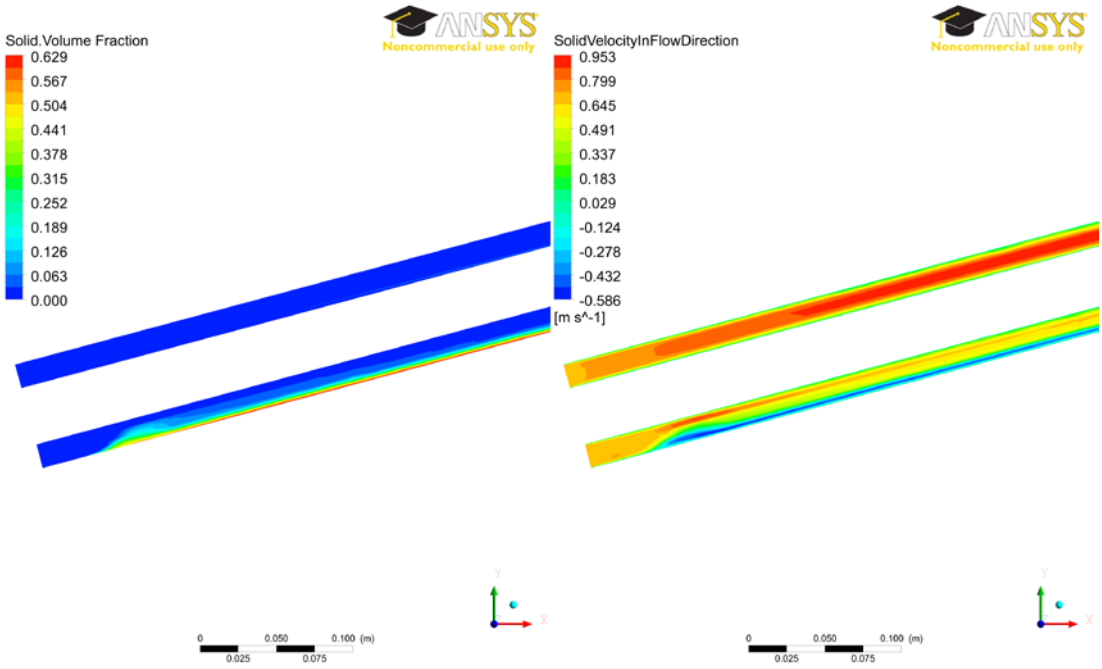

Figure 5.17 Cuttings volume fraction (left) and cuttings velocity in the direction of the annulus (right) on the symmetry plane at the entrance for Mud1-0.7m/s-0.068mm-5.0g/cc-1%-75°

The effect of cuttings concentration

To show the effect of cuttings concentration case

Mud2-1.3m/s-2.6mm-2.75g/cc-1%-45°

was simulated numerically where the solid concentration was increased from 1% v/v to 2% v/v. Figure 5.18 shows the solid volume fraction and solid velocity in the flow direction due to this change compared to Figure 5.9 which shows the original case results. The results indicate that the cuttings are distributed over more of the annulus cross section as their concentration is increased. In addition the cuttings near the lower wall are in stationary mode and therefore a higher flow velocity is required to put the particles in the moving bed state. Even though the cuttings volume has been increased the cuttings show no downward slippage or sliding as the mud rheology can hold them.

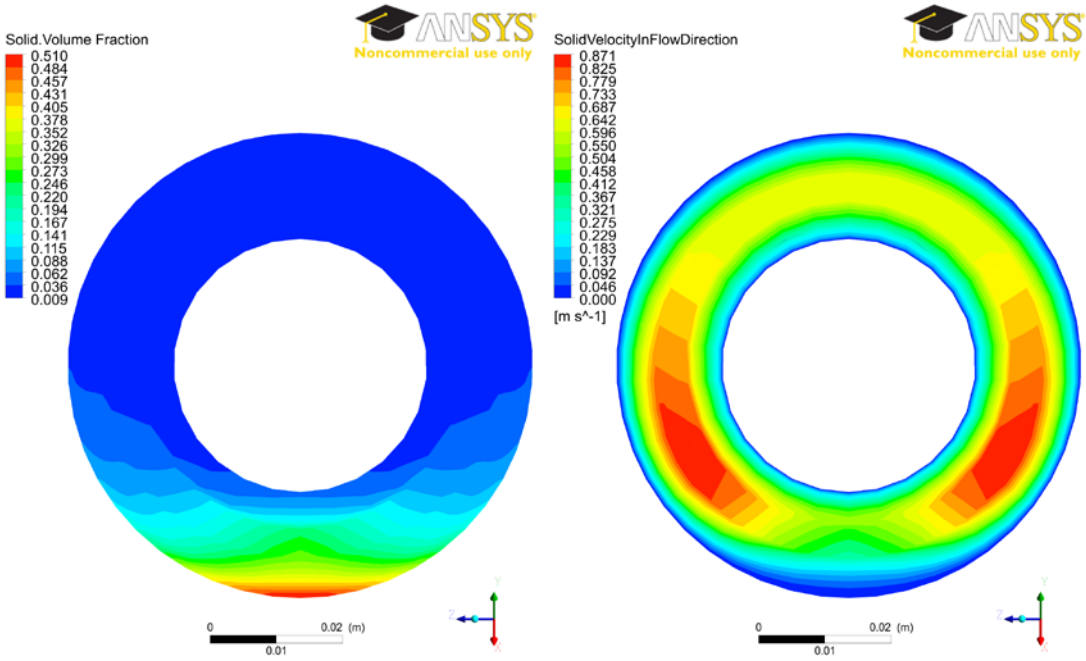

Figure 5.18 Cuttings volume fraction (left) and cuttings velocity in the direction of the annulus (right) on a cross section of the annulus 3m away from the entrance for Mud2-1.3m/s-2.6mm-2.75g/cc-2%-45°

5.5 Summary

In this chapter the results of numerical simulations of cuttings transportation were presented. Sensitivity analysis of various parameters was carried out and the results were validated against some laboratory flow loop experimental tests.

The results indicated that the developed model has the capability to determine cuttings movement in CT slim hole without allowing mixing of the cuttings to occur. The model can be used to determine the MTV and the state of cuttings in the annulus.

The next Chapter presents the conclusions and recommendations of this research study.

6 Conclusions and recommendations

This Chapter outlines the main conclusions drawn from this research and some recommendations are given for the continuation of the micro–borehole coiled tubing drilling research work.

6.1 Conclusions

The experimental studies detailed in Chapter 3 allowed the followings conclusions for the effect of the fine cuttings on the rheological properties of the drilling fluids:

- The effect of small size cuttings (rock flour) on drilling mud rheological properties is noticeable and must be considered in MBH hard rock drilling. This is somewhat contrary to the drilling in the O&G industry where the majority of cuttings are coarser and their effect on drilling fluid rheology is considered to be negligible.
- Increase in slurry viscosity from an increase in the fine cuttings concentration is more pronounced at higher shears rates (fluid velocities) that correspond more readily to MBHCTD scenarios. High drilling fluid velocities are required to function a downhole turbine or motor at very high speed for optimised drilling.
- An increase in the fine cuttings concentration from 0 to 5% v/v can increase the APLs by 15% in a 5cm/7cm MBH annulus.

The results of experimental work using the two flow loops to simulate both vertical and directional MBHs yielded the following conclusions:

- Experimental investigations performed with a mini flow loop showed that the smaller cuttings are easier to transport to the surface in vertical holes.
- As the viscosity of the drilling fluid increases the transition boundary occurs at higher Reynolds number. In addition higher flow velocity would be required to put the fluid into the transition or turbulent flow regime.

- Hole inclinations of 30° to 60° is the most difficult angles in terms of hole cleaning. This coincides with the results presented by previous research studies.
- While water is not used as the drilling fluid in O&G applications, in mineral exploration its use is preferred as it can drive the downhole motor and hammer more effectively due to its low viscosity.
- Ignoring water as a drilling fluid, higher viscosity drilling fluids found to perform better in terms of cuttings transportation and this contradicts with the findings in O&G. Including water as a drilling fluid, for bigger cuttings the statement in O&G complies with the finding in this study that water is the best fluid for cuttings transportation. However, this statement disproves the case of finer particles.
- With water as the drilling fluid, the MTV corresponding to different cuttings sizes are close to each other. However, for finer particles, with sizes less than 420 microns, the required velocity to carry the cuttings in moving bed mode is lower. In contrast, the profiles for higher viscosity muds are more parted.
- Dune and Boycott movement modes are rarely reported in cuttings transportation related to O&G applications. However, with water being used as the drilling fluid in minex drilling, these types of cuttings movement may be observed and therefore were investigated in this study.

The results of numerical simulations corresponding to cuttings transport in vertical and deviated boreholes while changing different input parameters resulted in following conclusions:

- The mini flow loop experimental results were modelled using EG model and the results were successfully validated. This showed the capability of this model to simulate the cuttings transportation process. Then the developed model was used to determine the sensitivity of parameters in transportation of the cuttings in vertical wells.
- The presented EG model is able to determine the MTV when the cuttings are at the stationary bed forms. Increasing the flow velocity will put the cuttings into moving bed profile.
- The developed model was used to determine the sensitivity of parameters in transportation of the cuttings in deviated boreholes assuming different mud

rheological models such as Newtonian, PL and HB as well as different flow velocities, cuttings sizes, hole inclinations and particle densities and concentrations.

- The results showed that the drilling fluids with higher viscosity can hold the cuttings more effectively than water. This results in more even distribution of the cuttings in the annulus space whereas in case of water as the drilling fluid the cuttings tend to attach more to the lower side of the annulus.
- The developed model could simulate the Boycott movement of the cuttings throughout the annulus space and this movement mode is of paramount importance to avoid mixing of the particles.

6.2 Recommendations for future work

- Further experimental work is required to be performed in order to incorporate the effect of the size of the cuttings on the rheological properties of the drilling fluid. The results would ultimately present in the form of equations or correlations to determine the rheology change due to addition of the cuttings to the drilling fluid. Also, the change in the pressure loss can be investigated experimentally with the flow loop and coupled with the equations presented in Section 3.4 of Chapter 3.
- Eccentricity of the CT was not studied here. In real situation of CTD in the deviated wells the CT would tend to lie on the bottom side of the wellbore and this worsen the cuttings transportation efficiency as the cuttings trap in a smaller clearance between the wellbore wall and the CT. Therefore experimental and numerical simulation to study this effect is important.
- In the current EG model an averaging method was used for the particles shape and size. Particles are assumed to be spherical and the particle size is presented as a single value. For more precise calculation a more accurate method to account for particle sphericity and size distribution should be used.
- Since the numerical simulation performed with transient model consumes a long time to reach a steady state condition, finding an alternative faster method would save the computational time and cost.
- Surge and swab are important elements in drilling operation and it becomes more significant in CTD. Because the annular clearance is very small in micro

boreholes, therefore sudden movement of the CT in the borehole will cause a high pressure loss in the hole which leads to kick occurrence or formation fracturing. Thus determination of surge and swab pressure loss and procedures to avoid this issue is an important topic for further study.

- Since CTD technology is planned to replace diamond coring in mineral exploration the samples recovered at the surface with the new method need to accurately represent the depth of origin of the cuttings. Particle tracking is the technique to be used to investigate the displacement of the particles in the wellbore. CFD simulations with Lagrangian approach can be performed in order to track the movement of single particles. This method is different from the Eulerian approach that was used in this study in which the particles were treated as continuum, i.e. based on an averaging method. In addition, experimental setup with the flow loop needs to be performed to validate the numerical results. For particle tracking studies the effect of various parameters need to be investigated. These include: mud properties (rheology, density, and flow rate); particle properties (size distribution, shape, concentration, and density); and annulus configuration (diameters, length and eccentricity).
- Borehole instability is one of the problems occurring during drilling operation. In minex, the type of borehole instability could be in the form of collapse of broken and fractured rocks at shallow depth, erosion of borehole wall due to high flow rate of the drilling fluid, instabilities associated with drilling into the unconsolidated formations and mud loss into fractured formations. Figure 6.1 shows two boreholes drilled at a mine site. The well shown on the left did not encounter collapse however, the top section of the second well experienced washout. Investigation of the causes of these instabilities and methods to prevent them is the subject of several future research studies.

Figure 6.1 The wells drilled with a hammer bit. Left: without washout, right: with washout

References

Al-Kayiem, H. H., Zaki, N. M., Asyraf, M. Z., & Elfeel, M. E. (2010). Simulation of the cuttings cleaning during the drillling operation. *American Journal of Applied Sciences, 7*(6), 800-806. doi: 10.3844/ajassp.2010.800.806

Albright, J., Dreesen, D., Anderson, D., Blacic, J., Thomson, J., & Fairbanks, T. (2005). Road map for a 5000-ft microborehole. Institution: Los Alamos National Laboratory. Retrieved from http://goo.gl/4GANkE

Ali, M. W. (2002). A parametric study of cutting transport in vertical and horizontal well using computational fluid dynamics (CFD). (Masters Degree), West Virginia University. Retrieved from http://goo.gl/zII2Tj

Ansys, Inc. (2011). Ansys Fluent Theory Guide Ver. 14

Bandelis, G. E., & Kelessidis, V. C. (2006). Solid bed erosion by liquids flowing in horizontal concentric annulus. Paper presented at the 2nd International Conference on Advances in Mineral Resources Management and Enviromental Geotechnology, Hania, Greece.

Bannister, C. E. (1934). United States Patent No. US 1965563 A. Retrieved from http://goo.gl/3DegBW

Bingham, E. C. (1922). Fluidity and plasticity. New York: McGraw-Hill.

Bourgoyne, A. T., Millheim, K. K., Chenevert, M. E., & Young, F. S. (1986). Applied drilling engineering. Richardson, TX, USA: Society of Petroleum Engineers.

Boycott, A. E. (1920). Sedimentation of blood corpuscles. *Nature, 104*, 532. doi: 10.1038/104532b0

Brown, N. P., Bern, P. A., & Weaver, A. (1989). Cleaning deviated holes: New experimental and theoretical studies. Paper presented at the SPE/IADC Drilling Conference, 28 February-3 March, New Orleans, Louisiana.

Buckingham, E. (1914). On physically similar systems; illustrations of the use of dimensional equations. *Physical Review, 4*(4), 345-376.

Byrom, T. G. (1999). Coiled-tubing drilling in perspective. *Journal of Petroleum Technology, 51*(6), 57-61. doi: 10.2118/51792-MS

Cengel, Y. A., & Cimbala, J. M. (2006). Fluid Mechanics: Fundamentals and Applications, Si Version: McGraw-Hill Education.

Corewell catalog. (2014). Product Data Sheet, Australian Mud Company. Retrieved from http://goo.gl/1pRdp5

Doron, P., & Barnea, D. (1993). A three-layer model for solid-liquid flow in horizontal pipes. *International Journal of Multiphase Flow, 19*(6), 1029-1043. doi: 10.1016/0301-9322(93)90076-7

Doron, P., & Barnea, D. (1996). Flow pattern maps for solid-liquid flow in pipes. *International Journal of Multiphase Flow, 22*, 273-283. doi: 10.1016/0301-9322(95)00071-2

Doron, P., Granica, D., & Barnea, D. (1987). Slurry flow in horizontal pipes-experimental and modeling. *International Journal of Multiphase Flow, 13*(4), 535-547. doi: 10.1016/0301-9322(87)90020-6

Deep Exploration Technologies Cooperative Research Centre. Driller Training Program. (2014). Retrieved 21 April, 2014, from http://goo.gl/4zU8tO

Eesa, M., & Barigou, M. (2009). CFD investigation of the pipe transport of coarse solids in laminar power law fluids. *Chemical Engineering Science, 64*(2), 322-333. doi: 10.1016/j.ces.2008.10.004

Enilari, M. G., Osisanya, S. O., & Ayeni, K. (2006). Development and evaluation of various drilling fluids for slim-hole wells. *Journal of Canadian Petroleum Technology, 48*(6), 30-32. doi: 10.2118/09-06-30-TB

Ergun, S. (1952). Fluid flow through packed columns. *Chem. Eng. Prog., 48*(2), 89-94.

Fangary, Y. S., Ghani, A. S., El Haggar, S. M., & Williams, R. A. (1997). The effect of fine particles on slurry transport processes. *Minerals engineering, 10*(4), 427-439. doi: 10.1016/S0892-6875(97)00019-8

Ford, J. T., Peden, J. M., Oyeneyin, M. B., Gao, E., & Zarrough, R. (1990). Experimental investigation of drilled cuttings transport in inclined boreholes. Paper presented at the SPE Annual Technical Conference and Exhibition, 23-26 September, New Orleans, Louisiana.

Fordham, E. J., Bittleston, S. H., & Tehrani, M. A. (1991). Viscoplastic flow in centered annuli, pipes, and slots. *Industrial and Engineering Chemistry, 30*(3), 517-524. doi: 10.1021/ie00051a012

Founargiotakis, K., Kelessidis, V. C., & Maglione, R. (2008). Laminar, transitional and turbulent flow of Herschel-Bulkley fluids in concentric annulus. *Canadian Journal of Chemical Engineering, 86*(4), 676-683. doi: 10.1002/cjce.20074

Gidaspow, D., Bezburuah, R., & Ding, J. (1992). Hydrodynamics of circulating fluidized beds: kinetic theory approach. Paper presented at the 7th international conference on fluidization, 3-8 May 1992, Gold Coast, Australia. http://goo.gl/9ey6qB

Hanks, R. W. (1979). The axial laminar flow of yield-pseudoplastic fluids in a concentric annulus. *Industrial and Engineering Chemistry, 18*(3), 488-493. doi: 10.1021/i260071a024

Hartnett, J. P., & Kostic, M. (1990). Turbulent friction factor correlations for power law fluids in circular and non-circular channels. *International communications in heat and mass transfer, 17*(1), 59-65. doi: 10.1016/0735-1933(90)90079-Y

Hemphill, T., Campos, W., & Pilehvari, A. (1993). Yield-power law model more accurately predicts mud rheology. *Oil and Gas Journal, 91*, 45-50.

Herschel, W. H., & Bulkley, R. (1926). Konsistenzmessungen von Gummi-Benzollösungen. *Colloid and Polymer Science, 39*(4), 291-300. doi: 10.1007/BF01432034

Hillis, R. (2012). Uncovering the future of drilling. *The AusIMM Bulletin*.

Hussain, Q. E., & Sharif, M. A. R. (1997). Viscoplastic fluid flow in irregular eccentric annuli due to axial motion of the inner pipe. *Canadian Journal of Chemical Engineering, 75*, 1038-1045. doi: 10.1002/cjce.5450750606

Hyun, C., Shah, S. N., & Osisanya, S. O. (2000). A three-layer modeling for cuttings transport with coiled tubing horizontal drilling. Paper presented at the SPE Annual Technical Conference and Exhibition, 1-4 October Dallas, Texas.

Hyun, C., Shah, S. N., & Osisanya, S. O. (2002). A three-segment hydraulic model for cuttings transport in coiled tubing horizontal and deviated drilling. *Journal of Canadian Petroleum Technology, 41*(6). doi: 10.2118/02-06-03

ICoTA. (2005). An introduction to coiled tubing. Retrieved from http://goo.gl/eQb0iK

Iyoho, A., & Azar, J. (1981). An accurate slot-flow model for non-Newtonian fluid flow through eccentric annuli. *SPE Journal, 21*(5), 565-572. doi: 10.2118/9447-PA

Kelessidis, V. C., & Bandelis, G. E. (2004). Flow patterns and minimum suspension velocity for efficient cuttings transport in horizontal and deviated wells in coiled-tubing drilling. *SPE Drilling & Completion, 19*(4), 213-227. doi: 10.2118/81746-PA

Kelessidis, V. C., Bandelis, G. E., & Li, J. (2007). Flow of dilute solid-liquid mixtures in horizontal concentric and eccentric annuli. *Journal of Canadian Petroleum Technology, 46*(5), 56-61. doi: 10.2118/07-05-06

Kelessidis, V. C., Dalamarinisa, P., & Maglione, R. (2011). Experimental study and predictions of pressure losses of fluids modeled as Herschel–Bulkley in concentric and eccentric annuli in laminar, transitional and turbulent flows. *Journal of Petroleum Science and Engineering, 77*, 305-312. doi: 10.1016/j.petrol.2011.04.004

Kelessidis, V. C., Maglione, R., Tsamantaki, C., & Aspirtakis, Y. (2006). Optimal determination of rheological parameters for Herschel-Bulkley drilling fluids and impact on pressure drop, velocity profiles and penetration rates during drilling. *Journal of Petroleum Science and Engineering, 53*, 203-224. doi: 10.1016/j.petrol.2006.06.004

Kelessidis, V. C., & Mpandelis, G. E. (2004). Hydraulic parameters affecting cuttings transport for horizontal coiled tubing drilling. Paper presented at the 7th National Congress on Mechanics, 24-26 June, Chania, Greece. http://goo.gl/Gg7aTp

Kelin, W., Tie, Y., Xiaofeng, S., Shuai, S., & Shizhu, L. (2013). Review and Analysis of Cuttings Transport in Complex Structural Wells. *Open Fuels & Energy Science Journal, 6*.

Lahiri, S. K., & Ghanta, K. C. (2010a). Regime identification of slurry transport in pipelines: A novel modelling approach using ANN & differential evolution. *Chemical Industry and Chemical Engineering Quarterly, 16*(4), 329-343. doi: 10.2298/CICEQ091030034L

Lahiri, S. K., & Ghanta, K. C. (2010b). Slurry flow modelling by CFD. *Chemical Industry and Chemical Engineering Quarterly, 16*(4), 295-308. doi: 10.2298/CICEQ091030031L

Laird, W. (1957). Slurry and Suspension Transport - Basic Flow Studies on Bingham Plastic Fluids. *Industrial and Engineering Chemistry, 49*, 138-141. doi: 10.1021/ie50565a041

Lang, R. (2006). Microhole Technology. Institution: U.S. Department of Energy. Retrieved from http://goo.gl/rqug7N

Leising, L. J., & Rike, E. A. (1994). Coiled-Tubing Case Histories. Paper presented at the SPE/IADC Drilling Conference, 15-18 February, Dallas, Texas.

Leising, L. J., & Walton, I. C. (2002a). Cuttings-transport problems and solutions in coiled-tubing drilling. *SPE Drilling & Completion, 17*(1), 54-66. doi: 10.2118/77261-PA

Leising, L. J., & Walton, I. C. (2002b). Cuttings-Transport Problems and Solutions in Coiled-Tubing Drilling. *SPE Drilling & Completion, 17*(SPE 77261-PA), 54-66. doi: 10.2118/77261-PA

Li, J., & Walker, S. (2001). Sensitivity analysis of hole cleaning parameters in directional wells. *SPE Journal, 6*(04), 356-363. doi: 10.2118/74710-PA

Li, Y., Bjorndalen, N., & Kuru, E. (2007). Numerical modelling of cuttings transport in horizontal wells using conventional drilling fluids. *Journal of Canadian Petroleum Technology, 46*(7). doi: 10.2118/07-07-TN

Littleton, B. L., Nicholson, S., & Blount, C. G. (2010). Improved drilling performance and economics using hybrid voiled tubing unit on the Chittim Ranch, West Texas. Paper presented at the IADC/SPE Drilling Conference and Exhibition, 2-4 February, New Orleans, Louisiana, USA.

Lun, C. K. K., Savage, S. B., Jeffrey, D. J., & Chepurniy, N. (1984). Kinetic theories for granular flow: inelastic particles in Couette flow and slightly inelastic particles in a general flow field. *Journal of Fluid Mechanics, 140,* 223-256. doi: 10.1017/S0022112084000586

Mandal, S. (2012). AMC drilling fluid products.

Marjoribanks, R. W. (1997). Geological Methods in Mineral Exploration and Mining: Springer Netherlands.

Martin, M., Georges, C., Bisson, P., & Konirsch, O. (1987). Transport of Cuttings in Directional Wells. Paper presented at the SPE/IADC Drilling Conference, 15-18 March 1987, New Orleans, Louisiana.

Matousek, V. (1996). Solids transportation in a long pipeline connected with a dredge. *Terra et Aqua, 62*.

McFadden, P. (2012). Uncover, Searching the Deep Earth: A vision for exploration geoscience in Australia. Institution: Australian Exploration Geoscience Research. Retrieved from http://goo.gl/aug9jJ

Metzner, A. B., & Reed, J. C. (1955). Flow of non-newtonian fluids-correlation of the laminar, transition, and turbulent-flow regions. *AIChE journal, 1*, 434-440. doi: 10.1002/aic.690010409

Department of Mines and Petroleum. (2013). Mineral exploration drilling - code of practice. Retrieved from http://goo.gl/zhFSva

Misiano, D. (2010). Exploration drilling. Institution: Atlas Copco. Retrieved from http://goo.gl/QE73Zs

Miska, S. Z., Reed, T., Kuru, E., Takach, N., Ashenayi, K., Ahmed, R., . . . Al-hosani, A. (2004). Advanced Cuttings Transport Study. Institution: The University of Tulsa. (DE-FG26-99BC15178), 57 Retrieved from http://goo.gl/xQnKQE

Nabil, T., El-Sawaf, I., & El-Nahhas, K. (2013). Computational fluid dynamics simulation of the solid-liquid slurry flow in a pipeline. Paper presented at the Seventeenth International Water Technology Conference, 5-7 November 2013, Istanbul.

Naganawa, S., & Nomura, T. (2006). Simulating Transient Behavior of Cuttings Transport over Whole Trajectory of Extended Reach Well. Paper presented at the IADC/SPE Asia Pacific Drilling Technology Conference and Exhibition, Bangkok, Thailand.

Nguyen, D., & Rahman, S. S. (1996). A three-layer hydraulic program for effective cuttings transport and hole cleaning in highly deviated and horizontal wells. *SPE/IADC Asia Pacific Drilling Technology*.

Nguyen, D., & Rahman, S. S. (1998). A three-layer hydraulic program for effective cuttings transport and hole cleaning in highly deviated and horizontal wells. *SPE Drilling & Completion, 13*(SPE 51186), 182-189. doi: 10.2118/51186-PA

Osgouei, R. E., Ozbayoglu, M. E., & Fu, T. K. (2013). CFD Simulation of Solids Carrying Capacity of a Newtonian Fluid Through Horizontal Eccentric

Annulus. Paper presented at the ASME 2013 Fluids Engineering Division Summer Meeting.

Ostwald, W. (1929). Ueber die rechnerische Darstellung des Strukturgebietes der Viskosität. *Kolloid-Zeitschrift, 47*(2), 176-187.

Ozbayoglu, E. M., Miska, S. Z., Reed, T., & Takach, N. (2002). Analysis of Bed Height in Horizontal and Highly-Inclined Wellbores by Using Artificial Neuraletworks. Paper presented at the SPE International Thermal Operations and Heavy Oil Symposium and International Horizontal Well Technology Conference.

Peden, J. M., Ford, J. T., & Oyeneyin, M. B. (1990). Comprehensive experimental investigation of drilled cuttings transport in inclined wells including the effects of rotation and eccentricity. Paper presented at the European Petroleum Conference, 21-24 October, The Hague, Netherlands.

Perry, K. (2009). Microhole coiled tubing drilling: a low cost reservoir access technology. *Journal of Energy Resources Technology, 131*. doi: 10.1115/1.3000100

Pigott, R. (1941). Mud flow in drilling. Paper presented at the Drilling and Production Practice, New York, US.

Pilehvari, A., Azar, J. J., & Shirazi, S. A. (1999). State-of-the-art cuttings transport in horizontal wellbores. *SPE Drilling & Completion, 14*(3), 196-200. doi: 10.2118/57716-PA

Pipe Line Under the Ocean (PLUTO). (2014). Retrieved 3 April 2014, 2014, from http://goo.gl/nvAVuQ

Ramadan, A., Skalle, P., & Johansen, S. T. (2003). A mechanistic model to determine the critical flow velocity required to initiate the movement of spherical bed particles in inclined channels. *Chemical Engineering Science, 58*(10), 2153-2163. doi: 10.1016/S0009-2509(03)00061-7

Ramadan, A., Skalle, P., & Saasen, A. (2005). Application of a three-layer modeling approach for solids transport in horizontal and inclined channels. *Chemical Engineering Science, 60*(10), 2557-2570. doi: 10.1016/j.ces.2004.12.011

American Petroleum Institute (API). (2010). Rheology and hydraulics of oil-well fluids. Retrieved from http://goo.gl/E8LQqS

Robertson, R. E., & Stiff Jr., H. A. (1976). An improved mathematical model for relating shear stress to shear rate in drilling fluids and cement slurries. *SPE Journal, 16*, 31-36. doi: 10.2118/5333-PA

Engineering ToolBox. Roughness & Surface Coefficients of Ventilation Ducts. (2014). from http://goo.gl/xy8DFT

Schlumberger. Rugosity. (2014). *Oilfield Glossary*. 2014, from http://goo.gl/if0Skr

Safaee Ardekani, O., & Shadizadeh, S. R. (2013). Development of drilling trip time model for southern Iranian oil fields: using artificial neural networks and multiple linear regression approaches. *Journal of Petroleum Exploration and Production Technology, 3*(4), 287-295. doi: 10.1007/s13202-013-0065-y

ESI CFD. Saxena, A. (2013). Guidelines for Specification of Turbulence at Inflow Boundaries. Retrieved 12 Nov, 2013, from http://goo.gl/FmZ9pU

Shah, S. N., Kamel, A., & Zhou, Y. (2006). Drag reduction characteristics in straight and coiled tubing - An experimental study. *Journal of Petroleum Science and Engineering, 53*(3-4), 179-188. doi: 10.1016/j.petrol.2006.05.004

Sharma, M. (1990). Cuttings transport in inclined boreholes. Paper presented at the paper OSEA-90159 presented at the 8th Offshore South Asia Conference, Singapore (4-7 December 1990).

Sifferman, T. R., & Becker, T. E. (1992). Hole cleaning in full-scale inclined wellbores. *SPE Drilling Engineering, 7*(2), 115-120. doi: 10.2118/20422-PA

Sorgun, M. (2010). Modeling of newtonian fluids and cuttings transport analysis in high inclination wellbores with pipe rotation. (PhD), Middle East Technical University, Ankara. Retrieved from http://goo.gl/bFfqP

Sorgun, M., Aydin, I., Ozbayoglu, E., & Schubert, J. J. (2012). Mathematical Modeling of Turbulent Flows of Newtonian Fluids in a Concentric Annulus with Pipe Rotation. *Energy Sources, Part A: Recovery, Utilization, and Environmental Effects*, *34*, 540-548. doi: 10.1080/15567036.2011.578105

Spears, R. (2003). Microhole initiative – workshop summary. Institution: Spears & Associates, Inc. Retrieved from http://goo.gl/AYzEuN

Syamlal, M., Rogers, W., & O'Brien, T. J. (1993). MFIX documentation: Theory guide. *Technical Note, DOE/METC-94/1004, NTIS/DE94000087, National Technical Information Service, Springfield, VA.* https://mfix.netl.doe.gov/documentation/Theory.pdf

Tomren, P. H., Iyoho, A. W., & Azar, J. J. (1986). Experimental study of cuttings transport in directional wells. *SPE Drilling Engineering, 1*(1), 43-56. doi: 10.2118/12123-PA

Amoco Production Company. (1996). Training to Reduce Unscheduled Events Retrieved from http://goo.gl/f4Tv4U

Tulsa Fluid Flow Projects. (2012). Retrieved 14 December, 2012, from http://goo.gl/N5zR4X

The University of Tulsa Drilling Research Projects. (2012). Retrieved 14 December, 2012, from http://goo.gl/d1JgV4

Versteeg, H. K., & Malalasekera, W. (2007). An introduction to computational fluid dynamics: the finite volume method: Pearson Education Ltd.

Walker, R. E., & Mayes, T. M. (1975). Design of Muds for Carrying Capacity. *Journal of Petroleum Technology*, *27*, 893-900. doi: 10.2118/4975-PA

Walker, S., & Li, J. (2000). The Effects of Particle Size, Fluid Rheology, and Pipe Eccentricity on Cuttings Transport. Paper presented at the SPE/ICoTA Coiled Tubing Roundtable, 5-6 April, Houston, Texas.

Wen, C., & Yu, Y. H. (1966). Mechanics of fluidization. Paper presented at the Chem. Eng. Prog. Symp. Ser.

Xan-Bore catalog. (2014). Product Data Sheet, Australian Mud Company. Retrieved from http://goo.gl/ygk08G

Xiao-le, G., Zhi-ming, W., & Zhi-hui, L. (2010). Study on three-layer unsteady model of cuttings transport for extended-reach well. *Journal of Petroleum Science and Engineering, 73*(1-2), 171-180. doi: 10.1016/j.petrol.2010.05.020

Yassin, M., Azam, A., Ismail, A. R., & Mohammad, A. (1993). Evaluation of formation damage caused by drilling fluid in deviated wellbore. Paper presented at the Seminar Penyelidikan Fakulti Kej. Kimia & Kej. Sumber Asli.

Zamora, M., Roy, S., & Slater, K. (2005). Comparing a basic set of drilling fluid pressure-loss relationships to flow-loop and field data. Paper presented at the AADE 2005 National Technical Conference and Exhibition, 5-7 April, Wyndam Greenspoint, Houston, Texas.

Zhou, Y., & Shah, S. N. (2004). Fluid flow in coiled tubing: a literature review and experimental investigation. *Journal of Canadian Petroleum Technology, 43*(6), 52-61. doi: 10.2118/04-06-03

Zhou, Y., & Shah, S. N. (2006). New Friction Factor Correlations of Non-Newtonian Fluid Flow in Coiled Tubing. *SPE Drilling & Completion, 21*(SPE 77960), 68-76. doi: 10.2118/77960-MS

Appendix A Cuttings collection, preparation and analyses

In this study actual cuttings were used instead of standard industry simulated drill solid particles such as rev dust or ball clay. The cuttings was recovered from the Brukunga mine site located 40km east of Adelaide, South Australia. This site is used as a research and training facility by the Deep Exploration Technologies Cooperative Research Centre (DET CRC) (DET CRC, 2014).

A.1 Sample preparation procedure for rheological tests

For the tests performed in Chapter 3 fine particles are required and therefore impregnated diamond cuttings have been used. They have been recovered from a diamond coring operation. The following procedure has been performed in order to prepare the samples for the rheology tests:

1. **Liquid removal and mixing**: The liquid from the mixture has first been removed by syphoning action with a plastic tube. Then the sample was mixed thoroughly to achieve a homogenous mixture.
2. **Plot particle size distributions (PSD)**: Using a Malvern Instruments Mastersizer 2000, the particle size distributions of the cuttings were determined. Most of the cuttings are in the size range of $1-100\mu m$. Figure A.1 shows the size distribution of the wet cuttings.
3. **Adding fluids**: A total of 11 different fluid samples were prepared to wash the cuttings. Selection of the fluid used to wash the cuttings is important as it should not have any chemical interaction when it is in contact with the cuttings.
4. **Add cuttings to fluid:** 20 grams of cuttings were added to the fluids (see Figure A.2). This was to determine in which drilling fluid the cuttings remain stable with similar size distributions before and after being exposed to these fluids. Then the most stable fluid was used to wash the remaining cuttings.

5. **Rolling test in the oven**: The samples were placed in the rolling oven for 15 hours to test whether the cuttings remain stable after this period or not. Oven temperature was kept at 177 °F (80 °C).
6. **Plot PSD**: The samples were removed from the oven and then allowed to cool down for a while. After that, particle size distribution tests were conducted for cuttings included in the different drilling fluids. 1% KCl mud shows the least change in cuttings size distribution, corresponding to minimum shattering or swelling of the particles. Therefore this mud was selected to wash all cuttings samples.
7. **Washing and drying cuttings**: The 1% KCl mud was used to wash the cuttings and then further washed using tap water to remove the salt from the cuttings. After draining off the water, the samples were placed in the oven. This was followed by repeating the cuttings size distribution analysis, which indicated that the cuttings kept their initial state to a large extent as is shown in Figure A.1. In this figure a shift is seen in the PSD curve of the dried sample to the right with respect to the original sample. This is due to the fact that the samples tended to agglomerate after being dried, so slightly larger samples are expected to be produced.
8. **X-Ray Diffraction (XRD)**: The XRD test was performed after drying the samples and the chemical components observed in the sample are listed in Table A.1. The results indicate no trace of active particles that could affect the viscosity of the samples. This shows that all components present in the samples are inert and will not change the rheology of the samples for any electrochemical interaction with water or hydration.

Cuttings density: Archimedes' principle was used to measure the density of the cuttings with the density bottle method. Because the cuttings sizes are small, using water forms foam which alters the measurements, therefore diesel oil was used in these experiments for density measurements. The measured density of the cuttings was 2.7007 g/cc.

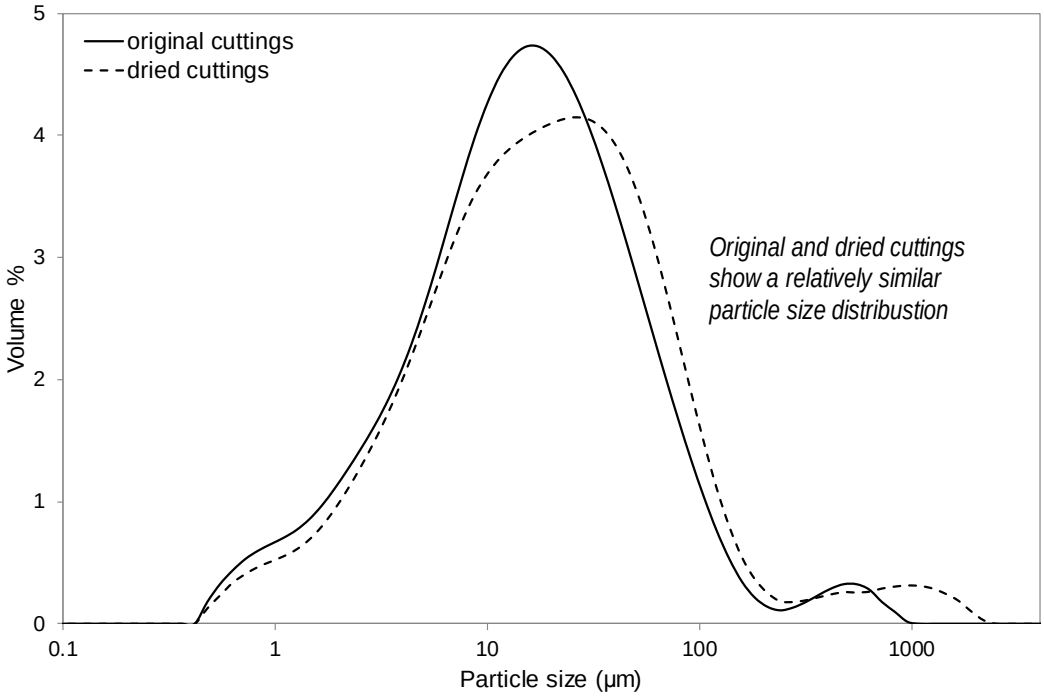

Figure A.1 PSD of cuttings before washing and after washing and drying

Figure A.2 Adding 20g of cuttings to the fluid samples

Table A.1 XRD results of cuttings

Phase	**Chemical formula**	**Weight %**
Albite	$NaAlSi_3O_8$	26.5
Calcite	$Ca(CO_3)$	0.95
Kaolinite-1A	$Al_2(Si_2O_5)(OH)_4$	0.35
Muscovite	$KAl_2Si_3AlO_{10}(OH)_2$	21
Pyrite	FeS_2	2.85
Pyrrhotite-3T	Fe_7S_8	10.5
Quartz	SiO_2	27.45
Amorphous Component*		10

*** may be due to the existence of non-crystalline material, or the difference between the experimental and the calculated data.**

A.2 Cuttings sample collection

For the tests performed in the flow loop the cuttings was recovered from a hammer drilling operation. In order to collect sufficient quantity of these cuttings, two un-

cased open holes were drilled to a total depth of 25m (82ft) with a multi-purpose Boart Longyear LX12 drilling rig in a rotary percussion mode.

A 60mm (2.4in) Wassara water-powered W50 drilling hammer was utilized to drill the well. Activation of the hammer requires a minimum flow rate and pressure of 75l/min and 180bar (2610psi), respectively. Figure A.3 shows the installed drilling hammer and bit in front of the drilling rod. The black channel next to the hammer bit cut in the surface allowed the returning annular fluid to carry the cuttings into a hole for collection.

Figure A.3 The Wassara downhole hammer connected to the drill bit

Rotation of the bit is caused by the drilling rig from the surface and the drilling fluid was water. The mean RPM and flow rate are 50rpm and 110l/min, respectively and the ROP is 0.7m/min. In this operation, rod handling takes a considerable time which CTD, as its advantage, can eliminate. Cuttings retrieved from 1st borehole are shown in Figure A.4.

Figure A.4 Cuttings collected from 1st well